Towards functional kidney organoids

Towards Functional Kidney Organoids: Insights from Kidney Organoid and Fetal Kidney Development

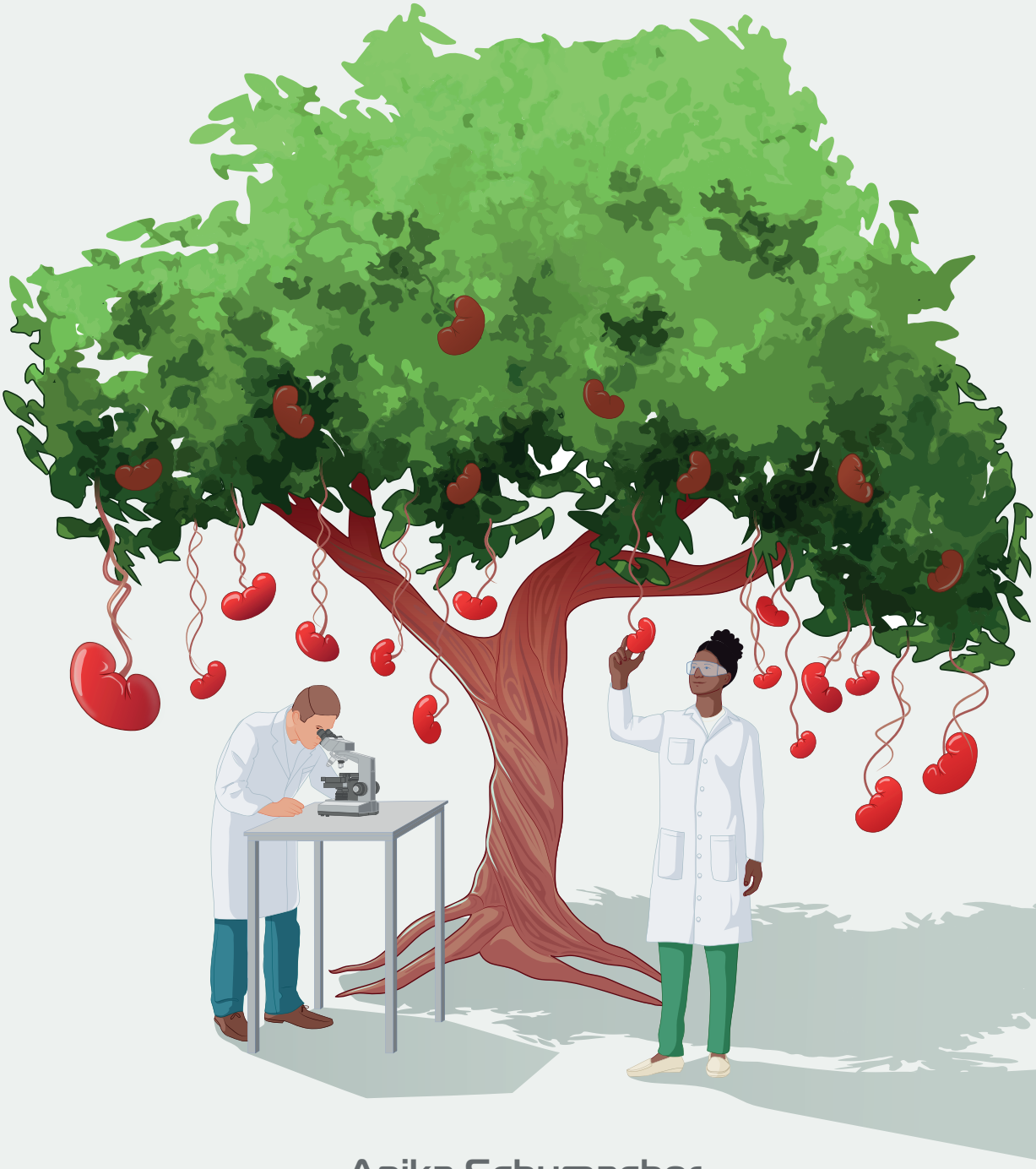

Anika Schumacher

Towards Functional Kidney Organoids: Insights from Kidney Organoid and Fetal Kidney Development

Anika Schumacher

The work described in this thesis was carried out at the Department of Cell Biology–Inspired Tissue Engineering (cBITE), MERLN Institute for Technology–Inspired Regenerative Medicine, Maastricht University, the Netherlands. We acknowledge some sponsoring by the Dutch Society for Microscopy (www.nvvm.microscopie.nl).

ISBN: 978-94-6469-489-5

Printed by: Proefschriftmaken.nl

Layout by: Anika Schumacher

Cover design by: Daniela Velasco

Towards Functional Kidney Organoids: Insights from Kidney Organoid and Fetal Kidney Development

Dissertation

To obtain the degree of Doctor at the Maastricht University,

on the authority of the Rector Magnificus,

Prof. dr. Pamela Habibović

in accordance with the decision of the Board of Deans,

to be defended in public on

Tuesday 26th of September 2023 at 10.00 hours

by

Anika Schumacher

born on 9th of March 1989 in Ulm (Germany)

Promotors:

Dr Vanessa LaPointe

Prof. dr. Martijn van Griensven

Assessment Committee:

Prof. dr. Mark Post (chair)

Dr Stefan Giselbrecht

Dr Martin Hoogduijn (Erasmus University Rotterdam)

Prof. dr. Marianne Verhaar (Utrecht University)

Paranymphs:

Gözde Sahin

Maria José Eischen-Loges

Contents

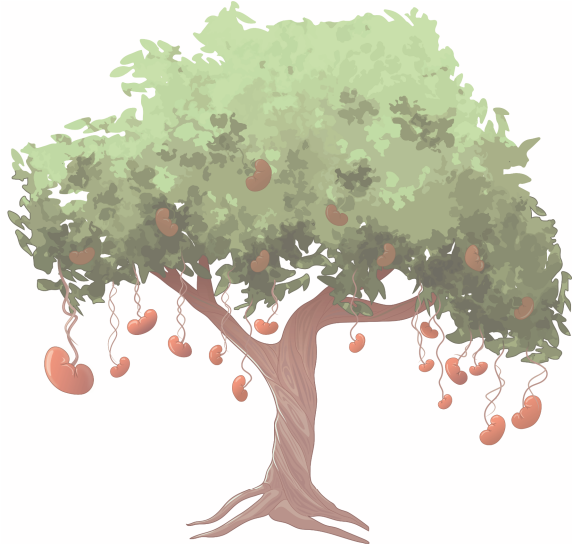

Chapter 1

Introduction

Anika Schumacher, Martijn van Griensven, Vanessa LaPointe

Department of Cell Biology–Inspired Tissue Engineering, MERLN Institute for Technology-Inspired Regenerative Medicine, Maastricht University, Maastricht, the Netherlands.

Creating kidney tissue from scratch: kidney organoids as transplantable grafts

Kidney disease affects more than 800 million people worldwide (10% of our population in 2022), and this number is predicted to increase, making it one of the leading burdens for healthcare and the economy.[1,2] Current treatment options are limited and there are no long-term solutions for patients with renal disease. Hemodialysis is still the major treatment option for patients with end-stage kidney disease – something unchanged since 1943. Over the decades, dialysis equipment has significantly improved by transitioning from cellulose to synthetic materials, from flat to capillary-sized hollow membranes, and through a significant reduction in size, allowing certain patient populations to undergo hemodialysis at home.

Nevertheless, hemodialysis remains a short-term solution as the average life expectancy on dialysis is 5–10 years, although this is strongly age-dependent.[3] The best solution currently is transplanting a matched donor organ. However, the waiting list is long due to an increasing donor shortage and ideal donor–patient matches are rare. Within 10 years post-transplantation, an average of 49.7% deceased donor transplants and 34.1% of living donor transplants fail.[4] Consequently, patients fall back on dialysis if no new donor organ is immediately available. More recently, stem cell therapy has been explored as an alternative. The majority of clinical trials tested the application of mesenchymal stem cells, and new trials are ongoing.[5,6] While challenges persist due to factors such as multifactorial diseases, patient age and co-morbidities, some clinical studies have shown improvements in, for instance, kidney function and reduction of proteinuria.[5,7] However, it remains to be determined if the benefits persist to make mesenchymal stem cells a long-term solution. More recently, xeno-transplantation of pig kidneys into a brain-dead human showed no adverse effects for 54 hours.[8,9] However, the ethically restricted duration of this study impairs any conclusions about long-term functionality. Clearly, there is currently no long-term solution with better outcomes than matched donor kidneys, and different treatment options are urgently needed.

Recent advances in the field of tissue engineering show promise for an alternative treatment method in the future. Tissue engineering is classically defined as the engineering of tissue constructs from cells, biomaterials and biochemical cues. Stem cell–derived micro-tissues such as organoids, which are frequently cultured without

biomaterials, have proven a valuable mimic of native tissues. The definition of organoids varies significantly according to the different tissue types and the culture methods that are applied.[10] What the definitions have in common is that they all describe a construct composed of a variety of cell types that self-organize (with or without the supplementation of an extracellular matrix–like material) into a three-dimensional shape with a structure and/or functionality comparable to the mature organ. Organoid models have become an intermediate step between monolayer cell cultures and animal research because of their greater cellular and architectural complexity resembling organs in three dimensions. They allow the studying of diseases, organogenesis, and pharmacological treatments in a more physiological environment without the immediate need for animal studies. Organoid dimensions are comparable to a small piece of tissue, ranging from a few hundred micrometers to several millimeters. To date, a large variety of organs have been replicated in the form of organoids (Figure 1). Their differentiation protocols are usually based on signaling events known from organ development.[11-13]

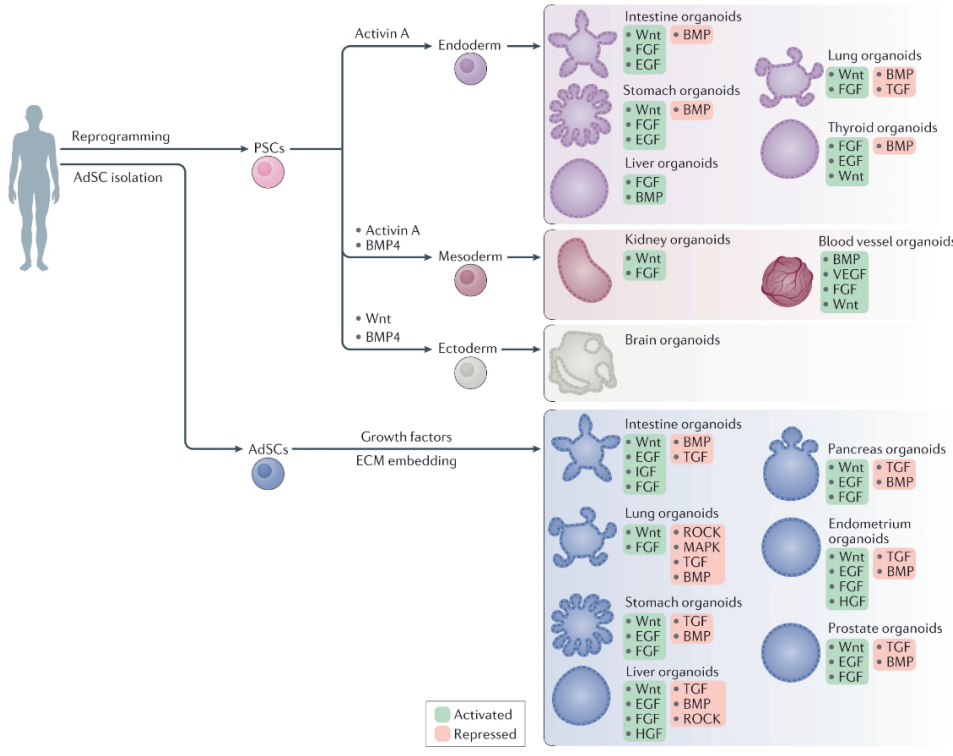

Figure 1: Overview of organoid types that have been developed to date and their major differentiation pathways, which are typically based on knowledge from signaling events in development. (AdSCs: adult–derived stem cells; PSCs: pluripotent stem cells.) Reproduced with permission from Kim, et al. [11]

Organoid technology has been successfully applied in the field of nephrology, serving as a disease model, for drug testing, and potentially in the future for transplantation. Kidney organoids are capable of recapitulating key aspects of human kidney development and renal diseases at the cellular and functional level, which is something that cell lines and animal models have failed to do in the past.[1] Nevertheless, 2D differentiation of rodent and human stem cells, including induced pluripotent stem cells (iPSCs), towards a variety of renal cell types was necessary to set the foundation for complex 3D kidney organoid culture.[14-16] Kidney organoid culture from stem cells was then pioneered by three groups in 2014–2015 by differentiating human embryonic stem cells (ESCs) in 2D and aggregating the progenitors to a 3D construct to allow self-organization into nephrons.[17-19] Only one year later, two research laboratories applied the same approach to iPSCs, thereby giving birth to the aim of universally transplantable tissue-engineered human kidneys.[19,20]

Since the introduction of the first iPSC–derived kidney organoid models, the number of kidney organoid culture protocols has strongly increased. Studies differ in terms of cell source, culture method, and the choice and timing of growth factors and small molecules (Figure 2). Culture methods are very diverse, ranging from transwell/air–liquid interface, Matrigel[21-23], other hydrogels[24], suspension[23,25] and bioreactor culture[26] to organoids-on-chip[27]. Recently, automated bioprinting of kidney organoid progenitors has reduced both the workload and variability in kidney organoid cultures.[28] Independent of the culture method, aggregation or condensation of the progenitors is an essential step for further maturation, as demonstrated by two earlier studies, where *in vitro* condensed progenitor clusters of nephron progenitors were shown to form nephrons *in vitro* and upon transplantation.[29,30] Increasingly, co-cultures are also being explored to establish more complete and more mature organoids (Figure 2).[31] Established co-cultures contain, for instance, endothelial cells[32], mesenchymal cells[29,33], ureteric bud and nephron progenitor cells[34] or amniotic fluid–derived cells[35].

Kidney organoids can be derived from either pluripotent stem cells (PSCs) such as ESCs and iPSCs or from adult tubular epithelial cells extracted from urine or renal cancer biopsies (Figure 2). Extrarenal stem cell sources, like bone marrow–derived stem cells, are unsuitable since they are devoid of nephrogenic potential, restricting the field to either PSCs or adult tubular cells.[36] Organoids of the latter are referred to as tubuloids, given their limited complexity and restricted development into only tubular cell types. They are cystic and therefore grow highly polarized, and they can be expanded over many passages while remaining genetically stable.[22] In contrast, PSC–derived kidney organoids are more complex. They self-organize into nephron-like structures and contain glomerular, tubular, stromal and endothelial cells. However, they cannot be passaged and can be kept in culture for a maximum of 25 days.[17,19,20,34] Consequently, their application and functionality are distinct. Tubuloids are particularly interesting for modeling tubular diseases, for drug testing and integration in bioengineering approaches, while PSC–derived organoids can model, for instance, glomerular diseases, fibrosis or kidney development, and have the potential to be used as a treatment for chronic kidney disease (CKD) with limited immune rejection.

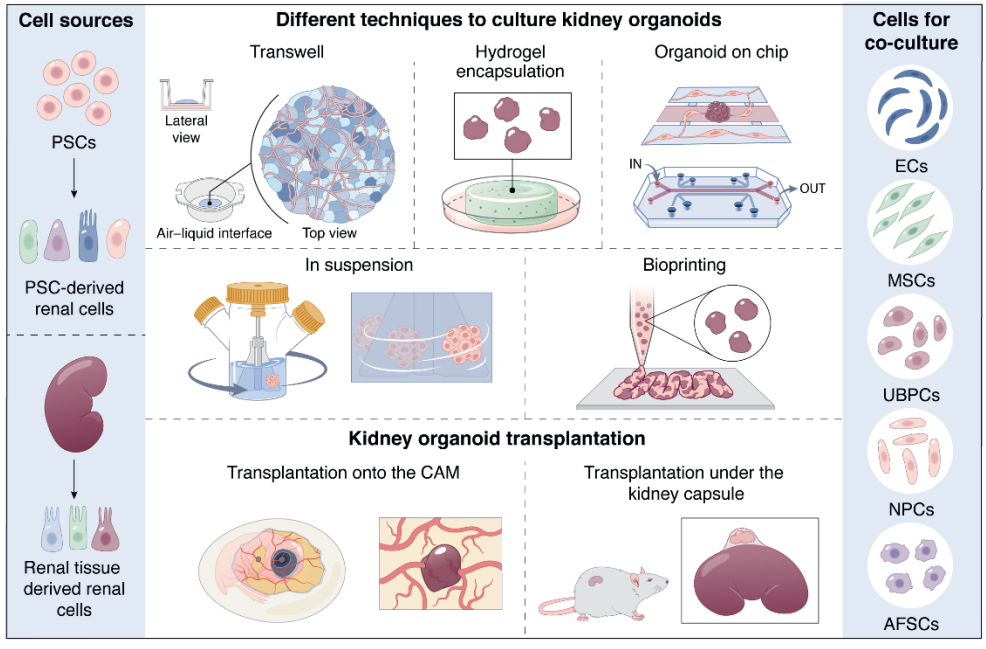

Figure 2: Schematic representation of potential cell sources, culture techniques and co-cultures to obtain kidney organoids. AFSCs: amniotic fluid stem cells, CAM: chorioallantoic membrane, ECs: endothelial cells, MSCs: mesenchymal stem cells, NPCs: nephron progenitor cells, PSCs: pluripotent stem cells, UBPCs: ureteric bud progenitor cells.

The progress made in kidney organoid culture over the past 9–10 years is extraordinary and has brought an alternative treatment method within reach for end-stage kidney disease. However, a variety of major limitations has engaged researchers across the world to further improve kidney organoid cultures. Limitations include the lack of vascularization, limited culture time, the appearance of up to 20% off-target cells, the lack of certain kidney cell types, the small dimensions compared to adult kidneys, and low reproducibility and maturity.[24,37-39] Clearly, the culture environment is still non-physiological on different levels (cellular composition, matrix/substrate and media complexity/growth factors). For instance, transwell-cultured kidney organoids, which is also the gold standard method for kidney explant culture, involve a stiff membrane and too high oxygen (21%) compared to developing fetal kidneys. Furthermore, the vascularization of kidney organoids and particularly the infiltration of vasculature into glomeruli, which is essential for future functionality, has not yet succeeded *in vitro*. These limitations indicate the need for improved *in vitro* cultures.

The issue of immaturity *in vitro* has had particular attention on the transcriptomic level following the introduction of single-cell RNA sequencing technology.[25,28,39-45] The gene expression profiles of iPSC–derived kidney organoids revealed that they are comparable to first trimester human fetal kidneys.[46] In general, the immaturity of stem cell–derived organoids is a well-known problem that researchers are now aiming to solve for future transplantation.[47] Along with the transcriptional immaturity, a largely neglected issue is the structural immaturity. To date, there has been no study on the structural development compared to human fetal kidneys and only selected features are shown, such as immature brush borders or podocyte foot processes[48], compared to adult kidneys. Undoubtedly, structural maturity is essential for future functionality of nephrons *in vivo* and therefore needs more attention in the future.

In vitro, stem cell–derived kidney organoids possess limited functionality. Nevertheless, organoids do express important transporters and receptors, such as organic anion transporter (OAT)1 and OAT3, megalin, and cubilin.[43,49] Fluorescein uptake into the lumen of the proximal tubule indicated OAT1- and OAT3-mediated active transport.[49] Furthermore, proximal tubules endocytosed dextran and responded to cisplatin treatment.[20,23,50] Additionally, cyclic adenosine monophosphate (AMP) stimulation resulted in the production of enzymatically active renin by a subtype of pericytes.[49] Most recently, active vitamin D metabolism was shown.[51] However, functional assays in 3D cultures are challenging and yet to be standardized to allow assessment of future upcoming culture modifications.[52]

Curiosity about post-transplantation functionality has incentivized researchers to implant iPSC–derived kidney organoids under the renal capsule of mice. Fourteen days after transplantation, nephrons in kidney organoids appeared more mature than their *in vitro*–cultured counterparts, but still less mature compared to the adult mouse kidney into which they were transplanted.[48,53] Mice developed new blood vessels that infiltrated organoid glomeruli to form structures similar to the glomerular filtration barrier.[48] After two months of implantation, the production of renin was retained.[49] Nevertheless, safety concerns are still valid given the cellular immaturity and off-target cells. Although no undifferentiated iPSCs could be found after 25 days of *in vitro* culture, pluripotency markers were still expressed in some cell populations. Once transplanted for 10 weeks, pluripotent cells were absent; however, tumors resembling Wilms' tumors and off-target cartilage populations expanded.[54] In light of these findings, it is clear that iPSC–derived kidney organoids are not yet translatable to the clinic and need to first be improved in terms of maturity and safety. Finally, the structural development of organoid nephrons, which is essential for their functionality, remains largely unstudied both *in vitro* and *in vivo* and its assessment is limited to immunofluorescence and histology. This lack of understanding has inspired the work of this thesis.

Aims and scope of this thesis

The present thesis aims to improve iPSC–derived kidney organoid culture methods by creating greater understanding of the structural human fetal kidney development and using this knowledge to find congruent and divergent features in kidney organoids. On this basis, suggestions for improvements are made.

As described in **Chapter 1**, stem cell–derived kidney organoids are a promising future treatment option for patients with end-stage kidney disease. However, many limitations need to be resolved before clinical translation is possible.

Chapter 2 and 3 create insights into human fetal kidney development that are essential to assess kidney organoid development. **Chapter 2** provides a review that aims to answer the longstanding question on the variety of renal cell types in developing and adult human kidneys, based on single-cell RNA sequencing technology. Understanding the emergence of cell types in developing human kidney supports the structural analysis of fetal kidneys performed in Chapter 3.

Chapter 3 tackles the issue that assessing ultrastructural development of kidney organoids has been hampered due to the lack of valid references. Therefore, this chapter presents an atlas of structural development of first-trimester human metanephric kidneys. Large transmission electron microscopy (EM) tile scans provide insights into the development of progenitors and various nephron segments, supported by reconstructions of volumetric EM data. Features of cell types and segments are clearly defined over the course of six weeks' development to make this chapter a reference for future work.

Chapter 4 uses the knowledge generated in Chapter 3 to assess structural kidney organoid development. Divergent and congruent features are elaborated, and given the abundance of glycogen, selected features are studied further in the context of

diabetic nephropathy. This chapter highlights that morphological assessment by EM can inform greatly on cellular functionality in organoids and argues that the organoid culture medium is hyperglycemic, leading to a variety of features known for hyperglycemic cultures and diabetic nephropathy.

Chapter 5 entails a methodological approach to overcome the known issue of the field, namely to perform whole mount immunofluorescence microscopy in high resolution. The kidney organoid model used in this thesis is one of the largest organoid models at several millimeters in size, posing a challenge for light microscopy. Therefore, this chapter presents a methodological overview of immunofluorescence staining and tissue clearing methods that were tested to enable refractive index matching and consequently high-resolution imaging.

Chapter 6 shifts focus to one specific limitation of the kidney organoid culture: the lack of vascularization. Again, inspired by human fetal kidney development, the organoid culture at standard 21% oxygen is questioned and changed to physiological 7% oxygen. The effect of this long-term hypoxic culture is investigated on VEGF-A growth factor expression and assessment of the endothelial network. This chapter uses the protocol developed in Chapter 5 to image endothelial cells in the organoids in 3D.

Chapter 7 provides a general discussion on the results described in this thesis and concludes with recommendations for future work.

Chapter 8 puts the future of kidney organoids into perspective towards clinical translation.

References

1 Wu, M. *et al.* Kidney organoids as a promising tool in nephrology. *Genes & Diseases* **9**, 585-597, doi:10.1016/j.gendis.2021.01.003 (2022).

2 Kovesdy, C. P. Epidemiology of chronic kidney disease: An update 2022. *Kidney Int Suppl (2011)* **12**, 7-11, doi:10.1016/j.kisu.2021.11.003 (2022).

3 *National Kidney Foundation*, https://www.kidney.org/atoz/content/dialysisinfo# Accessed: 14-7-2022.

4 Hart, A. *et al.* Optn/srtr 2017 annual data report: Kidney. *Am J Transplant* **19 Suppl 2**, 19-123, doi:10.1111/ajt.15274 (2019).

5 Wong, C. Y. Current advances of stem cell-based therapy for kidney diseases. *World J Stem Cells* **13**, 914-933, doi:10.4252/wjsc.v13.i7.914 (2021).

6 Dreyer, G. J. *et al.* Human leukocyte antigen selected allogeneic mesenchymal stromal cell therapy in renal transplantation: The neptune study, a phase i single-center study. *Am J Transplant* **20**, 2905-2915, doi:10.1111/ajt.15910 (2020).

7 Hickson, L. J., Eirin, A. & Lerman, L. O. Challenges and opportunities for stem cell therapy in patients with chronic kidney disease. *Kidney Int* **89**, 767-778, doi:10.1016/j.kint.2015.11.023 (2016).

8 Allison, S. J. A model of pig-to-human kidney transplantation. *Nat. Rev. Nephrol.* **18**, 199-199, doi:10.1038/s41581-022-00550-7 (2022).

9 Porrett, P. M. *et al.* First clinical-grade porcine kidney xenotransplant using a human decedent model. *Am. J. Transplant.* **22**, 1037-1053, doi:https://doi.org/10.1111/ajt.16930 (2022).

10 Simian, M. & Bissell, M. J. Organoids: A historical perspective of thinking in three dimensions. *J Cell Biol* **216**, 31-40, doi:10.1083/jcb.201610056 (2017).

11 Kim, J., Koo, B. K. & Knoblich, J. A. Human organoids: Model systems for human biology and medicine. *Nat Rev Mol Cell Biol* **21**, 571-584, doi:10.1038/s41580-020-0259-3 (2020).

12 Khoshdel Rad, N., Aghdami, N. & Moghadasali, R. Cellular and molecular mechanisms of kidney development: From the embryo to the kidney organoid. *Front. Cell Dev. Biol.* **8**, doi:10.3389/fcell.2020.00183 (2020).

13 Kaushik, G., Ponnusamy, M. P. & Batra, S. K. Concise review: Current status of three-dimensional organoids as preclinical models. *Stem Cells* **36**, 1329-1340, doi:10.1002/stem.2852 (2018).

14 Bruce, S. J. *et al.* In vitro differentiation of murine embryonic stem cells toward a renal lineage. *Differentiation* **75**, 337-349, doi:10.1111/j.1432-0436.2006.00149.x (2007).

15 Narayanan, K. *et al.* Human embryonic stem cells differentiate into functional renal proximal tubular-like cells. *Kidney Int* **83**, 593-603, doi:10.1038/ki.2012.442 (2013).

16 Song, B. *et al.* The directed differentiation of human ips cells into kidney podocytes. *PloS one* **7**, e46453, doi:10.1371/journal.pone.0046453 (2012).

17 Takasato, M. *et al.* Directing human embryonic stem cell differentiation towards a renal lineage generates a self-organizing kidney. *Nat Cell Biol* **16**, 118-126, doi:10.1038/ncb2894 (2014).

18 Taguchi, A. *et al.* Redefining the in vivo origin of metanephric nephron progenitors enables generation of complex kidney structures from pluripotent stem cells. *Cell Stem Cell* **14**, 53-67, doi:10.1016/j.stem.2013.11.010 (2014).

19 Morizane, R. *et al.* Nephron organoids derived from human pluripotent stem cells model kidney development and injury. *Nat Biotechnol* **33**, 1193-1200, doi:10.1038/nbt.3392 (2015).

20 Takasato, M. *et al.* Kidney organoids from human ips cells contain multiple lineages and model human nephrogenesis. *Nature* **526**, 564-568, doi:10.1038/nature15695 (2015).

21 Zeng, Z. *et al.* Generation of patterned kidney organoids that recapitulate the adult kidney collecting duct system from expandable ureteric bud progenitors. *Nat Commun* **12**, 3641, doi:10.1038/s41467-021-23911-5 (2021).

22 Schutgens, F. *et al.* Tubuloids derived from human adult kidney and urine for personalized disease modeling. *Nat Biotechnol* **37**, 303-313, doi:10.1038/s41587-019-0048-8 (2019).

23 Freedman, B. S. *et al.* Modelling kidney disease with crispr-mutant kidney organoids derived from human pluripotent epiblast spheroids. *Nat Commun* **6**, 8715, doi:10.1038/ncomms9715 (2015).

24 Geuens, T. *et al.* Thiol-ene cross-linked alginate hydrogel encapsulation modulates the extracellular matrix of kidney organoids by reducing abnormal type 1a1 collagen deposition. *Biomaterials* **275**, 120976, doi:10.1016/j.biomaterials.2021.120976 (2021).

25 Kumar, S. V. *et al.* Kidney micro-organoids in suspension culture as a scalable source of human pluripotent stem cell-derived kidney cells. *Development* **146**, doi:10.1242/dev.172361 (2019).

26 Przepiorski, A. *et al.* A simple bioreactor-based method to generate kidney organoids from pluripotent stem cells. *Stem cell reports* **11**, 470-484, doi:10.1016/j.stemcr.2018.06.018 (2018).

27 Homan, K. A. *et al.* Flow-enhanced vascularization and maturation of kidney organoids in vitro. *Nature methods* **16**, 255-262, doi:10.1038/s41592-019-0325-y (2019).

28 Lawlor, K. T. *et al.* Cellular extrusion bioprinting improves kidney organoid reproducibility and conformation. *Nat Mater* **20**, 260-271, doi:10.1038/s41563-020-00853-9 (2021).

29 Takebe, T. *et al.* Vascularized and complex organ buds from diverse tissues via mesenchymal cell-driven condensation. *Cell Stem Cell* **16**, 556-565, doi:10.1016/j.stem.2015.03.004 (2015).

30 Xinaris, C. *et al.* In vivo maturation of functional renal organoids formed from embryonic cell suspensions. *J Am Soc Nephrol* **23**, 1857-1868, doi:10.1681/asn.2012050505 (2012).

31 Zahmatkesh, E. *et al.* Evolution of organoid technology: Lessons learnt in co-culture systems from developmental biology. *Dev. Biol.* **475**, 37-53, doi:https://doi.org/10.1016/j.ydbio.2021.03.001 (2021).

32 Menéndez, A. B.-C. *et al.* Creating a kidney organoid-vasculature interaction model using a novel organ-on-chip system. *Sci. Rep.* **12**, 20699, doi:10.1038/s41598-022-24945-5 (2022).

33 Khoshdel-Rad, N. *et al.* Promoting maturation of human pluripotent stem cell-derived renal microtissue by incorporation of endothelial and mesenchymal cells. *Stem Cells Dev* **30**, 428-440, doi:10.1089/scd.2020.0189 (2021).

34 Taguchi, A. & Nishinakamura, R. Higher-order kidney organogenesis from pluripotent stem cells. *Cell Stem Cell* **21**, 730-746 e736, doi:10.1016/j.stem.2017.10.011 (2017).

35 Xinaris, C. *et al.* Functional human podocytes generated in organoids from amniotic fluid stem cells. *J. Am. Soc. Nephrol.* **27**, 1400-1411, doi:10.1681/asn.2015030316 (2016).

36 Pleniceanu, O., Harari-Steinberg, O. & Dekel, B. Concise review: Kidney stem/progenitor cells: Differentiate, sort out, or reprogram? *Stem Cells* **28**, 1649-1660, doi:10.1002/stem.486 (2010).

37 Nishinakamura, R. Human kidney organoids: Progress and remaining challenges. *Nat. Rev. Nephrol.* **15**, 613-624, doi:10.1038/s41581-019-0176-x (2019).

38 Takasato, M. & Wymeersch, F. J. Challenges to future regenerative applications using kidney organoids. *Curr. Opin. Biomed.* **13**, 144-151, doi:https://doi.org/10.1016/j.cobme.2020.03.003 (2020).

39 Phipson, B. *et al.* Evaluation of variability in human kidney organoids. *Nature methods* **16**, 79-87, doi:10.1038/s41592-018-0253-2 (2019).

40 Subramanian, A. *et al.* Single cell census of human kidney organoids shows reproducibility and diminished off-target cells after transplantation. *Nat. Commun.* **10**, 5462, doi:10.1038/s41467-019-13382-0 (2019).

41 Hale, L. J. *et al.* 3d organoid-derived human glomeruli for personalised podocyte disease modelling and drug screening. *Nat. Commun.* **9**, 5167, doi:10.1038/s41467-018-07594-z (2018).

42 Combes, A. N., Zappia, L., Er, P. X., Oshlack, A. & Little, M. H. Single-cell analysis reveals congruence between kidney organoids and human fetal kidney. *Genome Med* **11**, 3, doi:10.1186/s13073-019-0615-0 (2019).

43 Czerniecki, S. M. *et al.* High-throughput screening enhances kidney organoid differentiation from human pluripotent stem cells and enables automated multidimensional phenotyping. *Cell Stem Cell* **22**, 929-940.e924, doi:10.1016/j.stem.2018.04.022 (2018).

44 Wu, H. & Humphreys, B. D. Single cell sequencing and kidney organoids generated from pluripotent stem cells. *Clin J Am Soc Nephrol* **15**, 550-556, doi:10.2215/cjn.07470619 (2020).

45 Little, M. H. & Combes, A. N. Kidney organoids: Accurate models or fortunate accidents. *Genes & development* **33**, 1319-1345, doi:10.1101/gad.329573.119 (2019).

46 Morizane, R. & Bonventre, J. V. Kidney organoids: A translational journey. *Trends in molecular medicine* **23**, 246-263, doi:10.1016/j.molmed.2017.01.001 (2017).

47 Hofer, M. & Lutolf, M. P. Engineering organoids. *Nat Rev Mater* **6**, 402-420, doi:10.1038/s41578-021-00279-y (2021).

48 van den Berg, C. W. *et al.* Renal subcapsular transplantation of psc-derived kidney organoids induces neo-vasculogenesis and significant glomerular and tubular maturation in vivo. *Stem cell reports* **10**, 751-765, doi:10.1016/j.stemcr.2018.01.041 (2018).

49 Shankar, A. S. *et al.* Human kidney organoids produce functional renin. *Kidney Int.* **99**, 134-147, doi:10.1016/j.kint.2020.08.008 (2021).

50 Low, J. H. *et al.* Generation of human psc-derived kidney organoids with patterned nephron segments and a de novo vascular network. *Cell Stem Cell* **25**, 373-387.e379, doi:https://doi.org/10.1016/j.stem.2019.06.009 (2019).

51 Shankar, A. S. *et al.* Vitamin d metabolism in human kidney organoids. *Nephrol. Dial. Transplant.* **37**, 190-193, doi:10.1093/ndt/gfab264 (2022).

52 Freedman, B. S. Physiology assays in human kidney organoids. *Am. J. Physiol. Renal Physiol.* **322**, F625-F638, doi:10.1152/ajprenal.00400.2021 (2022).

53 Nam, S. A. *et al.* Graft immaturity and safety concerns in transplanted human kidney organoids. *Exp Mol Med* **51**, 1-13, doi:10.1038/s12276-019-0336-x (2019).

54 Shankar, A. S. *et al.* Kidney organoids are capable of forming tumors, but not teratomas. *Stem Cells* **40**, 577-591, doi:10.1093/stmcls/sxac009 (2022).

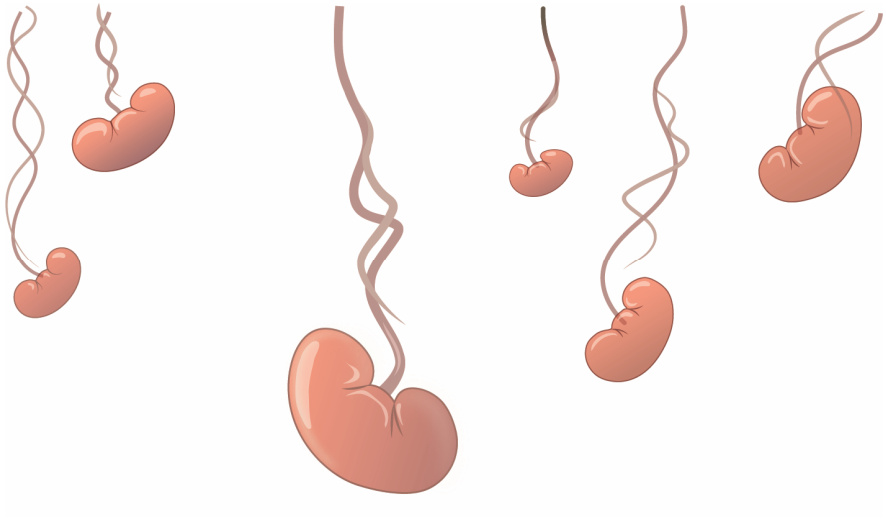

Chapter 2

Defining the variety of cell types in developing and adult human kidneys by single-cell RNA sequencing

A. Schumacher[1], M.B. Rookmaaker[2], J.A. Joles[2], R. Kramann[3,4] ,T.Q. Nguyen[5], M. van Griensven[1], V.L.S. LaPointe[1]

This chapter has been published as:

Schumacher, A., Rookmaaker, M.B., Joles, J.A. et al. Defining the variety of cell types in developing and adult human kidneys by single-cell RNA sequencing. npj Regen Med 6, 45 (2021). https://doi.org/10.1038/s41536-021-00156-w

Abstract

The kidney is among the most complex organs in terms of the variety of cell types. The cellular complexity of human kidneys is not fully unraveled and this challenge is further complicated by the existence of multiple progenitor pools and differentiation pathways. Researchers disagree on the variety of renal cell types due to a lack of research providing a comprehensive picture and the challenge to translate findings between species. To find an answer to the number of human renal cell types, we discuss research that used single-cell RNA sequencing on developing and adult human kidney tissue and compare these findings to literature of the pre-single-cell RNA sequencing era. We find that these publications show major steps towards the discovery of novel cell types and intermediate cell stages as well as complex molecular signatures and lineage pathways throughout development. The variety of cell types remains variable in the single-cell literature, which is due to limitations of the technique. Nevertheless, our analysis approaches an accumulated number of 41 identified cell populations of renal lineage and 32 of non-renal lineage in the adult kidney, and there is certainly much more to discover. There is still a need for a consensus on a variety of definitions and standards in single-cell RNA sequencing research, such as the definition of what is a cell type. Nevertheless, this early-stage research already proves to be of significant impact for both clinical and regenerative medicine, and shows potential to enhance the generation of sophisticated *in vitro* kidney tissue.

Introduction

The need for well-characterized renal cell types

A detailed understanding of the variety of cell types within the healthy kidney and their molecular composition will benefit scientists aiming to treat patients with kidney failure. The ideal treatment is kidney transplantation from a healthy immune-matching donor. However, donor kidney availability is far from meeting its demand, and waiting times are long so that many patients die while waiting for transplantation. There is great demand for new therapies, as current treatment methods, such as dialysis, do not provide all essential functionalities of a kidney and are not long-term solutions.[1] For example, toxins are insufficiently removed and the sodium and fluid homeostasis are distorted by intermittent treatment, while the metabolic and endocrine functions are completely neglected.[2,3] Dialysis can replace many functions of the kidney but is associated with high morbidity, mortality, reduced quality of life and high costs. Currently, the prevalence of patients with chronic kidney disease is as high as 9.1% with an age-dependent mortality rate of 1.5–6.3%.[4] Recent projections indicate that by 2030, nearly 5.5 million people worldwide could depend on renal replacement therapy.[5]

Due to the aforementioned shortcomings, clinicians and scientists aim to understand hurdles such as kidney development and regeneration, factors involved in kidney failure and disease, how to improve survival on dialysis and prevent donor tissue rejection. Furthermore, joint forces of (tissue) engineers, material scientists and (developmental) biologists are working worldwide on artificial and bioengineered kidneys as a replacement for current dialyses. They have made major advances in the de- and re-cellularization of rodent and human kidneys[3], renal tubule assist devices[6], lightweight miniaturized kidneys[7], and implantable bioartificial devices[7] and tissues,[8] among others. All these approaches would benefit from a greater understanding of the cellular and molecular composition of developing and adult kidney.

Creating kidneys *in vitro* is, however, a challenging task that involves the coordination of complex cellular and molecular events.[9] Starting in 2014, major breakthroughs were published on the creation of miniaturized self-assembled

kidney tissue (organoids) *in vitro* from induced pluripotent stem cells.[10-12] These organoids contain various renal cell types, patterned similarly to *in vivo* tissue. Nevertheless, they are incomplete and essential questions remain, such as: if the developmental lineage steps are being followed, why do some cell types emerge (e.g. podocytes and endothelial cells) while others do not (e.g. mesangial cells and parietal epithelial cells), why does the tissue deteriorate after a few weeks in culture, and why does it not mature beyond the first trimester[13,14], unless transplanted *in vivo*.[15] Finally, how can we achieve and maintain a complex 3D architecture of a nephron, tubulo-interstitium and vasculature? In order to answer such questions and to develop more mature tissues for transplantation, there is greater understanding needed of the large variety of renal cell types, their plasticity, lineage, cell state, phenotype switching, and functionality.

Divergent numbers of renal cell types

Outstanding research has been conducted in the past decades to unravel mammalian kidney development and nephrogenesis and to characterize adult kidneys.[16-21] However, the extraordinary developmental complexity has made scientists across fields struggle to determine the number of renal cell types and to replicate these cell types in vitro. Heterogeneity is a regular term appearing in these publications, being a clear indication of one of the major difficulties in kidney research. So far, the field generally agrees on certain heterogeneity between individuals such as the timing of kidney development (e.g. cessation of nephrogenesis from 32 weeks[22] to 37 weeks[23] of gestation), numbers of nephrons (210,000–1,825,000 nephrons per kidney with an average of 600,000–800,000[24,25]), cell numbers per segment (e.g. 431–746 podocytes per adult glomerulus[26]) and anatomical differences (e.g. number of renal papillae[27]). However, there is still little consensus on the number or range of distinct renal cell types; neither in humans nor in rodents.

More than 18 to 26 cell types have been described in mammalian mature kidneys[21,28-36] of which at least half are epithelial and/or located within nephrons.[37] While the source of these numbers is challenging to trace, possible reasons for the range can include the unclear definition of what is a distinct cell type, incomplete knowledge

of cell specific markers, technical limitations, a certain degree of variability in healthy subjects, and the difficulty of defining cell identities and distinguishing cell types. Additionally, inter-species differences could underlie these ranges, as often no species is mentioned apart from "mammalian kidneys." Clearly, part of the challenge is a lack of consensus on the definition of what constitutes a distinct cell type and the resolution of cell specific characteristics before we can elucidate the renal cellular complexity in humans in a comprehensive way.

Defining cell identity, plasticity and maturity

It remains questionable if it is possible to state a specific number of renal cell types and which techniques would lend the most appropriate data to do so. A specific cell number would imply a clear-cut definition of what is considered a distinct cell type. While researchers try to define cellular plasticity[38], this central, measurable definition of "cell type" has not yet been determined. Earlier, an evolutionary perspective was suggested, which states that a cell type can be defined by a core regulatory complex (CoRC), which is a set of transcription factors and their interacting factors.[39] In a recent publication, Morris [40] proposes a more complex viewpoint made of three major components: 1) phenotype and function (physical, molecular and functional features), 2) lineage, and 3) state (changes in cell state in response to stimuli). The general idea is that cell types cannot be clearly identified by solely assessing only one of the three components.

Many existing techniques for cell type detection and characterization have technical limitations. Initially histological stains were used, followed by techniques like immunostaining, (fluorescent) *in situ* hybridization (FISH) and flow cytometry. However, these techniques are biased by the existing knowledge of cellular markers, are by definition not designed to discover larger scales of novel markers, and are limited in the number of markers that can be simultaneously analyzed. This makes it technically impossible to assess a single cell on all three components of cellular identity. More recently, bulk RNA sequencing allowed the exploration of novel markers by providing average gene expression across a large population of cells.[41-43] However, the expression of low abundance genes is underrepresented in bulk

sequencing and cellular lineage cannot be determined.[41,44] Now, in the era of single-cell RNA (scRNA) sequencing, lineages can be determined and rare gene detection is possible. The heterogeneity within cell populations can be detected in high throughput,[41,42] as can the profiling of cell states and transitions during differentiation.[41,45-47] Therefore, while not free of limitations, scRNA sequencing is a promising technique to answer the long-standing question of the number of renal cell types.

This review aims to investigate the variety of renal cell types in the developing and adult human kidney by discussing common and conflicting findings of scRNA sequencing studies. Given our focus on regenerative medicine and tissue engineering, we excluded publications on renal pathology and drug testing. Briefly, the review first addresses the major stages of nephrogenesis to discuss the cellular lineages within these stages, which are important for researchers aiming to replicate development *in vitro*. Subsequently, findings on cellular variety of adult kidneys will be discussed. The discovery of novel cell types and markers, subpopulations, intermediate cell states, segment transitions, as well as phenotype-specific expression patterns and developmental trajectories will be covered. Finally, shortcomings and opportunities of scRNA sequencing will be discussed in the context of kidney research.

Main analysis

Structural development of the human metanephric kidney

Here we highlight the major stages of development, knowledge needed for the remainder of this review. Development of the human metanephric kidney begins around four weeks of gestation[17] from a close interaction of the metanephric mesenchyme (MM) and the ureteric bud (UB) (Figure 1). While both MM and UB derive from the intermediate mesoderm, it is in the MM where nephron progenitor cells (NPCs) differentiate into nephron tubules, the glomerulus and the renal stroma; whereas the UB gives rise to the collecting duct and ureter.[18] Simultaneous to the mesenchyme differentiation, UB differentiation and proliferation occur on the tip of the UB and lead to branching (bifurcation) into a tree-like pattern with later extensive elongation of the ureteric trunk.[48,49] The MM undergoes morphological changes during differentiation characterized as pretubular aggregate (PTA), renal vesicle (RV), comma-shaped bodies (CSB), and subsequently S-shaped bodies (SSB) before entering the capillary loop stage (CLS).[16,50,51] The first SSB is detected around Carnegie stage (CS) 18–19,[17] from which further differentiation occurs.

Cells of the distal nephron segment start invading the collecting duct epithelium at the SSB stage to connect the nephron to the collecting duct.[52] Subsequently, endothelial cells start to invade the proximal segment of the SSB, initiating the CLS. This stage is further characterized by the development of the vascular system, including the glomerular capillaries, arteries, veins, and the appearance of the primitive loop of Henle (LoH).[53] The first generation of glomeruli appears to be mature around week 9[54] and shortly after, glomerular filtration begins.[55] Eventually, 8–12 generations of glomeruli are formed, leading to nephrons in different developmental stages. Nephrogenesis ceases before birth, by week 38–41.[23]

Nephrogenesis is further supported by the surrounding interstitium and extracellular matrix.[56] The term interstitium describes a tissue with a variety of cell types such as renal fibroblasts, pericytes, and cells with endocrine functionalities (renin- and erythropoietin-producing cells), with possible distinct origins.[57] Although the discussion of the origin of renal interstitium is ongoing, one

perspective is that it emerges early in nephrogenesis from a FOXD1+ subpopulation of the MM.[57,58]

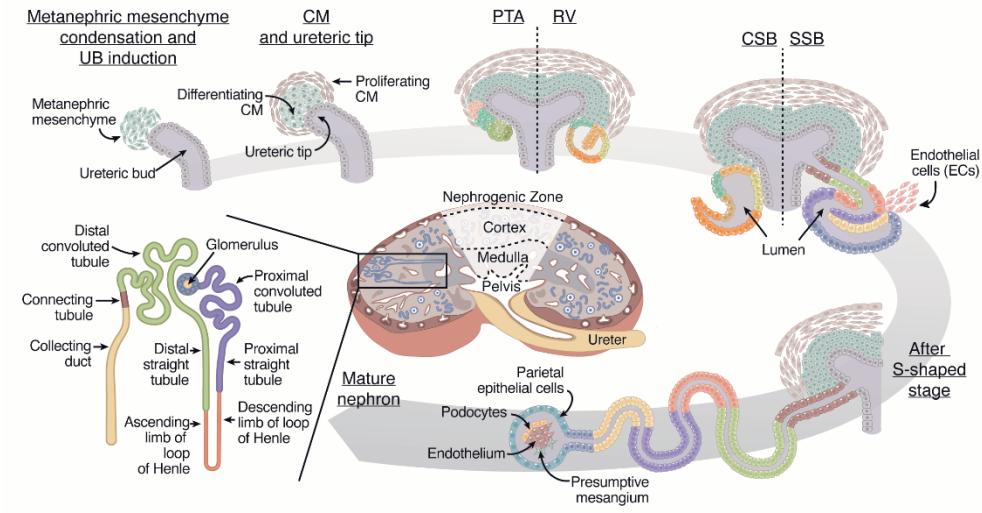

Figure 1: Schematic representation of nephrogenesis, starting with the interaction of the cap mesenchyme (CM) and ureteric bud (UB) in the nephrogenic zone. Differentiation takes place along morphologically determined stages known as pretubular aggregate (PTA), comma-shaped body (CSB), renal vesicle (RV), S-shaped body (SSB) and capillary loop stage (CLS) nephron. The mature nephron is located throughout the cortex, whereas the Loop of Henle and collecting duct extend into the medulla.

Renal cell type discoveries by single-cell RNA sequencing

Hereinafter, we highlight discoveries from scRNA studies on fetal and adult human renal tissue and contrast the findings with earlier literature using techniques like histology, immunostaining and FISH. We aim to elucidate the divergent numbers of clusters/cell types of the different scRNA and single nucleus RNA sequencing studies performed on human renal tissue to date, as summarized in Table 1 and Supplementary Table 2, and abbreviated as "scRNA sequencing papers" throughout this publication. Given the comprehensive topic, we decided to focus on kidney cells derived from the same intermediate mesoderm progenitor (excluding interstitial

cells) and summarize all findings in an updated lineage tree in Figure 2. Consequently, the discussion of the variety of immune cells, vascular and blood cells present in developing and adult kidney goes beyond the scope of this review; however, all findings of these cell types are summarized in Figure 3 and Supplementary Table 1.

Table 1: Donor information and detected cell clusters from single-cell RNA sequencing studies of healthy human kidney tissue.

Publication	**Donor age (Fetal in weeks; Adult in years)**		**Tissue source**	**Number of clusters**	**Number of clusters of metanephric mesenchyme lineage**
Young, et al. [59]	Fetal	8,9	Whole kidneys	7	6
Menon, et al. [60]	Fetal	12.4, 15, 15.7, 16.4, 18.8	Whole kidneys	11	18
Lindstrom, et al. [61]	Fetal	16	Nephrogenic zone	12/ 15	10
Wang, et al. [62]	Embryonic/ fetal	7–10, 13, 19, 22, 24, 25	Whole kidneys	13	10
Combes, et al. [63]	Fetal	16	Nephrogenic zone	16	13
Lindström, et al. [64] (preprint)	Fetal	14–17	Nephrogenic zone	18	18
Stewart, et al. [65]	Fetal	7 (F), 8 (M), 9 (F), 12 (M), 13 (F), 16 (F)	Whole kidneys	21	11
Tran, et al. [66]	Fetal	15, 17	Inner and outer cortex sections	21	18
Hochane, et al. [67]	Fetal	9 (M), 11 (M), 13 (F), 15 (F), 16 (M), 18 (F)	Whole kidneys	22	19
Lindstrom, et al. [68]	Fetal	17	Nephrogenic zone	22	15

Liao, et al. [69]	Adult	57–65 (2x M+1x F)	Whole kidney sections	10	8
Wu, et al. [70]	Adult	70 (M)	Biopsy	16	6
Wu, et al. [71]	Adult	62 (M)	Cortex	17	7
Young, et al. [59]	Adult	72	Interface or region-specific biopsies	19	10
Stewart, et al. [65]	Adult	44–72 (M+F)	Cortex, medulla, pelvis biopsy	25	12
Sivakamasundari, et al. [72] (preprint)	Adult	62–66 (M+F)	Resection samples	27	11
Kuppe, et al. [73]	Adult	50–84	Healthy tumor nephrectomy tissue	27	23
Lake, et al. [74]	Adult	>50 (M+F)	Cortex and medulla	30	19

* Biological sex (M=male/F=female) is indicated when known. A more detailed table can be found in the supplementary files (Supplementary Table 2).

Pseudo-time trajectory follows developmental flow

Pseudo-time analysis is a computational method to establish a dynamic process experienced by cells and arranges these cells based on their progression through this process. Pseudo-time trajectory analyses suggested that the identified kidney cells generally seem to follow the known developmental stages from NPCs, CSB and SSB to mature, differentiated cell types.[67] Interestingly, this analysis did not describe CLS as a separate stage during differentiation. The identified literature on fetal kidney (Table 1) agreed that podocytes emerge first from the SSB nephron progenitors, followed by proximal and distal tubules, and finally LoH. This confirms earlier knowledge on the timing of nephron patterning[75], where proximal, distal segments, and podocytes followed distinct lineages, and the distal tubule further differentiated into LoH and the connecting tubule (CNT). To our knowledge, the early podocyte emergence has, however, not been described before the scRNA sequencing era.

Additionally, Menon, et al. [60] distinguished the UB, stroma and nephron as three distinct developmental trajectories. Although podocytes in the same study had strong stress-related signaling, possibly a consequence of their dissociation, pseudo-time indicated an extraordinarily complex differentiation trajectory.[67] Needless to say, more studies are needed to confirm these findings to exclude interindividual differences and dissociation biases. Future research could consider reducing dissociation artifacts by, for instance, the addition of cold-active proteases.[76]

The balance of self-renewal and differentiation in early kidney development

The cap mesenchyme (CM) is considered the renal stem cell niche from which, in interaction with the ureteric epithelium, the mammalian kidney develops. Throughout development, the CM is maintained to repeatedly supply NPCs to undergo mesenchymal-to-epithelial transition (MET) and form the epithelial RV.[77] The number of different cell types at this stage has not yet been elucidated and scRNA sequencing research reveals that this will be a challenging task.

CM and NPCs populations were detected to various extents in the scRNA sequencing publications, with most papers describing one or the other, but not both populations (Supplementary Table 1). This could be explained by the different fetal ages. Studies of week 15–17 fetuses[61,66,68] might be less likely to detect CM clusters, since the CM population decreased with further differentiation and the markers are less likely to be detected compared to analyses at week 7–10.[59,62] However, differences can also be attributed to the process of assigning markers differently to certain populations as well as the definition of CM and NPC. The clear differences in markers used to identify both CM and NPC in the various publications indicate the challenge of distinguishing cell populations in early development (Supplementary Table 3). Clearly, both a consensus on the main population markers as well as terminology is required in order to ensure comparability of this complex research and provide a common ground for future studies.

Irrespective of the definition of CM and NPC, both differentiating and pluripotent populations were detected. For instance, Wang, et al. [62] distinguished two transcriptionally distinct populations, which are in line with earlier mouse[18,78-81] and

human studies[82] investigating the role of *SIX2* and *MUC1* expression in the progenitor pool, respectively. One such population expressed markers *SIX2*, *EYA1* and *COL1A1*, which are involved in the induction of CM and associated with the self-renewal capacity of stem cells indicated by high *HMGA1* and *HMGA2* expression.[62] Pseudo-time analysis suggested the self-renewing population sustained its proliferative capacity throughout nephrogenesis.[62] The second population was identified as gradually going through MET and expressing epithelial markers like *CLDN11* as well as *NPHS2*, indicating the onset of podocyte differentiation. The fact that Hochane, et al. [67] detected a self-renewing cluster clustered as NPCs could also indicate a gradual differentiation from CM to NPCs.

In terms of novel markers of the CM, Hochane, et al. [67] described *UNCX* as a novel marker for the *CITED1*$^{+}$ self-renewing population after validating their transcriptomic data with immunostainings. Although UNCX was found in early mouse studies[83-85] where it was described as a transcription factor involved in distal RV differentiation that disappears around E17.5, this seems to be the first study showing UNCX gene and protein expression in human tissue. Future studies might consider investigating its role by analyzing spatiotemporal expression along with common CM markers in human tissue. In summary, various scRNA sequencing studies in renal development support the presence of a self-renewing and differentiating population within the CM, while distinct NPC populations seem yet to emerge, and determination of specific cell types is challenging.

Segmentation and differentiation in early stages of developing nephrons

As development continues, the relative expression of CM genes decreases sharply after approximately week 10 with further cellular differentiation of NPCs and morphological organization into PTAs (Figure 1). At this stage in mice, PTAs are already well known to be segmented into proximal and distal segments.[86] Three-dimensional imaging of the developing human kidney revealed that NPCs already assign to certain lineages at the onset of the PTA. SIX1^{+} NPCs segment into two layers upon recruiting, where the earliest recruited NPCs are of distal lineage and the latest are of proximal lineage. The last NPCs recruited are hypothesized to be of

parietal lineage. Spatiotemporal location of NPCs within the early developing nephron could thus have an impact on their subsequent respective lineage. The latest research from the same group confirmed three distinct populations within the PTA-expressing proximal and distal markers.[64]

Simultaneously with NPC recruitment, the connection between NPC and PTA is gradually reduced until the late renal vesicle stage when it is broken and the $SIX2^+$ CM remains on the tip of the UB.[68] In this process, the PTA undergoes MET, polarizes, forms a lumen and cadherin-mediated cell–cell contacts emerge to finally result in the RV. Earlier research shows that the RV is segmented into proximal and distal parts in mice and shows priming for podocytes, parietal epithelial cells (PECs), proximal tubules (PTs) and distal tubules (DTs).[87] Few scRNA sequencing studies of human tissue detected the RV and only one detected more than one cluster, namely five in total, which were defined by patterns of *CDH1*, *JAG1* and *WT1* expression.[64] Since the latter study sequenced the nephrogenic zone only, it is clearly a challenge to detect the RV or even distinguish populations within whole kidneys.

In the final stage of nephrogenesis, the SSB-stage, further segmentation of the nephron starts to be noticeable. Divided into proximal, medial and distal segments, each segment differentiates further into distinct epithelia.[87] Few scRNA sequencing studies identified the SSB. Like in RVs, *MAFB* expression was associated with the podocyte progenitors within the proximal segment.[67] Correlation of scRNA sequencing and immunofluorescence confirmed the presence of precursors of distal, proximal, LoH populations and renal corpuscle within the SSB.[68] In a preprint, Lindström, et al. [64] identified six distinct populations by three-dimensional spatial mapping of single-cell transcriptomes, which agreed with the previously identified populations and additionally detected parietal epithelium, CNT, and macula densa/LoH. Interestingly, a single tubular progenitor population initially exists next to podocytes and parietal epithelium. As development proceeds, this tubular population differentiates further into distal and medial domains. Congruence in gene expression with the distinct adult cell types supports the assumption that these early populations are precursors that start to express some transcription factors and genes associated with specific cell type functionality as known from mature cells.

To conclude, while the SSB is distinguished by some scRNA sequencing papers, it clearly remains challenging to distinguish PTAs, RVs and CSBs. Identification by morphology and correlation to their respective transcriptome was done to overcome this challenge. This is an ideal example of the difficulty of distinguishing cells with subtle differences in the transcriptome following a gradual differentiation during development. However, the preprint of Lindström, et al. [64] indicates that better molecular and temporal resolution could be achieved by spatially mapping transcriptomes. Alternatively, pseudo-depth analysis could be applied. Furthermore, in combination with markers for the G2/M phase of mitosis, a distinction might be made between RV and CSB based on an assumption of reduced proliferation after the RV stage.[67] By fine-tuning the *in vitro* replication of kidney development based on such data, more diverse cell types could be generated according to natural lineage trajectories.

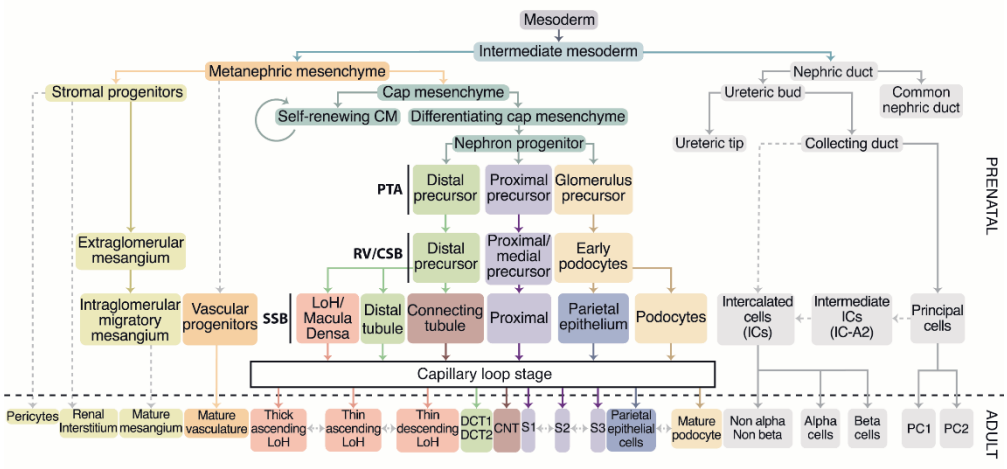

Figure 2: Lineage tree of renal cell types in development based on non-scRNA sequencing and scRNA sequencing literature. Dotted arrows indicate possible lineage relationships, which are not fully proven or not highlighted in the discussed scRNA sequencing publications. Pretubular aggregate (PTA), renal vesicle (RV), comma-shaped body (CSB), S-shaped body (SSB), Loop of Henle (LoH), connecting tubule (CNT), distal convoluted tubule 1 and 2 (DCT1/2), segment 1/2/3 (S1/S2/S3), intercalated cells (ICs), principal cells (PCs).

Mesangial cells in development and adulthood

The stromal population comprises a diverse cellular composition. Functionally, it guides nephrogenesis and provides essential signaling around mature nephrons. However, the diversity and functionality of stromal cells is not fully unraveled. Interstitial cells (ICs), mesangial cells (MCs), juxtaglomerular cells, fibroblasts, pericytes, and smooth muscle cells belong to the stromal populations, and all derive from a common FOXD1$^+$ precursor.[88] Mesangial cells, nowadays considered a special type of pericyte, are located within the glomerulus in direct contact with glomerular endothelial cells, while extra-glomerular endothelial cells are located at the stalk.[89,90] Less than half of the discussed scRNA sequencing publications detected a mesangial cluster, of which just one discriminated intra- and extraglomerular mesangium.[62] This is because the molecular signature of e-MCs is not yet well defined and distinguishing them from intraglomerular mesangial cells (i-MCs) is only possible by analyzing the microanatomy. This correlation of two techniques has led to interesting results.

Single-cell RNA sequencing revealed that e-MCs had higher proliferative potential, whereas i-MCs were more mature. Interestingly, until week 10, the expression of the mesenchymal cell marker *PDGFRb* and endothelial cell marker *CD31* were restricted to the stromal compartment and later migrated into the glomeruli.[62] This migratory phenomenon has been described in rat development[91] and aligns with the investigations of Menon, et al. [60] who presented the expression of *TAGL* in migratory mesangial cells. The molecular distinction of i-MCs and e-MCs was resolved via the co-expression of *PDGFRb* and *LAM4A* of i-MCs. Furthermore, *PIEZO2*, a gene encoding a stretch-gated ion channel, was identified in i-MCs of adult human kidneys. Stretch-gated ion channels in MCs were already described in 1989[92], but the research is very limited and *PIEZO2* has not been described earlier in this context.

While it is beyond the scope of this review to discuss all stromal cell types in detail and few papers resolved a variety of stromal populations, we would like to highlight recent scRNA sequencing publications investigating the interstitial heterogeneity in both rodent[93] and human kidneys[73,94]. A brief comparison with human datasets confirmed conservation of this heterogeneity. Given the important role these cells

play in extracellular matrix deposition and endocrine signaling, we hope that future research will continue in depth characterization.

Development and maturation of glomerular cells

Pseudo-time trajectories suggest that podocytes are the first differentiated cell type to emerge and mature along a complex genetic trajectory.[60] Remarkably, 228 genes are involved only for podocytes to develop from SSB podocytes to mature podocytes.[60,67] Comparing different gestational weeks showed that podocytes emerge around week 9 of human development.[65] The podocyte-specific markers *MAFB* and *TCF21* are first detected in renal vesicles overlapping with *SIX2* and *TMEM100*.[66] Accordingly, nephron progenitor markers *SIX2*, *EYA1* and *MEOX1* are downregulated over time and diminish with the onset of early podocyte markers *MAFB* and *TCF21*.[66,68] The developmental trajectory becomes increasingly complex as it continues from this point.

Four studies independently provided evidence for a transitional, immature podocyte population.[60,63,66,67] A small subpopulation of cells, located in the visceral part of the proximal segment of the SSB, follows the podocyte trajectory while expressing a distinct set of markers in the SSB phase until the capillary loop phase.[67] While not all studies agree on all markers of either immature or mature podocytes (Table 2), there is a general consensus that the transitional, immature podocytes express *OLFM3*, and do not express well-known mature podocyte markers such as *NPHS1*, *NPHS2* and *PTPRO*. Within each of these independent studies, the evidence confirms these findings as additional techniques such as single molecule FISH and immunofluorescent labeling delivered supporting information.[66-68] The marker heterogeneity between the studies of this transient population could be due to age differences of the individuals, technical differences, and the spatial heterogeneity caused by the gradually increasing maturity towards the medulla. However, all except one study detected *OLFM3* expression, confirming that the different studies found the same transitional podocyte cluster.

Within the immature podocyte cluster, *OLFM3* was most highly expressed compared to other genes, but diminished towards the CLS with the onset of mature

podocyte markers. Proliferation markers had low expression, which is expected for podocytes.[67,95] To date, no other publication has shown either *OLFM3* expression or a transitional podocyte population in human kidneys. The only transitional cell type related to podocytes was described as CD133$^+$/CD24$^+$ progenitors, which are located at the urinary pole within the Bowman's capsule and the proximal tubule and have been attributed to possess progenitor-like behavior by transdifferentiating into podocytes in case of injury.[96-98] However, this progenitor-like cell type is not to be confused with the *OLFM3*$^+$ population as the latter is a transient population in development, while the former was found to be resident in adults.

Interestingly Brunskill, et al. [99] extensively mapped the molecular signature of podocytes (144 podocyte-specific genes) in developing and adult mice and found a distinct set of podocyte-specific genes enriched in immature podocytes, with more mature markers emerging over time. These drastic gene expression changes can be associated with both the considerable morphological[100] and functional changes in podocyte development, where the immature *OLFM3*$^+$ population could represent pre-functional podocytes. Combes, et al. [63] and Tran, et al. [66] distinguished an additional maturing podocyte cluster that follows the transitional *OLFM3*$^+$ subcluster. This might indicate even more complex developmental stages. Markers related to microtubule modulation, such as *TUBA1A* and *STMN1*, were upregulated in this additional cluster, indicating the extensive morphological transformations known for podocyte development.[101] The field would benefit from more in depth studies elucidating the role of OLFM3 in the maturation of podocytes to support replication of differentiation in vitro.

Table 2: Overview of the number of clusters of podocyte progenitors and mature podocytes with their respective markers discovered using single-cell RNA sequencing of developing human kidney.

Author	Tissue age	Podocyte progenitor clusters	Markers early podocytes/ transitional cells	Podocyte clusters	Markers mature podocytes
Hochane, et al. [67]	w9, w11, w13, w16, w18	1	*OLFM3*$^+$/*MAFB*$^+$/*FOXC2*$^+$/*CLIC5*-^{LOW}/ *PTPRO*-^{LOW}, *NPHS1*-^{LOW}, *NPHS2*-^{LOW}	1	*MAFB*-^{LOW}, *NPHS2*$^+$, *PTPRO*$^+$, *PODXL*$^+$

Lindstrom, et al. [68]	w17	1	*CLDN5*$^{+}$, *OLMF3*$^{+}$	1	*TCF21*$^{+}$, *NPHS2*$^{+}$
Lindstrom, et al. [61]	w16	1	*PODXL*$^{+}$, *MAFB*$^{+}$, *NPHS2*$^{+}$	0	N/A
Menon, et al. [60]	w12.4, w15, w15.7, w16.4, w18.8	1	*OLFM3*$^{+}$/*MAFB*-^{LOW}	1	*PODXL*$^{+}$, *NPHS1*$^{+}$, *NPHS2*$^{+}$, *CLIC5*$^{+}$
Combes, et al. [63]	w16	1	ON1 CTGF+, *OLFM3*$^{+}$, *MAFB*$^{+}$, *NPHS1*$^{+}$, *LHX1*-^{LOW}, *PAX8*-^{LOW}	2	*PTPRO*$^{+}$, *SYNPO*$^{+}$, *VEGFA*$^{+}$, *WT1*$^{+}$
Tran, et al. [66]	w15, w17	1	*LHX1*+, *PAX8*$^{+}$, *FBLN2*$^{+}$, *OLFM3*$^{+}$, *PCDH9*$^{+}$, *SLC16A1*$^{+}$, *GFRA3*$^{+}$, *LEFTY1*$^{+}$	2	*PLA2R1*$^{+}$, *ARMH4*$^{+}$, *F3*$^{+}$, *SYNPO*$^{+}$, *NPHS2*$^{+}$, *MAFB*$^{+}$, *TGFBR3*$^{+}$, *COL4A3*$^{+}$, *COL4A4*$^{+}$, *TNNT2*$^{+}$, *PLCE1*$^{+}$, *ANXA1*$^{+}$
Wang, et al. [62]	w7, w8, w9, w10, w13, w19, w22, w24, w25	0	N/A	1	N/A
Stewart, et al. [65]	w7-16	0	N/A	1	*NPHS2*$^{+}$, *PTPRO*$^{+}$, *WT1*$^{+}$, *TCF21*$^{+}$, *PODXL*$^{+}$
Young, et al. [59]	w8,9	0	N/A	0	N/A
Lindström, et al. [64]	W14	1	*EFNB2*$^{+}$, *BMP4*$^{+}$, *OLFM3*$^{+}$, *MAFB*$^{+}$	1	N/A

w= weeks, N/A = information not available.

Another interesting glomerular cell type is the parietal epithelial cell. Terminally differentiated PECs are located as a monolayer on top of the Bowman's capsule and retain the capacity to proliferate. A variety of distinct PECs have been described according to the expression of different proteins, such as Pax-2 and claudin-1, but also their localization on the Bowman's capsule.[102] Additionally, PECs have frequently been a discussion point in terms of their transdifferentiation into podocytes in glomerular diseases.[96,97,102-104] Single-cell RNA sequencing research on the nephrogenic zone showed the existence of a common progenitor of PECs and podocytes until the RV stage.[64] A few weeks later in development, sequencing of the whole kidney showed distinct gene expression profiles for PECs and podocytes in a different study[60], indicating distinct maturation pathways. The potential to transdifferentiate has not been shown in the scRNA sequencing papers. We anticipate that the common progenitor is a starting point for more sophisticated research to investigate the role of PECs in injury and disease.

Surprisingly, only one of the published (single-cell) RNA sequencing papers could detect more than one PEC population, however characterization of these clusters is still needed.[73] A few other papers found a single cluster of PECs in either fetal kidney[60,66] or adult kidney[69,72] with enhanced expression of *CAV2*, *PTRF* (*CAVIN1*), *CLDN1*, *CLDN3*, *LIX1*, *CDH6* and *KRT8*, *KRT18*, *CD24*, *VCAM1* respectively. However, there was no discrimination between subpopulations, while at least two transitional cell types (in between PECs and podocytes) have been described in earlier research.[102] Therefore, future research would benefit from defining the molecular signature of PECs to unravel their complete lineage trajectory and functionalities in adulthood.

Patterning of tubular epithelial cells

From around week 12 onwards, more cell types are detectable, such as PT, LoH, CD and PE.[17,65] As previously described, PT and DT differentiate around the same stage and subsequently LoH and CNT emerge from the DT. While little information is provided on tubular maturation within the scRNA sequencing papers, interesting

findings provide insight into segment transitions and molecular signatures related to cell functions.

Generally, little is known about the molecular signature of the distinct PT segments. The proximal convoluted tubule (PCT) includes the segments S1 (early PCT) and S2 (late PCT). The proximal straight tubule (PST) is composed of the S2 (cortical PST) and S3 (medullary PST). All scRNA sequencing studies of adult kidney detected at least one PT cluster in adult tissue, of which about half found distinct populations that correlated with the different segments S1–3. However, earlier research has indicated a lack of discrete transitions in morphology in between the distinct segments and the likelihood of intermediate cell types.[105] A continuum of gene expression, as shown in similarity weighted nonnegative embedding (SWNE) analysis, confirmed the existence of such continuous transitions from PT to DCT.[74] A recent publication distinguished seven PT populations of which three expressed markers of both S1 and S2, also confirming a gradual transition.[73] This phenomenon of gradual transition could also explain why some papers resolved only a single PT population.[72]

Single-cell RNA sequencing provides more insight into both molecular anatomy and (patho)physiology. With the PT being the most abundant cell type in the kidney, 54 transcription factors were discriminated, many of which are restricted to the PT.[71] Although markers and transcription factors are identified in various studies[69,71], it is believed that differential gene expression along the PT trajectory indicates variation in metabolic processes and transport in the various segments.[74] Interestingly, next to metabolic markers, deep sampling revealed marker expressions with a role in immune defense against pathogens as well as inflammation and regeneration following kidney injury.[74]

The DCT can be distinguished from the PT by a decrease in fatty acid, glucose, amino acid and hormone metabolism.[62] Furthermore, the distal tubule, LoH and CNT are thought to derive from the same distal precursor within the SSB, which is distinct from the PT precursor.[64] Only one scRNA sequencing publication distinguished more than one DCT population[72], although previously two distinct populations have been confirmed. This might indicate a gradual transition between DCT cell types.[74] In contrast, there are indications for an abrupt transition of the thick ascending LoH

into the DCT since there was no overlap of the segment-specific markers SLC12A1 and SLC12A3.[72] Indeed the same lack of double-positive cells could be seen in the data set of, for example, Lake, et al. [74]. Morphologically an abrupt transition was already shown in rodents several decades ago.[106]

The CD consists of the cortical collecting duct (CCD) and outer medullary collecting duct (OMCD) and comprises intercalated (ICs) and principal cells (PCs).[105] Principal cells express the epithelial sodium channel (ENaC). Currently, classification of intercalated cells takes into account the expression of the chloride–bicarbonate exchanger SLC4A1, the multi-subunit H^+-ATPase and pendrin (subtype of the chloride–bicarbonate exchanger). Consequently, IC-A cells apically express H^+-ATPase, basolaterally express SLC4A1 and lack pendrin. IC-B express H^+-ATPase at their basolateral pole and non-A, non-B cells express both H^+-ATPase and pendrin at their apical membrane.

Non-A, non-B cells are, amongst others, located in the CNT[107], which, against earlier belief, develops from the distal tubule and not the CD in both humans[64] and mice[87]. The cellular complexity of the CNT could, however, only partly be resolved in the discussed papers. Only one CNT cluster has been reported throughout the studies, although the CNT is known to contain cell types with DCT2 and CD phenotypes.[74] This leads to the question of the identity of this single CNT cluster and why further clustering was or could not be shown. Future studies could include spatial information in their quest to distinguish subpopulations of the CNT and use spatial transcriptomics such as the Nanostring Whole Transcriptome Atlas (WTA) technology.

Nearly all scRNA sequencing papers of adult human kidney detected intercalated cells and most distinguished multiple populations and principal cells. Particularly, single nucleus RNA sequencing disclosed a remarkable resolution of the transitions from DCT to CD by distinguishing two PC and three IC populations. Within these transitions, IC-B, IC-A1 and PC-1 dominated within the cortex, while PC-3 and IC-A2 were highly abundant in the medulla. All IC and PC clusters expressed markers known for the collecting duct.[74] It remains to be determined if PCs and ICs located in the CNT can be distinguished on a transcriptional level. In the recent publication by Kuppe, et al. [73] a surprising eight distinct IC populations were detected in adult

kidneys. Future research could investigate if these clusters contain ICs located within the CNT. In sum, various scRNA sequencing papers succeeded in detecting more than the known cellular variety of populations within the CD, but limited populations within the CNT, which will be highly interesting to characterize further.

Interestingly, the PC marker *AQP2* was also expressed in a subpopulation of IC-A, here named IC-A2, in two independent studies of human kidney[62,74] as well as in mice[108,109], leading to the hypothesis that IC cells derive from the first emerging PC cell population with a double-positive transitional/intermediate stage (Figure 2). More characterization of the IC-A2 cell type is needed, particularly in terms of localization of SLC4A1 and H^+-ATPase, to clearly identify this cluster since earlier research did not distinguish different IC-A populations.[107] No non-A, non-B cells were detected, which were previously defined as expressing both H^+-ATPase and pendrin at their apical membrane and to be located in the CNT.[107] The detection of the additional IC subtype IC-A2 could inspire future research to investigate the lineage relationship between ICs and PCs.

All cell populations found in the discussed scRNA sequencing publications are summarized in Supplementary Table 1. Comparing the number of clusters for each cell type as described in each publication (excluding unassigned clusters such as "proliferating", "differentiating" and too general clusters such as "epithelial cells") provides insight into the cellular composition of developing and adult kidneys. Overall, 6–19 distinct cell populations of renal lineage were detected across the publications in the developing kidney and 6–33 distinct populations in the adult kidney, with a median of 14 populations in development and 13 in adult kidneys. Between 2–9 distinct non-renal populations were described, with a median of 4 in development and a range of 4–23 with a median of 7 in adult kidneys. Multiple factors could lead to these ranges including different tissue sources (biopsy, resection, whole kidney, etc.), tissue location (cortex vs medulla) or different digestion methods. Therefore, having the papers complement each other's findings by taking the sum of all different populations of all publications, likely provides a more realistic number. Thus, we counted the largest number of clusters for a specific cell types (i.e. seven PT clusters described by Kuppe, et al. [73]) and with this, the total sum was calculated. This approach helps us to provide an approximation for the

variety of cell types within human kidneys of both renal and non-renal lineage; namely in total 73 distinct populations in adult kidneys. Of this, 41 are populations of renal lineage and 32 are populations of non-renal lineage. (

Figure **2**) The fetal kidney comprised approximately 32 cell populations of renal lineage, however developing cells were likely counted repeatedly throughout the various stages of nephrogenesis. Clearly, these numbers are only an approximation of the true variety of cell types, due to the large variation in factors like tissue source, tissue age, dissociation method, terminology, and computational settings. Certain cell types, such as the large variety of stromal cells, are underrepresented in the current research and would need to be added. Furthermore, the definition of what defines a distinct cell type is yet unclear and heavily affects the number of identified cells. However, future studies with further developed protocols and novel technologies will certainly identify additional cell types, which cannot yet be resolved.

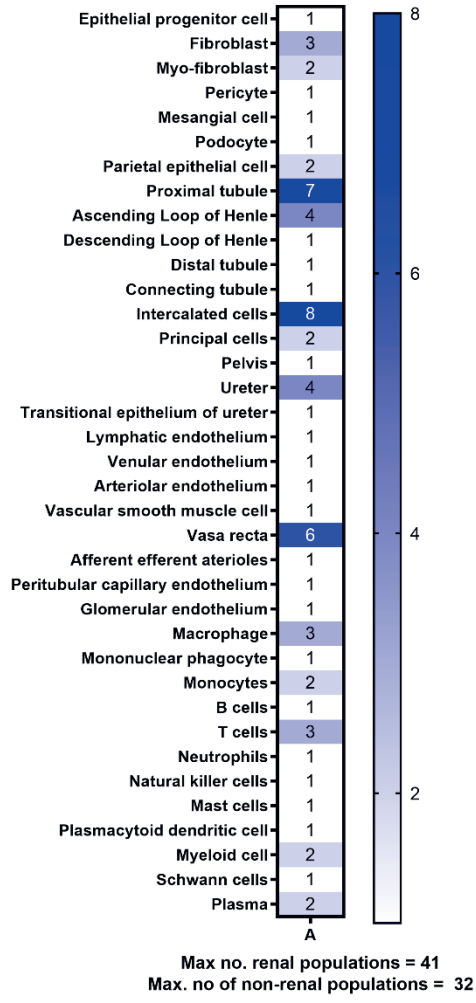

Figure 2: The variety of different renal cell populations identified by single-cell RNA sequencing to date. All cell types detected (accumulated) by all discussed scRNA sequencing publications. The number indicates the highest number of clusters distinguished by one or more of the discussed publications and with this, the total sum of populations was calculated. For the adult kidney, 41 renal and 32 non-renal populations were detected.

General discussion

In this review, we discuss new knowledge on the cellular composition of healthy developing and adult human kidneys based on scRNA sequencing studies. ScRNA sequencing has the unique potential to provide comprehensive information on the cellular and molecular complexity of various tissues. Therefore, we aimed to compare the current literature in the field to estimate the heterogeneity of kidney cell types. We conclude that scRNA sequencing is a valuable tool to detect a variety of cell types; for instance, transient cell populations such as developing podocytes and a new intercalated cell population.

However, there are also various issues with this technology such as the sparsity of the generated data. For instance, the biological sex of the studied patients was not considered in the analyses and has not been studied elsewhere on a single-cell transcriptomic level. Adding this could be of valuable impact. Differences in function, morphology and responses to injury are already known to exist between females and males in human developing and adult kidneys.[23,110,111] Recent scRNA sequencing of rodent kidneys also reveals transcriptomic differences between sexes.[112] For instance, markers of proximal tubule functionality, including organic anion, amino acid transport and drug and hormone metabolism, were differentially expressed in female and male mice. Future research could investigate conformity in humans and particularly elaborate on differences in the developmental trajectory in pseudo-time. Additionally, the variety of cell types detected with scRNA sequencing is strongly determined by factors such as computational settings, dissociation methods, tissue source, markers used to identify clusters, and patient age. Standardized reporting of factors such as gestational age would facilitate the integration of multiple datasets and allow further analysis of, for example, transcriptome development in relation to gestational age.

Certain differences of used terminologies, technical limitations and the lack of the definition of a cell type impede the data comparability and integration. Several comprehensive reviews have been published on solving technical limitations of scRNA sequencing, such as distinguishing rare transcripts from noise, dropouts and computational challenges such as user defined clustering.[42,113,114]

While many limitations are being addressed, additional techniques will be needed to confirm cellular identity besides the transcriptomic profile. These techniques could be applied to answer research questions in terms of the previously discussed three pillars of cellular identity. They could include anatomical localization of the scRNA sequencing markers by in situ hybridization, in situ sequencing and studying ligand–cell interactions[115]. Determining cellular functionality and state in response to stimuli in human tissue will primarily require explantation since cell types outside their native environment, in 2D culture, will probably lose their phenotypic characteristics. Clearly, there is still no straightforward definition of a cell type, however, a combination of the aforementioned techniques and models could make a large step towards an atlas of functional human kidney cell types.

Discrimination of early nephrogenic stages and cell type precursors using scRNA sequencing appeared to be consistently challenging throughout various studies due to the subtle molecular and spatial changes. Comparing different studies is particularly difficult, since the transcriptome significantly changes during differentiation and thus the time point of cell isolation is very important. Consequently, additional validation experiments are needed e.g. using staining of identified markers. Alternatively, differentiation paths in development could be regarded more as a continuum rather than distinct clusters.[116] For instance, podocytes would consequently not be distinguished as separate RV-, CSB-, SSB-podocytes, but as podocytes expressing gradients of transcriptomes throughout development. For this trajectory interference could be a more suitable method. As such, pseudo-time trajectory analysis has shown that podocytes differentiate prior to the differentiation of tubular cell types and that there is a distinct differentiation pathway for proximal and distal tubular segments. Finding master regulators along these differentiation pathways can support both the understanding of disease as well as *in vitro* replication of development. Additionally, more insight could be generated into much earlier development; on how the degeneration of temporary pro-and mesonephros could influence the pattering of the permanent metanephric kidney.

Sequencing cells from distinct anatomical locations, such as the nephrogenic zone as shown in various publications of Lindstrom, et al. [68], can help to achieve a higher

resolution of the early nephrogenesis. This approach might then also lead to detection of the cells of the capillary loop stage. To conclude, the scRNA sequencing studies on human kidneys to date have shown a detailed transcriptomic complexity and future research will likely discover more.

Future clinical relevance and impact on regenerative medicine

ScRNA studies have already given us unprecedented insights into renal development and disease and the technology holds the promise to answer several longstanding questions in the field of nephrology. The higher resolution of molecular mechanisms could provide more insight into complex renal diseases.[73] Cell type–specific gene expression related to chronic kidney disease, diabetes and hypertension could for instance help to identify cell-specific and disease specific targets and guide the development of urgently needed targeted therapeutics.[74] The diagnosis and treatment of various kidney diseases could be improved based on molecular data of research on pathogenic mechanisms and potential biomarker discovery.[43] ScRNA sequencing is already getting more patient oriented by the possibility to sequence a variety of kidney cells from urine.[117]

Basic research to develop kidney grafts, such as kidney organoids from induced pluripotent stem cells for future transplantation rely on data on molecular signaling pathways of developing tissue. Currently, these models often lack certain cell types and segments such as the collecting duct, mesangial cells and PECs. More information on the molecular pathways of these cell types is needed in order to reproduce these *in vitro*. ScRNA sequencing research on developing kidney can provide such data. Additionally, the transcriptome of developing kidneys and *in vitro* models can be compared as previously shown[71] to confirm the formation of the appropriate cell types, cellular maturity and timing. A more comprehensive discussion on this topic can be found in the recent review of Wu and Humphreys [118].

Conclusion

In conclusion, we extensively discussed findings of all identified scRNA sequencing publications to date of healthy human developing and adult kidneys and compared their outcome in terms of differences in cellular variety. Together, the publications detected approximately 41 distinct cell populations of renal lineage in the adult human kidney. However, to determine a definite number of cell types, a clear definition of a cell type should be determined and various limitations of the technique need to be resolved. Due to the subtle and gradual changes in transcriptome in development, we suggest that cells in developing kidneys may best be regarded as a continuum instead of distinct cell types. Detecting master regulators will then help to guide *in vitro* work along the same differentiation pathways. In the future, advanced technologies such as combined scRNA sequencing and measurement of DNA accessibility, increasing depth as well as improved analysis methods will likely improve our understanding of the variety of cell types in the adult and developing nephron. Nevertheless, the studies to date provide essential insight into the molecular signature of a large variety of cell populations in adulthood and in development and therefore enabled us to present an updated lineage tree for cell types of renal lineage. On a final note, we trust that these studies will shape the future of regenerative medicine by unraveling lineage trees at an even higher resolution and thus help in organoid and tissue engineering approaches.

References

1 van Gelder, M. K. *et al.* From portable dialysis to a bioengineered kidney. *Expert Rev Med Devices* **15**, 323-336, doi:10.1080/17434440.2018.1462697 (2018).

2 Humes, H. D., Buffington, D., Westover, A. J., Roy, S. & Fissell, W. H. The bioartificial kidney: Current status and future promise. *Pediatr Nephrol* **29**, 343-351, doi:10.1007/s00467-013-2467-y (2014).

3 Song, J. J. *et al.* Regeneration and experimental orthotopic transplantation of a bioengineered kidney. *Nat Med* **19**, 646-651, doi:10.1038/nm.3154 (2013).

4 Bikbov, B. *et al.* Global, regional, and national burden of chronic kidney disease, 1990–2017: A systematic analysis for the global burden of disease study 2017. *The Lancet* **395**, 709-733, doi:10.1016/s0140-6736(20)30045-3 (2020).

5 Liyanage, T. *et al.* Worldwide access to treatment for end-stage kidney disease: A systematic review. *Lancet (London, England)* **385**, 1975-1982, doi:10.1016/S0140-6736(14)61601-9 (2015).

6 Humes, H. D. *et al.* Initial clinical results of the bioartificial kidney containing human cells in icu patients with acute renal failure. *Kidney Int* **66**, 1578-1588, doi:10.1111/j.1523-1755.2004.00923.x (2004).

7 Huff, C. How artificial kidneys and miniaturized dialysis could save millions of lives. *Nature* **579**, 186-188, doi:10.1038/d41586-020-00671-8 (2020).

8 Morizane, R. & Bonventre, J. V. Kidney organoids: A translational journey. *Trends Mol Med* **23**, 246-263, doi:10.1016/j.molmed.2017.01.001 (2017).

9 Clapp, W. L. in *Silva's diagnostic renal pathology* (eds Tibor Nadasdy, Vivette D. D'Agati, Xin Jin Zhou, & Zoltan G. Laszik) 1-56 (Cambridge University Press, 2017).

10 Takasato, M. *et al.* Directing human embryonic stem cell differentiation towards a renal lineage generates a self-organizing kidney. *Nat Cell Biol* **16**, 118-126, doi:10.1038/ncb2894 (2014).

11 Lam, A. Q. *et al.* Rapid and efficient differentiation of human pluripotent stem cells into intermediate mesoderm that forms tubules expressing kidney proximal tubular markers. *J Am Soc Nephrol* **25**, 1211-1225, doi:10.1681/ASN.2013080831 (2014).

12 Taguchi, A. *et al.* Redefining the in vivo origin of metanephric nephron progenitors enables generation of complex kidney structures from pluripotent stem cells. *Cell Stem Cell* **14**, 53-67, doi:10.1016/j.stem.2013.11.010 (2014).

13 Nishinakamura, R. Human kidney organoids: Progress and remaining challenges. *Nature reviews. Nephrology* **15**, 613-624, doi:10.1038/s41581-019-0176-x (2019).

14 Takasato, M. & Wymeersch, F. J. Challenges to future regenerative applications using kidney organoids. *Current Opinion in Biomedical Engineering* **13**, 144-151, doi:10.1016/j.cobme.2020.03.003 (2020).

15 van den Berg, C. W. *et al.* Renal subcapsular transplantation of psc-derived kidney organoids induces neo-vasculogenesis and significant glomerular and tubular maturation in vivo. *Stem Cell Reports* **10**, 751-765, doi:10.1016/j.stemcr.2018.01.041 (2018).

16 Lindstrom, N. O. *et al.* Conserved and divergent molecular and anatomic features of human and mouse nephron patterning. *J Am Soc Nephrol* **29**, 825-840, doi:10.1681/ASN.2017091036 (2018).

17 Lindstrom, N. O. *et al.* Conserved and divergent features of human and mouse kidney organogenesis. *J Am Soc Nephrol* **29**, 785-805, doi:10.1681/ASN.2017080887 (2018).

18 Kobayashi, A. *et al.* Six2 defines and regulates a multipotent self-renewing nephron progenitor population throughout mammalian kidney development. *Cell Stem Cell* **3**, 169-181, doi:10.1016/j.stem.2008.05.020 (2008).

19 Costantini, F. & Kopan, R. Patterning a complex organ: Branching morphogenesis and nephron segmentation in kidney development. *Dev Cell* **18**, 698-712, doi:10.1016/j.devcel.2010.04.008 (2010).

20 Maeshima, A., Sakurai, H. & Nigam, S. K. Adult kidney tubular cell population showing phenotypic plasticity, tubulogenic capacity, and integration capability into developing kidney. *J Am Soc Nephrol* **17**, 188-198, doi:10.1681/ASN.2005040370 (2006).

21 Challen, G. A., Bertoncello, I., Deane, J. A., Ricardo, S. D. & Little, M. H. Kidney side population reveals multilineage potential and renal functional capacity but also cellular heterogeneity. *J Am Soc Nephrol* **17**, 1896-1912, doi:10.1681/ASN.2005111228 (2006).

22 Sutherland, M. R. *et al.* Accelerated maturation and abnormal morphology in the preterm neonatal kidney. *J Am Soc Nephrol* **22**, 1365-1374, doi:10.1681/ASN.2010121266 (2011).

23 Ryan, D. *et al.* Development of the human fetal kidney from mid to late gestation in male and female infants. *EBioMedicine* **27**, 275-283, doi:10.1016/j.ebiom.2017.12.016 (2018).

24 Hoy, W. E. *et al.* A stereological study of glomerular number and volume: Preliminary findings in a multiracial study of kidneys at autopsy. *Kidney Int Suppl* **63**, S31-37, doi:10.1046/j.1523-1755.63.s83.8.x (2003).

25 Hughson, M., Farris, A. B., 3rd, Douglas-Denton, R., Hoy, W. E. & Bertram, J. F. Glomerular number and size in autopsy kidneys: The relationship to birth weight. *Kidney Int* **63**, 2113-2122, doi:10.1046/j.1523-1755.2003.00018.x (2003).

26 Puelles, V. G. *et al.* Podocyte number in children and adults: Associations with glomerular size and numbers of other glomerular resident cells. *J Am Soc Nephrol* **26**, 2277-2288, doi:10.1681/ASN.2014070641 (2015).

27 Cullen-McEwen, L., Sutherland, M. R. & Black, M. J. in *Kidney development, disease, repair and regeneration* (ed Melissa H. Little) 27-40 (Academic Press, 2016).

28 Takasato, M. *et al.* Kidney organoids from human ips cells contain multiple lineages and model human nephrogenesis. *Nature* **526**, 564-568, doi:10.1038/nature15695 (2015).

29 Little, M., Georgas, K., Pennisi, D. & Wilkinson, L. in *Organogenesis in development* Vol. 90 *Current topics in developmental biology* (ed Peter Koopman) 193-229 (Academic Press, 2010).

30 Kretzler, M. & Menon, R. Single-cell sequencing the glomerulus, unraveling the molecular programs of glomerular filtration, one cell at a time. *J Am Soc Nephrol* **29**, 2036-2038, doi:10.1681/ASN.2018060626 (2018).

31 Clevers, H. Modeling development and disease with organoids. *Cell* **165**, 1586-1597, doi:10.1016/j.cell.2016.05.082 (2016).

32 Li, Y. & Wingert, R. A. Regenerative medicine for the kidney: Stem cell prospects & challenges. *Clin Transl Med* **2**, 11, doi:10.1186/2001-1326-2-11 (2013).

33 Schutgens, F., Verhaar, M. C. & Rookmaaker, M. B. Pluripotent stem cell-derived kidney organoids: An in vivo-like in vitro technology. *European journal of pharmacology* **790**, 12-20, doi:10.1016/j.ejphar.2016.06.059 (2016).

34 Thiagarajan, R. D. *et al.* Identification of anchor genes during kidney development defines ontological relationships, molecular subcompartments and regulatory pathways. *PLoS One* **6**, e17286, doi:10.1371/journal.pone.0017286 (2011).

35 Al-Awqati, Q. & Oliver, J. A. Stem cells in the kidney. *Kidney Int* **61**, 387-395, doi:10.1046/j.1523-1755.2002.00164.x (2002).

36 McMahon, A. P. Development of the mammalian kidney. *Current topics in developmental biology* **117**, 31-64, doi:10.1016/bs.ctdb.2015.10.010 (2016).

37 Humphreys, B. D. Mapping kidney cellular complexity. *Science* **360**, 709-710, doi:10.1126/science.aat7271 (2018).

38 Assmus, A. M., Mullins, J. J., Brown, C. M. & Mullins, L. J. Cellular plasticity: A mechanism for homeostasis in the kidney. *Acta Physiol (Oxf)* **229**, e13447, doi:10.1111/apha.13447 (2020).

39 Arendt, D. *et al.* The origin and evolution of cell types. *Nat Rev Genet* **17**, 744-757, doi:10.1038/nrg.2016.127 (2016).

40 Morris, S. A. The evolving concept of cell identity in the single cell era. *Development* **146**, doi:10.1242/dev.169748 (2019).

41 Vallejos, C. A., Risso, D., Scialdone, A., Dudoit, S. & Marioni, J. C. Normalizing single-cell rna sequencing data: Challenges and opportunities. *Nat Methods* **14**, 565-571, doi:10.1038/nmeth.4292 (2017).

42 Potter, S. S. Single-cell rna sequencing for the study of development, physiology and disease. *Nature reviews. Nephrology* **14**, 479-492, doi:10.1038/s41581-018-0021-7 (2018).

43 Malone, A. F., Wu, H. & Humphreys, B. D. Bringing renal biopsy interpretation into the molecular age with single-cell rna sequencing. *Semin Nephrol* **38**, 31-39, doi:10.1016/j.semnephrol.2017.09.005 (2018).

44 Lun, A. T., Bach, K. & Marioni, J. C. Pooling across cells to normalize single-cell rna sequencing data with many zero counts. *Genome Biol* **17**, 75, doi:10.1186/s13059-016-0947-7 (2016).

45 Hicks, S. C., Townes, F. W., Teng, M. & Irizarry, R. A. Missing data and technical variability in single-cell rna-sequencing experiments. *Biostatistics* **19**, 562-578, doi:10.1093/biostatistics/kxx053 (2018).

46 Xia, B. & Yanai, I. A periodic table of cell types. *Development* **146**, dev169854, doi:10.1242/dev.169854 (2019).

47 Trapnell, C. *et al.* The dynamics and regulators of cell fate decisions are revealed by pseudotemporal ordering of single cells. *Nat Biotechnol* **32**, 381-386, doi:10.1038/nbt.2859 (2014).

48 Sweeney, D., Lindstrom, N. & Davies, J. A. Developmental plasticity and regenerative capacity in the renal ureteric bud/collecting duct system. *Development* **135**, 2505-2510, doi:10.1242/dev.022145 (2008).

49 Michael, L. & Davies, J. A. Pattern and regulation of cell proliferation during murine ureteric bud development. *J Anat* **204**, 241-255, doi:10.1111/j.0021-8782.2004.00285.x (2004).

50 Dressler, G. R. Advances in early kidney specification, development and patterning. *Development* **136**, 3863-3874, doi:10.1242/dev.034876 (2009).

51 O'Brien, L. L. & McMahon, A. P. Induction and patterning of the metanephric nephron. *Semin Cell Dev Biol* **36**, 31-38, doi:10.1016/j.semcdb.2014.08.014 (2014).

52 Kao, R. M., Vasilyev, A., Miyawaki, A., Drummond, I. A. & McMahon, A. P. Invasion of distal nephron precursors associates with tubular interconnection during nephrogenesis. *J Am Soc Nephrol* **23**, 1682-1690, doi:10.1681/ASN.2012030283 (2012).

53 Faa, G. *et al.* Morphogenesis and molecular mechanisms involved in human kidney development. *Journal of cellular physiology* **227**, 1257-1268, doi:10.1002/jcp.22985 (2012).

54 Black, M. J. *et al.* When birth comes early: Effects on nephrogenesis. *Nephrology (Carlton, Vic.)* **18**, 180-182, doi:10.1111/nep.12028 (2013).

55 Rosenblum, S., Pal, A. & Reidy, K. Renal development in the fetus and premature infant. *Semin Fetal Neonatal Med* **22**, 58-66, doi:10.1016/j.siny.2017.01.001 (2017).

56 Das, A. *et al.* Stromal-epithelial crosstalk regulates kidney progenitor cell differentiation. *Nat Cell Biol* **15**, 1035-1044, doi:10.1038/ncb2828 (2013).

57 Zeisberg, M. & Kalluri, R. Physiology of the renal interstitium. *Clin J Am Soc Nephrol* **10**, 1831-1840, doi:10.2215/CJN.00640114 (2015).

58 Little, M. H. & McMahon, A. P. Mammalian kidney development: Principles, progress, and projections. *Cold Spring Harbor perspectives in biology* **4**, doi:10.1101/cshperspect.a008300 (2012).

59 Young, M. D. *et al.* Single-cell transcriptomes from human kidneys reveal the cellular identity of renal tumors. *Science* **361**, 594-599, doi:10.1126/science.aat1699 (2018).

60 Menon, R. *et al.* Single-cell analysis of progenitor cell dynamics and lineage specification in the human fetal kidney. *Development* **145**, doi:10.1242/dev.164038 (2018).

61 Lindstrom, N. O. *et al.* Conserved and divergent features of mesenchymal progenitor cell types within the cortical nephrogenic niche of the human and mouse kidney. *J Am Soc Nephrol* **29**, 806-824, doi:10.1681/ASN.2017080890 (2018).

62 Wang, P. *et al.* Dissecting the global dynamic molecular profiles of human fetal kidney development by single-cell rna sequencing. *Cell Rep* **24**, 3554-3567 e3553, doi:10.1016/j.celrep.2018.08.056 (2018).

63 Combes, A. N., Zappia, L., Er, P. X., Oshlack, A. & Little, M. H. Single-cell analysis reveals congruence between kidney organoids and human fetal kidney. *Genome Med* **11**, 3, doi:10.1186/s13073-019-0615-0 (2019).

64 Lindström, N. O. *et al.* Spatial transcriptional mapping of the human nephrogenic program. *bioRxiv*, 2020.2004.2027.060749, doi:10.1101/2020.04.27.060749 (2020).

65 Stewart, B. J. *et al.* Spatiotemporal immune zonation of the human kidney. *Science* **365**, 1461-1466, doi:10.1126/science.aat5031 (2019).

66 Tran, T. *et al.* In vivo developmental trajectories of human podocyte inform in vitro differentiation of pluripotent stem cell-derived podocytes. *Dev Cell* **50**, 102-116 e106, doi:10.1016/j.devcel.2019.06.001 (2019).

67 Hochane, M. *et al.* Single-cell transcriptomics reveals gene expression dynamics of human fetal kidney development. *PLoS Biol* **17**, e3000152, doi:10.1371/journal.pbio.3000152 (2019).

68 Lindstrom, N. O. *et al.* Progressive recruitment of mesenchymal progenitors reveals a time-dependent process of cell fate acquisition in mouse and human nephrogenesis. *Dev Cell* **45**, 651-660 e654, doi:10.1016/j.devcel.2018.05.010 (2018).

69 Liao, J. *et al.* Single-cell rna sequencing of human kidney. *Sci Data* **7**, 4, doi:10.1038/s41597-019-0351-8 (2020).

70 Wu, H. *et al.* Single-cell transcriptomics of a human kidney allograft biopsy specimen defines a diverse inflammatory response. *J Am Soc Nephrol* **29**, 2069-2080, doi:10.1681/ASN.2018020125 (2018).

71 Wu, H. *et al.* Comparative analysis and refinement of human psc-derived kidney organoid differentiation with single-cell transcriptomics. *Cell Stem Cell* **23**, 869-881 e868, doi:10.1016/j.stem.2018.10.010 (2018).

72 Sivakamasundari, V. *et al.* Comprehensive cell type specific transcriptomics of the human kidney. *bioRxiv*, 238063, doi:10.1101/238063 (2017).

73 Kuppe, C. *et al.* Decoding myofibroblast origins in human kidney fibrosis. *Nature* **589**, 281-286, doi:10.1038/s41586-020-2941-1 (2021).

74 Lake, B. B. *et al.* A single-nucleus rna-sequencing pipeline to decipher the molecular anatomy and pathophysiology of human kidneys. *Nat Commun* **10**, 2832, doi:10.1038/s41467-019-10861-2 (2019).

75 Dressler, G. R. The cellular basis of kidney development. *Annu Rev Cell Dev Biol* **22**, 509-529, doi:10.1146/annurev.cellbio.22.010305.104340 (2006).

76 Adam, M., Potter, A. S. & Potter, S. S. Psychrophilic proteases dramatically reduce single-cell rna-seq artifacts: A molecular atlas of kidney development. *Development* **144**, 3625-3632, doi:10.1242/dev.151142 (2017).

77 Park, J. S. *et al.* Six2 and wnt regulate self-renewal and commitment of nephron progenitors through shared gene regulatory networks. *Dev Cell* **23**, 637-651, doi:10.1016/j.devcel.2012.07.008 (2012).

78 Hendry, C., Rumballe, B., Moritz, K. & Little, M. H. Defining and redefining the nephron progenitor population. *Pediatr Nephrol* **26**, 1395-1406, doi:10.1007/s00467-010-1750-4 (2011).

79 Boyle, S. C., Kim, M., Valerius, M. T., McMahon, A. P. & Kopan, R. Notch pathway activation can replace the requirement for wnt4 and wnt9b in mesenchymal-to-epithelial transition of nephron stem cells. *Development* **138**, 4245-4254, doi:10.1242/dev.070433 (2011).

80 Self, M. *et al.* Six2 is required for suppression of nephrogenesis and progenitor renewal in the developing kidney. *EMBO J* **25**, 5214-5228, doi:10.1038/sj.emboj.7601381 (2006).

81 Kobayashi, A. *et al.* Identification of a multipotent self-renewing stromal progenitor population during mammalian kidney organogenesis. *Stem Cell Reports* **3**, 650-662, doi:10.1016/j.stemcr.2014.08.008 (2014).

82 Fanni, D. *et al.* Muc1 in mesenchymal-to-epithelial transition during human nephrogenesis: Changing the fate of renal progenitor/stem cells? *J Matern Fetal Neonatal Med* **24 Suppl 2**, 63-66, doi:10.3109/14767058.2011.613159 (2011).

83 Neidhardt, L. M., Kispert, A. & Herrmann, B. G. A mouse gene of the paired-related homeobox class expressed in the caudal somite compartment and in the developing vertebral column, kidney and nervous system. *Dev Genes Evol* **207**, 330-339, doi:10.1007/s004270050120 (1997).

84 Kispert, A. T-box genes in the kidney and urinary tract. *Current topics in developmental biology* **122**, 245-278, doi:10.1016/bs.ctdb.2016.06.002 (2017).

85 Brunskill, E. W. *et al.* Single cell dissection of early kidney development: Multilineage priming. *Development* **141**, 3093-3101, doi:10.1242/dev.110601 (2014).

86 Mugford, J. W., Yu, J., Kobayashi, A. & McMahon, A. P. High-resolution gene expression analysis of the developing mouse kidney defines novel cellular compartments within the nephron progenitor population. *Dev Biol* **333**, 312-323, doi:10.1016/j.ydbio.2009.06.043 (2009).

87 Georgas, K. *et al.* Analysis of early nephron patterning reveals a role for distal rv proliferation in fusion to the ureteric tip via a cap mesenchyme-derived connecting segment. *Dev Biol* **332**, 273-286, doi:10.1016/j.ydbio.2009.05.578 (2009).

88 Sequeira-Lopez, M. L. *et al.* The earliest metanephric arteriolar progenitors and their role in kidney vascular development. *Am J Physiol Regul Integr Comp Physiol* **308**, R138-149, doi:10.1152/ajpregu.00428.2014 (2015).

89 Schlondorff, D. & Banas, B. The mesangial cell revisited: No cell is an island. *J Am Soc Nephrol* **20**, 1179-1187, doi:10.1681/ASN.2008050549 (2009).

90 Goligorsky, M. S. *et al.* Role of mesangial cells in macula densa to afferent arteriole information transfer. *Clin Exp Pharmacol Physiol* **24**, 527-531, doi:10.1111/j.1440-1681.1997.tb01240.x (1997).

91 Daniel, C. *et al.* Transgelin is a marker of repopulating mesangial cells after injury and promotes their proliferation and migration. *Lab Invest* **92**, 812-826, doi:10.1038/labinvest.2012.63 (2012).

92 Craelius, W., el-Sherif, N. & Palant, C. E. Stretch-activated ion channels in cultured mesangial cells. *Biochem Biophys Res Commun* **159**, 516-521, doi:10.1016/0006-291x(89)90023-5 (1989).

93 England, A. R. *et al.* Identification and characterization of cellular heterogeneity within the developing renal interstitium. *Development* **147**, dev.190108, doi:10.1242/dev.190108 (2020).

94 Barwinska, D. *et al.* Molecular characterization of the human kidney interstitium in health and disease. *Science Advances* **7**, eabd3359, doi:10.1126/sciadv.abd3359 (2021).

95 Kriz, W. The inability of podocytes to proliferate: Cause, consequences, and origin. *Anatomical record (Hoboken, N.J. : 2007)* **303**, 2588-2596, doi:10.1002/ar.24291 (2020).

96 Ronconi, E. *et al.* Regeneration of glomerular podocytes by human renal progenitors. *J Am Soc Nephrol* **20**, 322-332, doi:10.1681/ASN.2008070709 (2009).

97 Benigni, A., Morigi, M. & Remuzzi, G. Kidney regeneration. *Lancet (London, England)* **375**, 1310-1317, doi:10.1016/S0140-6736(10)60237-1 (2010).

98 Romagnani, P., Lasagni, L. & Remuzzi, G. Renal progenitors: An evolutionary conserved strategy for kidney regeneration. *Nature reviews. Nephrology* **9**, 137-146, doi:10.1038/nrneph.2012.290 (2013).

99 Brunskill, E. W., Georgas, K., Rumballe, B., Little, M. H. & Potter, S. S. Defining the molecular character of the developing and adult kidney podocyte. *PLoS One* **6**, e24640, doi:10.1371/journal.pone.0024640 (2011).

100 Ichimura, K. *et al.* Morphological process of podocyte development revealed by block-face scanning electron microscopy. *J Cell Sci* **130**, 132-142, doi:10.1242/jcs.187815 (2017).

101 Ichimura, K. *et al.* Three-dimensional architecture of podocytes revealed by block-face scanning electron microscopy. *Sci Rep* **5**, 8993, doi:10.1038/srep08993 (2015).

102 Shankland, S. J., Smeets, B., Pippin, J. W. & Moeller, M. J. The emergence of the glomerular parietal epithelial cell. *Nature reviews. Nephrology* **10**, 158-173, doi:10.1038/nrneph.2014.1 (2014).

103 Kopp, J. B. Replenishment of the podocyte compartment by parietal epithelial cells. *Kidney Int* **88**, 934-935, doi:10.1038/ki.2015.256 (2015).

104 Romagnani, P. Parietal epithelial cells: Their role in health and disease. *Contributions to nephrology* **169**, 23-36, doi:10.1159/000313943 (2011).

105 Chen, L. *et al.* Renal-tubule epithelial cell nomenclature for single-cell rna-sequencing studies. *J Am Soc Nephrol* **30**, 1358-1364, doi:10.1681/ASN.2019040415 (2019).

106 Madsen, K. M. & Tisher, C. C. Structural-functional relationships along the distal nephron. *Am J Physiol* **250**, F1-15, doi:10.1152/ajprenal.1986.250.1.F1 (1986).

107 Roy, A., Al-bataineh, M. M. & Pastor-Soler, N. M. Collecting duct intercalated cell function and regulation. *Clin J Am Soc Nephrol* **10**, 305-324, doi:10.2215/CJN.08880914 (2015).

108 Chen, L. *et al.* Transcriptomes of major renal collecting duct cell types in mouse identified by single-cell rna-seq. *Proc Natl Acad Sci U S A* **114**, E9989-E9998, doi:10.1073/pnas.1710964114 (2017).

109 Park, J. *et al.* Single-cell transcriptomics of the mouse kidney reveals potential cellular targets of kidney disease. *Science* **360**, 758-763, doi:10.1126/science.aar2131 (2018).

110 Si, H. *et al.* Human and murine kidneys show gender- and species-specific gene expression differences in response to injury. *PLoS One* **4**, e4802, doi:10.1371/journal.pone.0004802 (2009).

111 Sabolic, I. *et al.* Gender differences in kidney function. *Pflugers Arch* **455**, 397-429, doi:10.1007/s00424-007-0308-1 (2007).

112 Ransick, A. *et al.* Single-cell profiling reveals sex, lineage, and regional diversity in the mouse kidney. *Dev Cell* **51**, 399-413 e397, doi:10.1016/j.devcel.2019.10.005 (2019).

113 Chen, G., Ning, B. & Shi, T. Single-cell rna-seq technologies and related computational data analysis. *Front Genet* **10**, 317, doi:10.3389/fgene.2019.00317 (2019).

114 Kiselev, V. Y., Andrews, T. S. & Hemberg, M. Challenges in unsupervised clustering of single-cell rna-seq data. *Nat Rev Genet* **20**, 273-282, doi:10.1038/s41576-018-0088-9 (2019).

115 Ren, X. *et al.* Reconstruction of cell spatial organization from single-cell rna sequencing data based on ligand-receptor mediated self-assembly. *Cell Res* **30**, 763-778, doi:10.1038/s41422-020-0353-2 (2020).

116 Han, X. *et al.* Construction of a human cell landscape at single-cell level. *Nature* **581**, 303-309, doi:10.1038/s41586-020-2157-4 (2020).

117 Abedini, A. *et al.* Urinary single-cell profiling captures the cellular diversity of the kidney. *Journal of the American Society of Nephrology*, ASN.2020050757, doi:10.1681/ASN.2020050757 (2021).

118 Wu, H. & Humphreys, B. D. Single cell sequencing and kidney organoids generated from pluripotent stem cells. *Clin J Am Soc Nephrol* **15**, 550-556, doi:10.2215/CJN.07470619 (2020).

The Supplementary Tables 1-3 can be viewed online (https://doi.org/10.1038/s41536-021-00156-w).

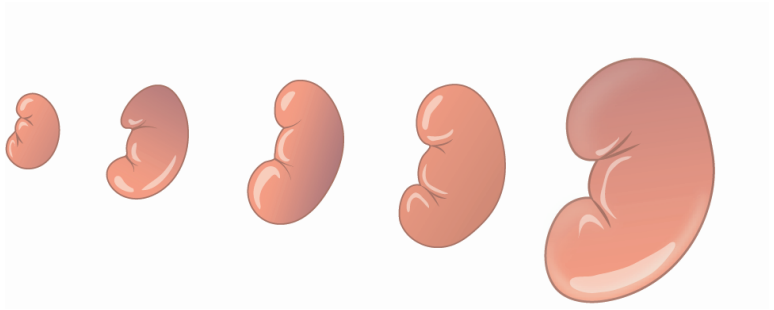

Chapter 3

Structural development of the human fetal kidney: new stages and cellular dynamics in nephrogenesis

Anika Schumacher, Tri Q. Nguyen, Roel Broekhuizen, Martijn van Griensven, Vanessa LaPointe

This chapter has been submitted for publication:

Schumacher, A., Nguyen, T.Q., Broekhuizen, R. et al. *Structural development of the human fetal kidney: new stages and cellular dynamics in nephrogenesis.*

and is available as preprint:

Schumacher, A., Nguyen, T.Q., Broekhuizen, R. et al. *Structural development of the human fetal kidney: new stages and cellular dynamics in nephrogenesis.* bioRxiv, 2023.03. 24.534074 (2023). https://doi.org/10.1101/2023.03.24.534074

Chapter 4

Ultrastructural comparison of human kidney organoids and human fetal kidneys reveals features of hyperglycemic culture

Anika Schumacher, Virginie Joris, Martijn van Griensven, Vanessa LaPointe

This chapter has been submitted for publication:

Schumacher, A., Joris, V., van Griensven, M. et al. *Ultrastructural comparison of human kidney organoids and human fetal kidneys reveals features of hyperglycemic culture*.

and is available as preprint:

Schumacher, A., Joris, V., van Griensven, M. et al. *Ultrastructural comparison of human kidney organoids and human fetal kidneys reveals features of hyperglycemic culture*. bioRxiv, 2023.03. 27.534124 (2023). https://doi.org/10.1101/2023.03.27.534124

Chapter 5

A practical guide to immunostaining and tissue clearing of large organoid models: lessons learned

Anika Schumacher, Martijn van Griensven, Vanessa LaPointe

Department of Cell Biology–Inspired Tissue Engineering, MERLN Institute for Technology-Inspired Regenerative Medicine, Maastricht University, Maastricht, the Netherlands.

Introduction to tissue clearing

The emergence of 3D cultures such as spheroids and organoids has opened up a large variety of possibilities to better recapitulate complex cell behaviour *in vitro*, but has also created new technical challenges. Standard culture methods, assays, and imaging techniques are not always applicable and have therefore had to evolve alongside the 3D culture methodology (Figure 1).

In particular, microscopy, which is highly dependent on tissue dimension and complexity, is not optimised to image these novel 3D cultures. While paraffin embedding and cryosectioning are suitable techniques, they are labour-intensive, do not preserve the 3D complexity and the resulting sections are often not representative of the entire organoid or spheroid. Similarly, most available microscopes cannot image large specimens at high resolution. Confocal microscopy and super-resolution microscopy are best at filtering out the out-of-focus light, however, they have limited light penetration and therefore sample thickness. In contrast, two-photon microscopy allows deep, even intra-vital imaging, but does not allow imaging at a resolution comparable to confocal or spinning-disk confocal microscopy. Light sheet microscopy allows imaging of intact organisms and tissues at high speed and high resolution, but requires the samples to be transparent.

To circumvent the issue of low light penetration, researchers came up with the idea to change the tissue properties instead of the techniques or tissue dimensions. By making the tissue transparent through refractive index matching, light is able to propagate through the tissue with less diffraction. This concept of tissue clearing was first implemented in 1914[1], soon after the invention of the first fluorescence microscope, however it was rarely applied for decades. Since 2007, when the successful imaging of a cleared whole mouse brain was shown[2], the field has truly evolved and today's protocols enable imaging a whole mouse in high-resolution[3].

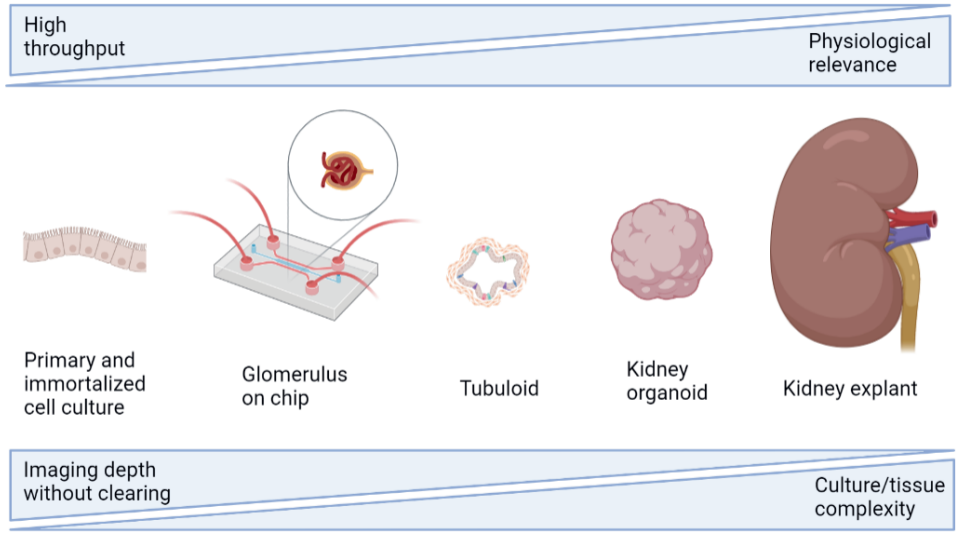

Figure 1: The culture of physiological, complex structures brings along new technical challenges for microscopy. Longer acquisition times and more complex data analysis further complicate microscopic assessment.

Over the past decade, various tissue clearing methods have been developed and more recently extensively reviewed.[4-7] This chapter will focus on practical matters applied specifically to kidney organoids and will outline the methodology development that was part of this thesis.

Briefly, tissue clearing methods can be clustered into three major categories: solvent-based, aqueous, and hydrogel-based tissue clearing. Solvent-based protocols usually comprise two steps: 1. dehydration leading to lipid solvation, and 2. refractive index (RI) matching with additional lipid solvation. Dehydrated proteins have an RI of > 1.5 and therefore samples need perfusion with solutions with a comparable RI.[8] Aqueous tissue clearing methods were developed due to the drawbacks of solvent-based clearing: solvents' nature to dissolve glues, and the toxicity and quenching of fluorescent proteins. Aqueous tissue clearing methods follow the following principles: passive immersion in a solution that is refractive index–matched to the tissue 1. without or 2. with prior active or passive removal of lipids or 3. removal of

lipids followed by hydration of the sample to lower the refractive index of the remaining tissue components (hyperhydration).[4] Since the passive immersion techniques often do not fully clear lipids, it is believed that they need to have an RI > 1.45.[4] Although aqueous clearing by simple immersion has the above-stated advantages, it generally performs worse and is much slower than solvent-based techniques. Another aqueous method is hyperhydration, which removes lipids to lower the RI. Lipid removal in an aqueous environment relies on long incubation with detergents such as Triton X-100, and hyperhydration is achieved through an osmotic gradient by, for instance, the addition of urea. Hyperhydration leads to swelling of the tissue and therefore longer imaging time due to the larger sample size. Besides, efficient clearing is usually achieved only after weeks of incubation. Finally, hydrogel-based clearing methods aim to circumvent the issues of damage or removal of proteins in the process of lipid solvation, as seen in aqueous and solvent-based tissue clearing. This strategy is done by embedding the tissue in hydrogel, then tediously removing lipids by detergents or electrophoresis and finally immersing it in an RI-matched solution. This process is the basis of expansion microscopy, where swelling of hydrogel-perfused tissue increases resolution by increasing the size of small structures. However, this swelling can be a disadvantage for fragile subcellular structures.

In sum, tissue clearing methods aim to create a homogenous RI of the tissue, matched to both mounting method and objectives, thereby reducing non-forward scatter and resulting in a transparent tissue. While tissue clearing was not applied on organoids at the start of this work, it was certainly needed. Uncleared kidney organoids, particularly the transwell-cultured organoids used in this thesis, are several millimetres in size and highly turbid. The imaging depth and resolution were therefore inadequate to answer our research questions and new approaches were needed. Our aim was to achieve single-cell resolution throughout the organoids to distinguish cell types and their specific location. This information was needed, for instance, in Chapter 6 of this thesis to quantify endothelial cells in 3D. As it turned out, the organoids did not have a homogeneous cellular distribution since the different cell types form different segments of nephrons, making whole mount imaging of cleared organoids particularly relevant.

Whole mount organoid immunostaining: general considerations

Along with the clearing of organoids, the whole mount immunostaining protocol needed to be optimised to allow antibody perfusion and homogeneous labelling. Initially, by staining overnight in the fridge, the organoid was stained heterogeneously, with weak staining in its core and intense staining in its periphery. Researchers previously addressed this problem by developing a method that required treatment with 2% Triton X-100, 20% dimethyl sulfoxide (DMSO) and 5% bovine serum albumin (BSA) in PBS along with increasing the antibody concentration.[9] We applied this protocol to 3D kidney organoids, and doubled the primary antibody concentration compared to 2D. The samples were incubated at room temperature for 5 days for each antibody incubation. Washing required a 2-day incubation at room temperature in the same buffer.

The staining was then assessed by cryosectioning (Figure 2). Although the staining appeared equally intense throughout the organoid, the harsh treatment with high concentrations of DMSO and Triton X-100 changed the tissue morphology, making the images more blurry and leading to nonspecific binding of antibodies in the periphery (Figure 2A, white arrowheads). Reducing the incubation time and concentrations to a quarter did not significantly change the results, indicating that DMSO could be too harsh. Furthermore, after immunostaining using this protocol, the organoid was significantly more fragile and likely would not have remained intact during the ethyl cinnamate (ECi) clearing afterwards.

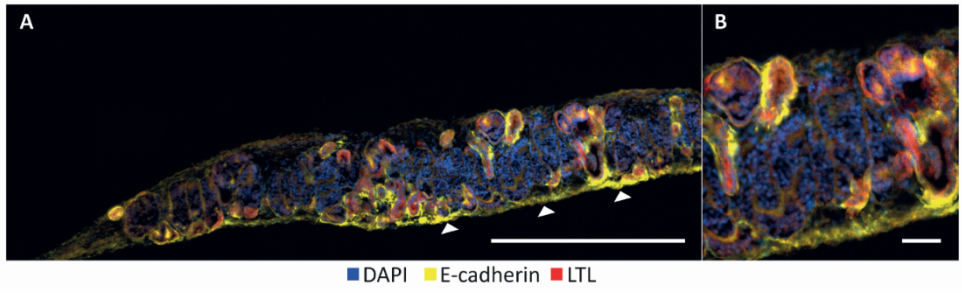

Figure 2: Cryosections of an organoid treated with a Triton X-100 and DMSO–based permeabilisation method. A. Full cross-section of an organoid and B. a zoomed imaged show that the harsh permeabilisation leads to artefacts. White arrows: nonspecific binding of E-cadherin antibody (yellow). LTL: Lotus tetragonolobus lectin. Scale bars: A. 500 μm, B. 50 μm.

Alternatively, we tested simply prolonging the incubation times of our standard immunostaining protocol to 3 days per incubation step instead of overnight at 4 °C. Additionally, the Triton X-100 concentration was increased from 0.06% to 0.5% in the blocking step to increase permeabilisation. We achieved satisfactory results with this revision for most antibodies. Additionally, we carefully selected secondary antibodies based on the abundance and location of the proteins, following these two principles:

1. Fluorophores with longer wavelength excitation for abundant proteins and fluorophores with shorter wavelength excitation for scarce proteins.
2. Fluorophores with longer wavelength excitation for proteins located deeper in the organoid and fluorophores with shorter wavelength excitation for proteins located towards the periphery of the organoid.

Tissue clearing kidney organoids

Since starting this project, the variety of tissue clearing protocols and the details of the published protocols have increased tremendously. Before, important details for the successful execution of these protocols were often lacking. When tissue clearing was applied to kidney organoids as part of this thesis, tissue clearing of organoids in general was not yet described in the literature. Therefore, a variety of clearing protocols were tested on the kidney organoids, of which a selection will be covered in this chapter.

To start, two conditions were set to make a selection for clearing methods to test. Since the organoids did not have the structural strength or complexity of a real tissue, but were more comparable to a soft gel, we assumed that simple immersion techniques would be most suitable and no harsh clearing would be required. Furthermore, we tried to avoid toxic reagents given the heavy usage of the microscopes and potential risk of leakage during long imaging time. Accordingly, a variety of protocols were chosen and tested on fixed kidney organoids, of which a selection is shown in Figure 3 and Table 1.

Table 1: Characteristics of different clearing methods tested on kidney organoids.

	METHOD				
	FRUIT	**TDE**	**SCALE**	**SWITCH**	**ECi**
Original article	Hou, et al. [10]	Costantini, et al. [11]	Hama, et al. [12]	Murray, et al. [13]	Klingberg, et al. [14]
Technique	aqueous clearing	aqueous clearing	aqueous clearing	aqueous clearing	solvent-based
Final RI	40% = 1.4	1.42	1.38	1.47	1.56
Toxic components	no	no	no	yes	no
Usage of detergent/solvent	none	yes	yes	yes	yes
Lipids preserved	yes	no	no	no	no
Tunable RI	yes	yes	unknown	likely	no
Duration of protocol	days	days	weeks	days	hours–days
Changes in tissue morphology	minor expansion	none	expansion	none described & none seen	shrinkage
Success rate on kidney organoids	medium	low	low	low	high

Although the FRUIT method showed potential, only the method using ECi, a non-toxic compound stated to have a high RI of 1.56, was successful in reducing blurriness significantly and allowing imaging at a single-cell resolution (Figure 3). Kidney organoids were extensively dehydrated in a series of ethanol to remove lipids before immersion in ECi. However, the RI of ECi is dependent on the wavelength of light it is exposed to due to dispersion (Figure 4). Therefore, imaging with short wavelengths such as 460 nm to visualize DAPI was not possible. Furthermore, due to the high refractive index, imaging was limited to maximally 20× magnification and a numerical aperture (NA) of 0.8, since higher NA led to more blurriness due to the higher sensitivity for low signals. In an attempt to lower the RI of ECi, ECi was diluted with ethanol to a refractive index of 1.47, but the fixed organoid dissolved immediately upon immersion. To date, no study has been published that describes that the RI of ECi is adjustable.

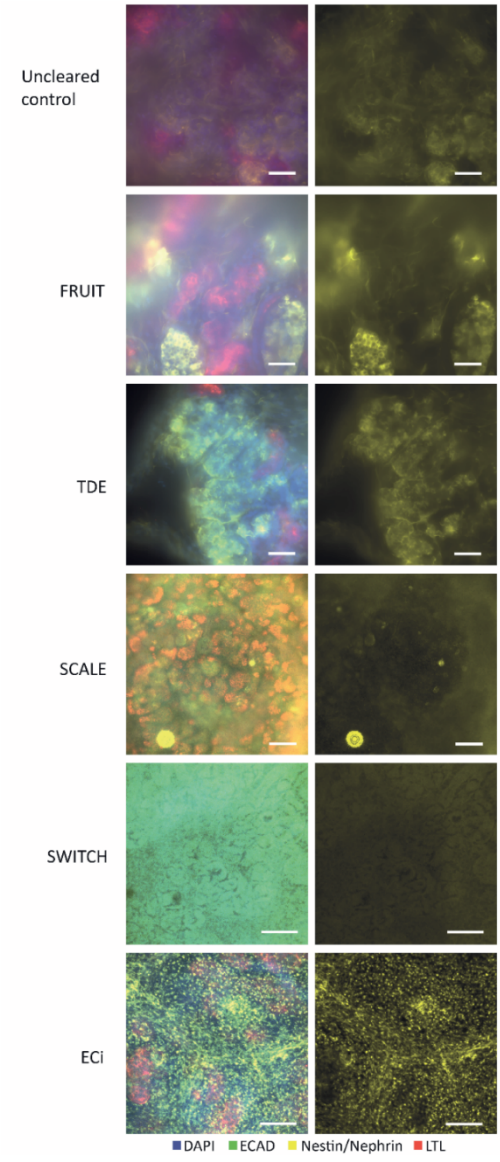

Figure 3: Examples of clearing methods tested on D7+18 kidney organoids. Compared to the uncleared control, ethyl cinnamate (ECi) produced the best resolution with the lowest out-of-focus signal. Conclusions should only be drawn on the clarity of the images given the differences between the individual experiments. ECAD: E-cadherin (tubules), DAPI (nuclei), LTL: Lotus tetragonolobus lectin (proximal tubules), Nestin/Nephrin: (podocytes). Scale bars: A–C: 50 μm, D: 200 μm, E: 100 μm.

With ECi, extensive dehydration of the organoids had important consequences. First, the sample shrunk up to approximately 10 times. If the organoid was left on the transwell membrane during clearing, this shrinking was not isotropic; it occurred largely in thickness, while the diameter remained comparable to the uncleared organoid. Second, the harsher lipid solvation by ethanol, compared to for instance the FRUIT method, resulted in the removal of lipid-anchored proteins such as nephrin.

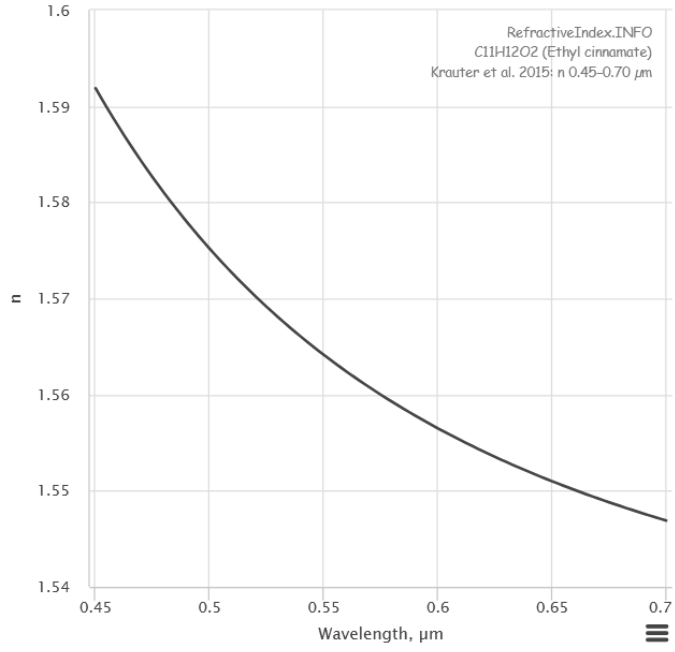

Figure 4: Dispersion of light in ethyl cinnamate. The refractive index (n) is highest for the DAPI channel, and is ill-suited for regular air and water immersion objectives. Reproduced with permission from [15] based on the data of Krauter, et al. [16].

To conclude, due to the scarcity of samples at the time of optimization of these methods, it should be emphasised that certain methods, such as FRUIT, might have proven more successful with additional optimization. Different adjustments to the protocols, especially more precise tuning of the clearing solutions to specific RIs, might have resulted in better clearing results. ECi gave the best results in the first

trials and therefore was chosen for further optimization. Subsequent experiments proved this method advantageous due to the quick clearing, lack of toxicity, and long preservation of fluorescence.

Mounting of ECi-cleared kidney organoids – an underestimated challenge

Mounting of cleared explanted tissue is rather straightforward and therefore usually not included in the methods section of publications. Due to the large extracellular matrix (ECM) content, the integrity of tissue explants after clearing is still sufficient to pick the tissue up with forceps for transfer to an imaging dish. Tissue can therefore be easily mounted. For instance, cleared brain tissue can be glued to the imaging dish with common Superglue or even a hot glue gun. However, this option is dependent on the size of the tissue, since the glue is highly fluorescent and therefore the regions adjacent to it cannot be imaged. In contrast, cleared and uncleared organoids can be neither handled with forceps nor glued to a dish due to their size and fragility. Handling the organoid without any additional support matrix leads to deformation and damage.

Several mounting methods were investigated for transwell-cultured kidney organoids, of which three were proven possible (Figure 5):

1. Gel embedding and fixation to the imaging dish with glue.
2. Keeping the organoid on the transwell filter and loading with heavy O-rings.
3. Keeping the organoid on the transwell filter and glueing the organoid to the dish.

For the first option (Figure 5A), the fixed and stained organoid is detached from the transwell filter embedded in 1% Phytagel in PBS. The gel is pipetted as thin as possible on the organoid after removal of the transwell filter, followed by the dehydration series of the clearing protocol. Once the dehydration is completed, the gel including the organoid is glued with a few microliters of glue to the imaging dish. The glue used for the experiments of this thesis is Loctite 401 Superglue.

Importantly, the glue does not come into contact with the organoid. This option makes handling of the organoid easier, since the surrounding gel protects it. However, since the gel needs to be dehydrated together with the organoid, the dehydration and incubation time in ECi takes longer.

The second option (Figure 5B) does not require the detachment of the organoid from the transwell filter. Instead, the membrane is cut around the organoid and the organoid can thereby be easily picked up with forceps on the membrane. After the final dehydration step, the organoid is transferred upside down into the imaging dish and several layers of O-rings with increasing size are placed around the organoid to weigh it to the bottom of the dish. This method requires very careful carrying and storing of the sample to not displace the O-rings. Furthermore, it has the advantage of speed and no risk of autofluorescence by attached glue. However, this method is only applicable if the stage speed of the microscope can be set to a maximum of 2.5 mm/s to prevent sample movement.

The third option (Figure 5C) follows the same steps as the second method until after the last dehydration step. Once dehydrated, the transwell membrane is glued to the dish (with the organoid facing the glass bottom) as far as possible from the organoid to prevent the glue attaching to the organoid. When the glue is dried, the process is continued with ECi.

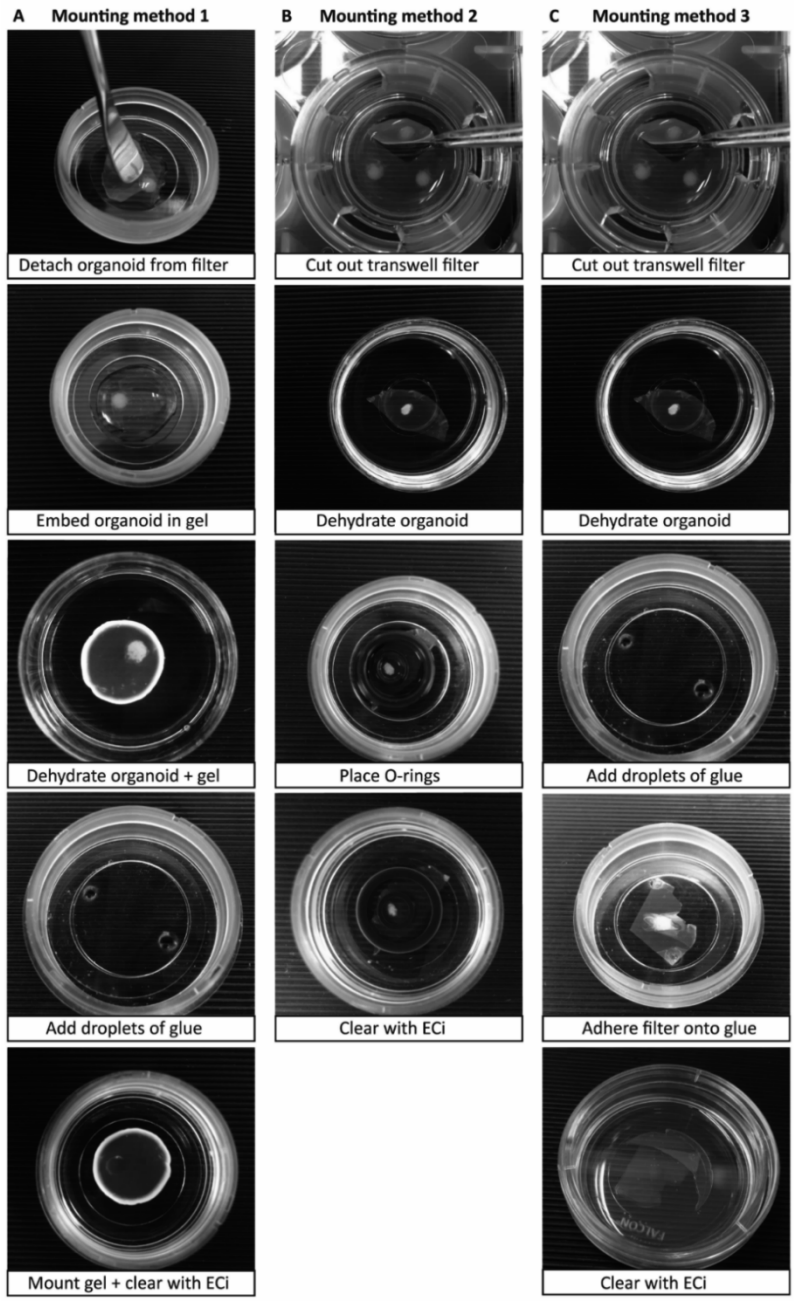

Figure 5: Photos illustrating the steps (top to bottom) of three different mounting methods (columns) of cleared kidney organoids.

Furthermore, there are a couple more attention points in these protocols. First, solvents such as ethanol dissolve many types of glue. Therefore, mounting with glue should only take place after dehydration, and the spot of the gel or membrane that will come in contact with glue should be "dried" with a fibre-free tissue to avoid a large amount of ethanol touching the glue. The glue should first dry for a few minutes in the imaging dish before adding the sample, until it is just liquid enough to still adhere to the dehydrated gel or the transwell membrane. This delay is to avoid a long exposure of the organoid to air, which would lead to rehydration.

Second, the organoid should not be touched once removed from the filter, since it easily deforms (Figure 6A). Movement of the organoid can be achieved by pipetting the liquid around the organoid in the needed direction.

Third, ECi dissolves certain types of plastic and glues; therefore, the choice of the imaging dish should be made carefully. Trials to understand if and how long a dish is resistant to ECi should be performed before continuing with microscopy. Objectives contain rubbers and glues that can be dissolved by ECi, and the damage of a leak can therefore be substantial. The Ibidi glass-bottom dish (cat. no. 81158) was found to be suitable. Both the glass bottom and the glue attaching the glass bottom to the dish were resistant to dissolving by ECi. However, the lid is not resistant and will dissolve; therefore, the dish should not be tilted when ECi is inside. Additionally, the dehydration should not be performed in this dish because this makes the glue of the dish vulnerable to ECi, leading to detachment of the glass bottom.

Finally, dehydration results in a complete hardening of the organoid (and if embedded in gel, also the gel) and makes it very brittle. Applying pressure on the organoid when mounting should be strictly avoided to prevent the formation of cracks (Figure 6B). Nevertheless, it is essential to mount the organoid for all three methods as flat as possible since a small tilt can increase both the imaging time and the size of the data file tremendously. If these tips are followed, then mounting should result in an artefact-free organoid image (Figure 6C).

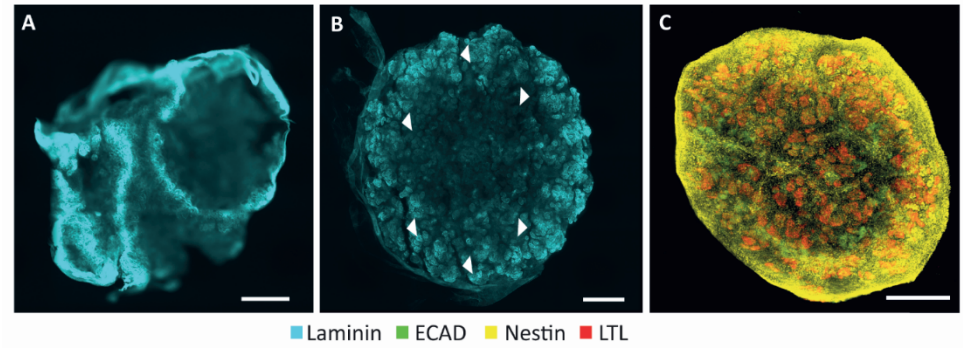

Figure 6: Examples of mounting cleared kidney organoids. A. Cleared organoid detached from the membrane easily deforms during clearing or mounting. B. Dehydrated organoids become brittle and the slightest pressure or bending can result in cracks (white arrowheads). C. Cleared organoid following any of the three types of mounting can be successfully imaged without artefacts. Scale bars: 500 μm.

Storage of ECi-cleared kidney organoids

ECi has a melting point of 6.5–8.0 °C. Consequently, it crystallizes at the standard storage temperature (4 °C) of fluorescently labelled samples. ECi-cleared samples should therefore be stored at room temperature. However, even though the lid of the Ibidi imaging dish limits evaporation, placing the imaging dish on certain types of plastics (such as polystyrene Petri dishes) will eventually dissolve the Petri dish along with the glass bottom compartment of the Ibidi dish. Polypropylene cases, such as tip boxes, are more suitable storage containers. After several months, the clearing effect can reduce. This reduction is solved by re-clearing the sample by immersing it in 100% ethanol overnight (during which ethanol should be replaced a few times), followed by ECi incubation as described in the protocol.

Imaging and processing

The best balance between resolution, imaging time and file size was achieved by imaging with a spinning disk confocal microscope equipped with either a 10× air (CFI Plan Fluor DL 10X) or a 20× extra-long working distance air objective (CFI S Plan Fluor ELWD ADM 20X). Objectives with higher magnifications and

consequently higher NA were not suitable, since more scattering would be caused by the high RI of ECi. Before imaging, shading correction was applied for each channel to assure artefact-free stitching. If the signal was significantly dimmer in the centre of the stack, z-intensity correction was applied after deconvolution.

Additional tips learned beyond the available literature

To conclude, there are a couple of additional tips and tricks that were acquired throughout testing clearing methods or that were mentioned by other researchers at conferences and meetings.

- Organoids should be mounted in the clearing solution and not in a mounting medium that is supposed to have the same RI.
- The clearing solution should not be replaced immediately before imaging, since the smallest changes in RI can create scattering of light.
- Generally, the sample should be first stained and then cleared, since proteins could be damaged in the process of clearing. However, some methods allow repeated staining after clearing.
- The tissue to be cleared should be as fresh as possible since fresher tissue clears better.
- Molecular grade ethanol gives better clearing results than washing grade ethanol.
- Tissue should be cleared in large volume (e.g., 15–50 mL) tubes.
- Concentrations of antibodies are still a matter of debate – some researchers advise to not increase but lower the concentration when labelling in the centre of the tissue is insufficient. Other researchers state that 5–15× the concentration used in 2D should be used for 3D tissue that will undergo clearing.[13] Certainly, the concentration needs to be optimized for each antibody.
- An antibody that works reliably for whole mount and on sections is not guaranteed to work after clearing.

- Some antibodies that do not interact on sections when combined could interact in 3D, leading to false labelling. Furthermore, tissue clearing has been shown to modify the intensity of the emitted light and to shift the absorption and emission peaks. These changes can result in leak-through into other filters/channels and consequently result in false interpretation.[17] It is therefore essential to validate antibodies individually on uncleared organoids, such as on sections in 2D, and use the results as a reference for 3D.
- If there is a halo or the periphery is strongly stained and the centre is dim, there are several solutions:
    - Modify the antibody concentration.
    - Increase the antibody incubation time at 4 °C.
    - Increase laser intensity in z-depth during imaging (z-intensity correction).
    - Perform post z-intensity correction. (However, this correction may be challenging with a poor signal-to-noise ratio because noise will be strongly amplified in depth).
- Some antibodies might lose their binding strength over time or after freezing and thereby no longer be suitable for clearing. The latter happened for one antibody (CD31 used in Chapter 6), even though it could be frozen according to datasheet. However, two weeks after freezing, it kept failing in the clearing protocol and only the fresh antibody (not yet frozen) could be used. At the same time, the frozen antibody worked reliably on cryosections after 1.5 years.
- Specifically for the ECi protocol:
    - Ethanol solutions containing PBS used for dehydration of samples will precipitate phosphate after about 1.5–2 hours at 4 °C. The solutions should therefore be changed frequently, and the incubation times should be kept short or executed at room temperature (although the latter might affect the clearing result).
    - Preparing the dehydration solutions should be done at least a couple of hours in advance, since the solutions warm up and produce air bubbles when ethanol and PBS are combined.

To conclude, tissue clearing has proven a suitable technique to allow high-resolution whole mount imaging of kidney organoids. More specifically, clearing with ECi gave the best result, although FRUIT might be a suitable alternative with more optimization. The lower and adjustable RI of FRUIT would allow imaging with higher magnification or lower wavelengths.

Furthermore, nanobodies have been shown to solve the issue of heterogeneous staining of large samples, due to their 10× smaller size. Light-sheet microscopy has already been in use for a few years (more recently on organoids) and stands out for its quick imaging time. A recent perspective showed that in the past four years, all of the three clearing techniques (solvent-based, aqueous and hydrogel-embedded) have proven applicable for spheroid and organoid clearing.[18] While we critically note that direct comparisons between methods are often lacking and this dearth hampers finding the ideal method, it could be argued that the ideal clearing method will remain dependent on the organoid type, the research question, and the available microscopes. Nevertheless, tissue clearing will likely become the standard for large organoid models with high morphological complexity, eventually allowing 3D organoid microscopy data to be integrated in single-cell transcriptomic datasets and contribute to aims such as the Organoid Cell Atlas.[19]

References

1 Spalteholz, W. *Ueber das durchsichtigmachen von menschlichen und tierischen praeparaten und seine theoretischen bedingungen*. (S. Hirzel, 1914).

2 Dodt, H. U. *et al.* Ultramicroscopy: Three-dimensional visualization of neuronal networks in the whole mouse brain. *Nat Methods* **4**, 331-336, doi:10.1038/nmeth1036 (2007).

3 Cai, R. *et al.* Panoptic imaging of transparent mice reveals whole-body neuronal projections and skull-meninges connections. *Nat Neurosci* **22**, 317-327, doi:10.1038/s41593-018-0301-3 (2019).

4 Richardson, D. S. & Lichtman, J. W. Clarifying tissue clearing. *Cell* **162**, 246-257, doi:10.1016/j.cell.2015.06.067 (2015).

5 Nowzari, F. *et al.* Three-dimensional imaging in stem cell-based researches. *Front Vet Sci* **8**, 657525, doi:10.3389/fvets.2021.657525 (2021).

6 Gomez-Gaviro, M. V., Sanderson, D., Ripoll, J. & Desco, M. Biomedical applications of tissue clearing and three-dimensional imaging in health and disease. *iScience* **23**, 101432, doi:10.1016/j.isci.2020.101432 (2020).

7 Ariel, P. A beginner's guide to tissue clearing. *Int J Biochem Cell Biol* **84**, 35-39, doi:10.1016/j.biocel.2016.12.009 (2017).

8 Voros, J. The density and refractive index of adsorbing protein layers. *Biophys J* **87**, 553-561, doi:10.1529/biophysj.103.030072 (2004).

9 Zukor, K. A., Kent, D. T. & Odelberg, S. J. Fluorescent whole-mount method for visualizing three-dimensional relationships in intact and regenerating adult newt spinal cords. *Dev Dyn* **239**, 3048-3057, doi:10.1002/dvdy.22441 (2010).

10 Hou, B. *et al.* Scalable and dii-compatible optical clearance of the mammalian brain. *Front Neuroanat* **9**, 19, doi:10.3389/fnana.2015.00019 (2015).

11 Costantini, I. *et al.* A versatile clearing agent for multi-modal brain imaging. *Sci Rep* **5**, 9808, doi:10.1038/srep09808 (2015).

12 Hama, H. *et al.* Scale: A chemical approach for fluorescence imaging and reconstruction of transparent mouse brain. *Nat Neurosci* **14**, 1481-1488, doi:10.1038/nn.2928 (2011).

13 Murray, E. *et al.* Simple, scalable proteomic imaging for high-dimensional profiling of intact systems. *Cell* **163**, 1500-1514, doi:10.1016/j.cell.2015.11.025 (2015).

14 Klingberg, A. *et al.* Fully automated evaluation of total glomerular number and capillary tuft size in nephritic kidneys using lightsheet microscopy. *J Am Soc Nephrol* **28**, 452-459, doi:10.1681/ASN.2016020232 (2017).

15 *RefractiveIndex.INFO: Refractive Index Database*, https://refractiveindex.info/?shelf=organic&book=ethyl_cinnamate&page=Krauter Accessed: 16-04-2023.

16 Krauter, P. *et al.* Optical phantoms with adjustable subdiffusive scattering parameters. *J Biomed Opt* **20**, 105008, doi:10.1117/1.JBO.20.10.105008 (2015).

17 Eliat, F. *et al.* Tissue clearing may alter emission and absorption properties of common fluorophores. *Sci Rep* **12**, 5551, doi:10.1038/s41598-022-09303-9 (2022).

18 Susaki, E. A. & Takasato, M. Perspective: Extending the utility of three-dimensional organoids by tissue clearing technologies. *Front Cell Dev Biol* **9**, 679226, doi:10.3389/fcell.2021.679226 (2021).

19 Bock, C. *et al.* The organoid cell atlas. *Nat Biotechnol* **39**, 13-17, doi:10.1038/s41587-020-00762-x (2021).

Chapter 6

Enhanced microvasculature formation and patterning in iPSC–derived kidney organoids cultured in physiological hypoxia

A. Schumacher[1], N. Roumans[1], T. Rademakers[1], V. Joris[1], M. Eischen-Loges[1,2], M. van Griensven[1], V.L.S. LaPointe[1*]

This chapter has been published as:

Schumacher, A, Roumans, N, Rademakers, et al. *Enhanced Microvasculature Formation and Patterning in iPSC–Derived Kidney Organoids Cultured in Physiological Hypoxia*. Front. Bioeng. Biotechnol. 10:860138. (2022) https://doi.org/10.3389/fbioe.2022.860138

Graphical abstract

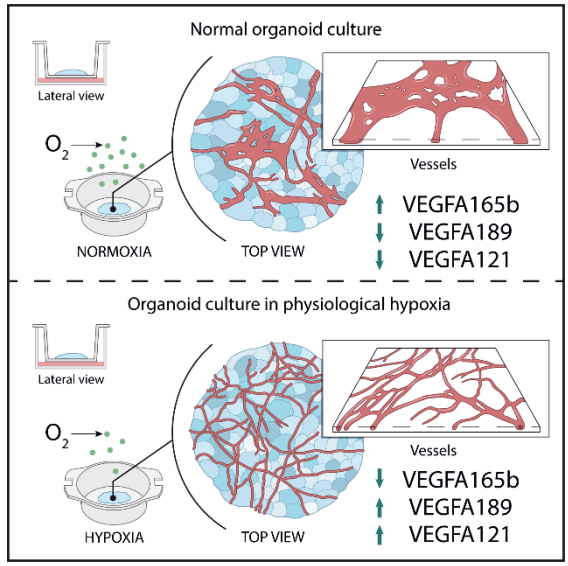

Abstract

Stem cell–derived kidney organoids have been shown to self-organize from induced pluripotent stem cells into most important renal structures. However, the structures remain immature in culture and contain endothelial networks with low connectivity and limited organoid invasion. Furthermore, the nephrons lose their phenotype after approximately 25 days. To become applicable for future transplantation, further maturation *in vitro* is essential. Since kidneys *in vivo* develop in hypoxia, we studied the modulation of oxygen availability in culture. We hypothesized that introducing long-term culture at physiological hypoxia, rather than the normally applied non-physiological, hyperoxic 21% O_2, could initiate angiogenesis, lead to enhanced growth factor expression and improve the endothelial patterning. We therefore cultured the kidney organoids at 7% O_2 instead of 21% O_2 for up to 25 days and evaluated nephrogenesis, growth factor expression such as VEGF-A and vascularization. Whole mount imaging revealed a homogenous morphology of the endothelial network with enhanced sprouting and interconnectivity when the

kidney organoids were cultured in hypoxia. Three-dimensional vessel quantification confirmed that the hypoxic culture led to an increased average vessel length, likely due to the observed upregulation of VEGF-A189 and VEGF-A121 mRNA and downregulation of the antiangiogenic protein VEGF-A165b measured in hypoxia. This research indicates the importance of optimization of oxygen availability in organoid systems and the potential of hypoxic culture conditions in improving the vascularization of organoids.

Introduction

Organoid models have become an irreplaceable alternative to two-dimensional cell culture because of their greater cellular and architectural complexity, which is alike native tissue. Induced pluripotent stem cells can be differentiated into kidney organoids that develop nephrons resembling capillary loop–stage nephrons.[1] The large variety of renal cell types they possess, similar to the developing kidney[2], makes them promising models for regenerative medicine, drug testing and developmental biology[3]. However, these organoids have several drawbacks—such as the limited culture duration, loss of nephrogenic potential, immaturity and lack of vasculature[4,5]—perhaps due the lack of an *in vivo*–like culture environment, which is increasingly being investigated.[6] Moreover, kidney organoids are one of the largest organoid models, growing up to 1.5 mm in thickness.[1] This draws attention to one aspect of a physiological environment, which is the oxygenation of the tissue.

Cell culture in hypoxia, defined as a state where cells no longer have sufficient oxygen available to use oxidative phosphorylation to generate ATP[7], has been performed for more than a decade, for example to maintain stem cells[8]. Hypoxia is also known to act as a morphogen in cell communication of various cell lineages and for certain cell types to partially determine cellular differentiation.[9] If not optimized to the model system, hypoxia is known to have detrimental effects in cell and tissue culture. Nevertheless, to date, there is little knowledge on the effects of hypoxia in organoid cultures. Briefly, hypoxic culture (5% O_2) of intestinal organoids was considered detrimental due to a reduced number of crypts.[10] In contrast, microwell-cultured kidney organoids cultured for 24 h in hypoxia (1 and 3% O_2) showed

enhanced functionality measured by secretion of erythropoietin (EPO).[11] These results argue that oxygen levels critically affect maturation of organoids, in a model-sensitive manner.

Kidney organoids are cultured, like explanted kidneys[12], at an air–liquid interface and therefore are directly exposed to incubator air (21% O_2), commonly defined as normoxia. However, it has been previously well described that 21% O_2 is non-physiological.[7] For this reason, and the fact that the physiological environment of the developing kidney is hypoxic, we do consider 21% O_2 to be hyperoxic and non-physiological. This is particularly the case for endothelial cells, which largely reside on the organoids' surface. Hyperoxia is known to negatively impact kidney development *in vivo,* such as significantly reducing the size of the nephrogenic zone and glomeruli.[13] *In vitro*, the detrimental effects of hyperoxic cell and tissue culture are also well established[14,15], such as the formation of reactive oxygen species in endothelial cells[16]. By contrast, there is significant evidence that hypoxia enhances the proliferation of endothelial cells as well as stem cell differentiation towards an endothelial lineage.[17-23] Murine metanephric explants showed enhanced endothelial cell proliferation when cultured in hypoxia (3% O_2).[24,25] Furthermore, the mammalian uterus is hypoxic and fetal organs develop in hypoxic environments.[26,27] Therefore, modulating the oxygen concentrations could be a step towards *in vivo*–like kidney organoid culture with improved vascularization.

In developing kidneys in the hypoxic mammalian uterus[26,28], nephrogenesis starts in the avascular nephrogenic zone.[29,30] Later in the capillary loop stage of nephrogenesis, mainly angiogenesis and to a lesser extent vascularization start to take place.[4] Only when blood vessels enter the kidney and new vessels are formed, oxygen levels increase to finally reach 4–9.5 kPa (30–71 mmHg) in the adult human cortex and 2 kPa (15 mmHg) in the adult human medulla.[31] Due to the invasive nature of the measurements, the oxygen tensions in developing human cortex and medulla have not been determined. Recapitulating this *in vivo* hypoxic environment in the kidney organoid culture could enable the transcription of genes essential in kidney organogenesis. Below 5% O_2, binding of prolyl hydroxylases to cytoplasmic hypoxia-inducible factor alpha (HIFα) is inhibited, leading to reduced or inhibited proteosomal degradation. Consequently, HIFα rapidly accumulates, translocates

into the nucleus and its dimerization with HIFβ is initiated.[29] Dimer binding to hypoxia responsive element (HRE) promoters leads to the transcription of a variety of genes. While this process occurs in all tissue types, it is known that various HIF-regulated genes are implicated in angiogenesis and vascularization in kidney organogenesis. In kidney development, nuclear HIF translocation occurs in metanephric mesenchyme and subsequently in podocytes, leading to VEGF-A transcription, which attracts endothelial cells to vascularize the nephrons.[32,33]

Developmentally, kidney organoids, normally cultured at non-physiological hyperoxic 21% O_2 (≈160 mmHg), are comparable to kidneys in the first to early second trimester.[34] Since, however, the oxygen concentrations in the developing human kidney are unknown, we hypothesized whether a culture at 7% O_2 (≈53 mmHg), comparable to the adult human cortex, would lead to intra-organoid oxygen concentrations more closely resembling developing non-vascularized kidneys *in vivo,* and initiate angiogenesis in the organoids. After up to 25 days of culture, we analyzed nephrogenesis, the expression of angiogenic markers (particularly VEGF) and endothelialisation to determine whether hypoxic cultures of the organoids improved these characteristics compared to cultures at 21% O_2. We found that long-term hypoxic culture enhances endothelial patterning and sprouting and consequently could enhance kidney organoid cultures towards a more *in vivo*–like model.

Materials and Methods

Induced pluripotent stem cell differentiation and kidney organoid culture

Induced pluripotent stem cells (iPSCs) were differentiated and the organoids were cultured according to the previously published protocol by van den Berg, et al. [35] (Figure 1A). Briefly, the iPSC line LUMC0072iCTRL01 (male fibroblasts reprogrammed using RNA Simplicon reprogramming kit, Millipore) obtained from the hiPSC core facility at the Leiden University Medical Center, were passaged biweekly and maintained in 3 mL of Essential 8 Medium (Thermo Fisher Scientific) supplemented with 1% penicillin–streptomycin in 6-well plates coated with truncated recombinant human vitronectin (Thermo Fisher Scientific). The iPSC line

was previously assessed for pluripotency and normal karyotype.[36] For differentiation, 80,000 cells per well were seeded into a six well plate and differentiated according to the published protocol in organoid culture medium composed of STEMdiff APEL2 medium (STEMCELL Technologies), supplemented with 1% antibiotic-antimycotic and 1% protein-free hybridoma medium II (PFHM 2) (Thermo Fisher Scientific) and the respective growth factors and small molecules (8 μM GSK-3 inhibitor CHIR99021 (R&D Systems), 200 ng/mL FGF9 (fibroblast growth factor 9; R&D Systems), and 1 μg/mL heparin (Sigma-Aldrich)). After 7 days of differentiation, the cells were aggregated by centrifugation and spotted on transwell tissue culture plates with 0.4 μm pore polyester membrane inserts (Corning) and cultured at an air–liquid interface. For an additional 5 days, denoted as day 7+5, the organoids were cultured in organoid medium containing the growth factors and small molecules. From day 7+5 onwards, the organoids were cultured in organoid culture medium either in a hypoxia incubator (37°C, 5% CO_2, 7% O_2) or in normoxia (37°C, 5% CO_2, 21% O_2). The medium was refreshed every 2 days. At day 7+18 and day 7+25, the organoids were assessed.

Darkfield imaging

The organoids were fixed at day 7+18 and day 7+25 in 2% (v/v) paraformaldehyde (20 min, 4°C) and were subsequently embedded in 10% gelatin in PBS (phosphate-buffered saline) in a cryomold. Once hardened, the gel was pealed out of the mold and placed on a darkfield imaging stage with circular illumination (Nikon). Images were acquired using a 1× air objective on a Nikon SMX25 automated stereomicroscope with a customized Nikon darkfield illumination holder.

Cryopreservation and cryosectioning

After fixing the organoids at day 7+18 or day 7+25 in 2% (v/v) paraformaldehyde (20 min, 4°C), the organoids were cryoprotected. The organoids were immersed in 15% (w/v) sucrose in 0.1 M phosphate buffer containing 0.1 M dibasic sodium phosphate and 0.01 M monobasic sodium phosphate in MilliQ water (24 h, 4°C, rotating), and

subsequently in 30% (w/v) sucrose in 0.1 M phosphate buffer (48 h, 4°C, rotating). After cryoprotection, the organoids were embedded in freezing medium (15% (w/v) sucrose and 7.5% (w/v) gelatin in 1 M phosphate buffer) and hardened on ice. Freezing was performed in an isopentane bath in liquid nitrogen and the blocks were stored at -30°C until cryosectioning at -18°C into 12 μm–thick sections. The sections were stored at -80°C until use.

Oxygen measurement

The oxygen concentration within the organoids was measured using an optical oxygen microsensor (PM-PSt7, Presens in Regensburg, Germany). The probe was calibrated according to the manufacturer's instructions. Briefly, the pressure settings were set to the elevation of the lab (997 kPa) and the probe was calibrated in an oxygen-depleted solution (water containing 70 mM sodium sulfite and 500 mM cobalt nitrate) followed by an oxygen-enriched solution (water connected to a room air valve). All solutions were equilibrated to room temperature before calibration and room temperature (20°C) was put as standard in the software. At day 7+18 and day 7+25, organoids in both normoxia and hypoxia were measured using the calibrated sensor. The sensor was fixed to a micromanipulator and was inserted into the bottom of the organoid, approximately 1 mm in depth, close to the insert membrane of the transwell. The incubator was kept closed to ensure a stable gas concentration and measurements were continued until the signal reached a steady state (taking approximately 30–90 min).

Hypoxia imaging

Hypoxia was measured in living organoids using the Image-iT Green Hypoxia Reagent (Thermo Fisher Scientific), which produces a green fluorescent signal below 5% O_2. The organoid was fully immersed in 5 μM ImageIT Green reagent dissolved in organoid culture medium for 4 h in normoxia. Subsequently, the staining solution was replaced with fresh medium and the organoids were moved to the incubator set to either the 7% O_2 or the 21% O_2 for 6 h, after which they were fixed for

cryosectioning or imaged live. For live imaging, the organoids were imaged using a 10× air objective on an automated Nikon Eclipse Ti-E equipped with a spinning disk with a 70 μm pore size, a Lumencor Spectra X light source and Photometrics Prime 95B sCMOS camera. For cryosectioning, the method in Section 2.3 was applied. The sections were imaged with the same microscope using a 20× air objective and a 40× oil objective. All images were processed using Fiji[37], in which the rolling ball function was applied in the case of poor signal to noise ratio.

Immunofluorescence

The cryosections were warmed to RT (room temperature) and subsequently incubated in pre-warmed PBS (15 min, 37°C), to remove the sucrose and gelatin. Next, the cryosections were blocked with PBS containing 0.2% (v/v) Tween, 10% (w/v) BSA (bovine serum albumin) and 0.1 M glycine (20 min, RT) and incubated in primary antibodies (Supplementary Table 1) diluted in the dilution buffer of PBS containing 0.2% (v/v) Tween, 1% (w/v) BSA and 0.1 M glycine (overnight, 4°C). After washing in PBS containing 0.2% (v/v) Tween, the slides were incubated with appropriate secondary antibodies (Supplementary Table 1) diluted in the dilution buffer (1 h, RT). Finally, the slides were washed and mounted with Prolong Gold (Thermo Fisher Scientific). After curing for two days, imaging was performed on the automated Nikon Eclipse Ti-E microscope using a 20× air and a 40× oil objective. All images were processed using Fiji[37], in which the rolling ball function was applied in the case of poor signal to noise ratio.

Luminex assay

The VEGF-A concentration in the culture medium was analyzed using a VEGF-A Human ProcartaPlex Simplex Kit (Cat. no. EPX01A-10277-901, Invitrogen), specific for the detection of VEGF-A165. The medium was collected on days 7+7, 7+12, 7+17, 7+21, and 7+24 and centrifuged (10 min, 4°C, 239 x g). The supernatant was immediately stored at -80°C. The assay was performed according to the manufacturer's instructions. In brief, samples were diluted 1:50 in universal assay

buffer and 50 μL was added to the wells containing the antibody-coupled beads, along with the standards provided with the assay (30 min, RT, shaking). After an overnight incubation (4°C) and a final incubation (30 min, RT, shaking), detection antibody–biotin reporters were added to each well (30 min, RT, shaking). Next, fluorescent conjugate streptavidin–phycoerythrin was added (30 min, RT, shaking). After a final washing step, the beads were resuspended in 120 μL reading buffer. Fluorescence intensities were measured using a Luminex100 instrument (Bio-Rad) which was calibrated before each use. Data acquisition was done with the Bio-Plex Manager 6.0 software. The data were normalized to the standard curve dilutions delivered with the kit according to manufacturer's instructions.

Western blot

After snap freezing in liquid nitrogen, the organoids were resuspended in 70 μL RIPA (radioimmunoprecipitation assay) lysis buffer (Sigma-Aldrich) supplemented with phosphatase inhibitor tablets PhosSTOP (Sigma-Aldrich) and protease inhibitor cOmplete ULTRA Tablets (Sigma-Aldrich). The protein concentrations were determined using a Pierce BCA Protein Assay Kit (Thermo Fisher Scientific) according to the manufacturer's protocol. Per well, 15 μg of protein was loaded. The migration was performed in migration buffer (Tris [tris(hydroxymethyl)aminomethane]-EDTA (ethylenediaminetetraacetic acid), SDS (sodium dodecyl sulfate), glycine, Bio-Rad) at 120 V. Subsequently, the proteins were transferred onto a nitrocellulose membrane at 350 mA for 90 min in a transfer buffer (Tris-base, glycine, SDS, 20% methanol). After the transfer, the membranes were blocked in blocking buffer (TBS (Tris-buffered saline), 0.1% Tween (v/v), 5% BSA (w/v)) (1 h, RT, shaking). Next, the membranes were incubated with primary antibodies (Table 1) (overnight, 4°C, shaking) in TBS-Tween, 5% BSA (w/v). The membranes were washed in TBS-Tween and incubated with the peroxidase-conjugated secondary antibody (Bio-Rad, Table 1) for 1 h at RT. The membranes were incubated with Clarity Western ECL substrate (Bio-Rad) and were developed using a ChemiDoc (Bio-Rad). The protein bands were quantified by densitometry using ImageJ, normalized to GAPDH.[38]

RNA isolation and qPCR

Organoids stored in TRIzol at -80°C were thawed and pipetted vigorously to homogenize the samples. Then, 500 µL was transferred to a Phasemaker tube (Thermo Fisher Scientific) after which, 100 µL of chloroform were added, shaken thoroughly and incubated for 5 min at RT. The mixture was centrifuged at 12,000 × g (15 min, 4°C). The aqueous phase was carefully transferred to a new microcentrifuge tube containing 250 µL isopropanol and 1 µL glycogen. After an additional centrifugation step (15 min, 4°C, 12,000 × g) the pellet was washed twice with 200 mM NaOAc in 75% ethanol. The supernatant was discarded, and the pellet was dried at 55°C, resuspended in 25 µL nuclease-free water, and incubated at 55°C with shaking. CDNA was synthesized using the iScript cDNA synthesis kit (Bio-Rad) and 500 ng/µL of RNA was loaded per sample. Quantitative PCR was carried out with iQ SYBR Green Supermix (Bio-Rad), 5 ng cDNA per reaction, on a CFX96TM Real-Time system (Bio-Rad). Primer sequences (Supplementary Table S2) were verified using total human kidney RNA (Takara Bio). *PSMB4* was determined as the most stable housekeeping gene using the method described by Xie, et al. [39], and *GAPDH* was used as a second housekeeping gene to ensure valid results. The data were normalized to *PSMB4* and plotted relative to the expression of the control samples day 7+18 normoxia. Each data point represents one organoid of three distinct iPSC differentiations. The statistics were performed on the log (fold change) and plotted onto the fold change graphs.

Whole mount immunofluorescence, tissue clearing and automated imaging

Whole organoids were fixed in 2% paraformaldehyde (20 min, 4°C) and blocked in PBS containing 10% goat serum, 0.1 M glycine and 0.5% Triton X-100 (overnight, 4°C, shaking). They were incubated in primary antibodies (Supplementary Table S1) diluted in PBS containing 10% goat serum, 0.1 M glycine and 0.06% Triton X-100 (3 days, 4°C, shaking). After two washes in 0.3% Triton X-100 in PBS (2 h, RT, shaking), the organoids were incubated with the appropriate secondary antibodies (Supplementary Table S1) diluted in PBS containing 1% goat serum, 0.1 M glycine and 0.06% Triton X-100 (3 days, 4°C, shaking). After two washes (2 h, RT, shaking),

the organoids were cleared using the method of Klingberg, et al. [40]. Briefly, the organoids were dehydrated in a series of 30%–100% molecular biology–grade ethanol and submerged in ethyl cinnamate (overnight, RT followed by 1 h, 37°C). Imaging was done immediately after on an automated Nikon Eclipse Ti-E with the 70 μm spinning disk in place. Imaging was automated using a Nikon JOBS tool. Briefly, a 10× air objective was used for automated detection of the organoid, while a 20× air objective with an extra-long working distance was used to image at higher resolution with a z increment size of 5 μm.

Automated image processing and vessel quantification

Immunofluorescence of VEGF-A on cryo-sections was quantified using FIJI. The FIJI default threshold was applied on the DAPI channel and the Renyi Entropy threshold on the VEGF-A channel. Next, the area of both thresholded signals was measured and the area of VEGF-A was normalized to the area of DAPI signal to correct for different sizes of sections. The results are presented as percent area.

Whole mount images were processed within a processing and quantification JOB specifically made for these samples, integrated in the NIS-Elements AR (Advance Research) (Nikon) software. In summary, background was removed using the clarify AI tool prior to the segmentation of the CD31 signal. The CD31 signal was thresholded by intensity and segmented by measuring the longest medial axis in 3D. Falsely segmented pixels, due to intense background signal, were excluded by circularity and minimal size if needed. The volume of the segmented signal was measured in 3D for the full organoid. The volume of the total organoid was measured by segmenting the organoid based on the strong background. The percentage of vascularization was determined by calculating the CD31+ cell volume as a fraction of the total organoid volume. Furthermore, the segmented CD31 signal was skeletonized to measure the cumulative and average length of all fragments in 3D. Stepwise details on the used JOB can be found in Supplementary Figure S1.

Statistical analysis

All statistical analyses were performed using GraphPad Prism 9. For all immunofluorescence protein analyses, three organoids (n=3) each arising from one of three independent organoid cultures (N=3) were assessed. One organoid (n=1) arising from one of three (N=3) independent organoid cultures was quantified in 3D. For the gene expression analysis and Luminex assay, three organoids (n=3) each arising from one of two independent organoid cultures (N=2) were analyzed. Two organoids (n=2), each arising from one of three independent organoid cultures (N=3) were assessed for the darkfield measurement and oxygen measurement. Individual samples were excluded only for technical failures. For each figure, the exact N and n are reported in the figure caption. A two-way ANOVA was performed for each experiment to assess the contribution of both row (time point) and column (oxygen concentration) factors. All *p*-values can be found in the Results section. Statistical significance was only concluded for *p*-values below 0.05.

Results

Macro-morphology and oxygen concentrations in normoxic and hypoxic organoid culture

To replicate the *in vivo* hypoxic environment, we cultured kidney organoids in 7% O_2 and compared them to their counterparts cultured in 21% O_2 (Figure 1A). Brightfield analysis revealed no differences in macro morphology, density or size until day 7+25 (Figure 1B, Supplementary Figure 2). Darkfield imaging was performed to assess the shape and thickness of the organoids (Figure 1C). No statistically significant differences in thickness were found comparing organoids cultured in normoxia and hypoxia ($p = 0.839$; Figure 1D).

To quantify the oxygen concentration, we inserted an optical microsensor into the bottom of the organoid (close to the filter). In normoxia, the lowest oxygen concentration we measured was 7.53 ± 1.47% on day 7+18, which significantly decreased to 2.15 ± 0.66% by day 7+25 ($p < 0.0001$). This value at day 7+25 was not significantly different from the oxygen concentration measured in the organoids

cultured in hypoxia on day 7+18 (1.28 ± 0.76%; $p = 0.439$) or day 7+25 (1.00 ± 0.21%; $p = 0.211$) (Figure 1E).

To investigate whether the organoids had a hypoxic core, we imaged living organoids and cryosections at the center of the organoids with a hypoxia dye (ImageIT Green) (Figure 1F). The cryosections, cut through the center of the organoids, revealed a higher intensity (meaning lower O_2) in hypoxia. We saw the dye localized largely to nephron structures and less to the surrounding stroma. We did not see evidence of a hypoxic core in the center of any organoids.

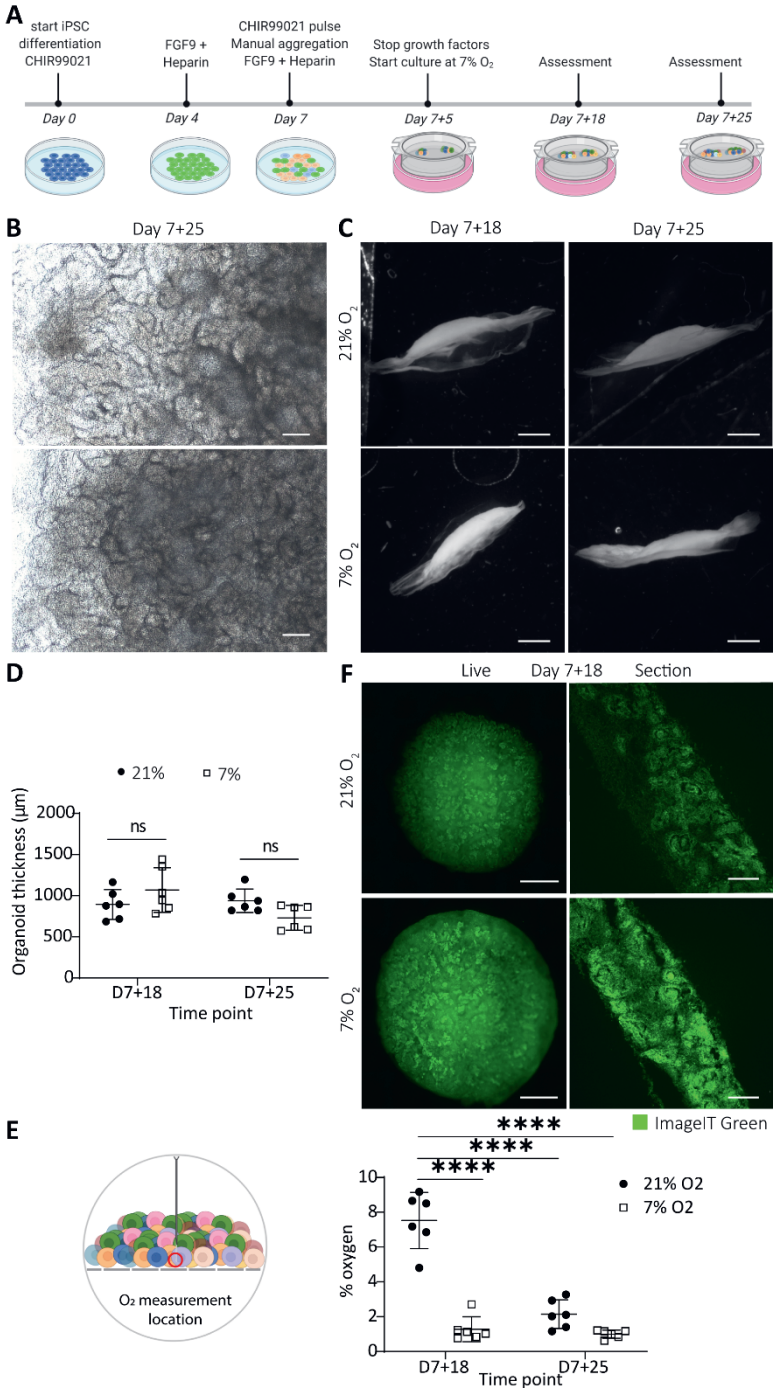
A
start iPSC differentiation CHIR99021
FGF9 + Heparin
CHIR99021 pulse Manual aggregation FGF9 + Heparin
Stop growth factors Start culture at 7% O2
Assessment
Assessment
Day 0
Day 4
Day 7
Day 7+5
Day 7+18
Day 7+25
B
Day 7+25
C
Day 7+18
Day 7+25
21% O2
7% O2
D
21%
7%
Organoid thickness (µm)
2000
1500
1000
500
0
ns
ns
D7+18
D7+25
Time point
E
O2 measurement location
F
Live
Day 7+18
Section
21% O2
7% O2
ImageIT Green
****
****
****
% oxygen
10
8
6
4
2
0
21% O2
7% O2
D7+18
D7+25
Time point

Figure 1: Kidney organoids cultured in uterine-like hypoxic environment structurally form like their normoxic counterparts without the appearance of a hypoxic core. A. Schematic representation of the iPSC differentiation and organoid culture. Human iPSCs are differentiated for 7 days, after which aggregates are spotted on the air–liquid interface and cultured as organoids for up to 25 additional days (termed day 7+25). B. Brightfield images display comparable morphologies of the organoids cultured in 7% and 21% O_2 at the culture endpoint day 7+25. Scale bar: 200 μm. C. Darkfield images show that the macro-anatomy of the organoids is comparable in both oxygen concentrations. Scale bar: 2 mm. D. Quantification of the organoid thickness from the darkfield images shows no difference between 21% O_2 and 7% O_2. (n=2, N=3). E. Oxygen measurement in the bottom part of the organoids towards the transwell filter shows that organoids in 7% oxygen have a comparable oxygen concentration to their normoxic counterparts at day 7+25, which is significantly lower compared to the normoxic condition at day 7+18. (n=2, N=3; **** = $p \leq 0.0001$) F. Organoids (left column) and cryosections of their central core (right column) stained on day 7+18 with the hypoxia dye ImageIT Green that produces a fluorescent signal below 5% O_2. The organoids display no hypoxic core but the dye stains all3 nephrons. Scale bar "live": 1 mm, scale bar "section": 100 μm.

Next, we explored if culture in hypoxia would affect the differentiation and organization of various cell types in the kidney organoids. To assess this, we stained vertically cut cryosections throughout the whole organoids for well-established markers to label the major cell types found in kidney organoids. We found no differences in either the presence of the cell types or their organization into proximal tubules (LTL), distal tubules (ECAD), loop of Henle (SLC12A1) or glomeruli (NPHS1-positive podocytes) (Figure 2A,B).

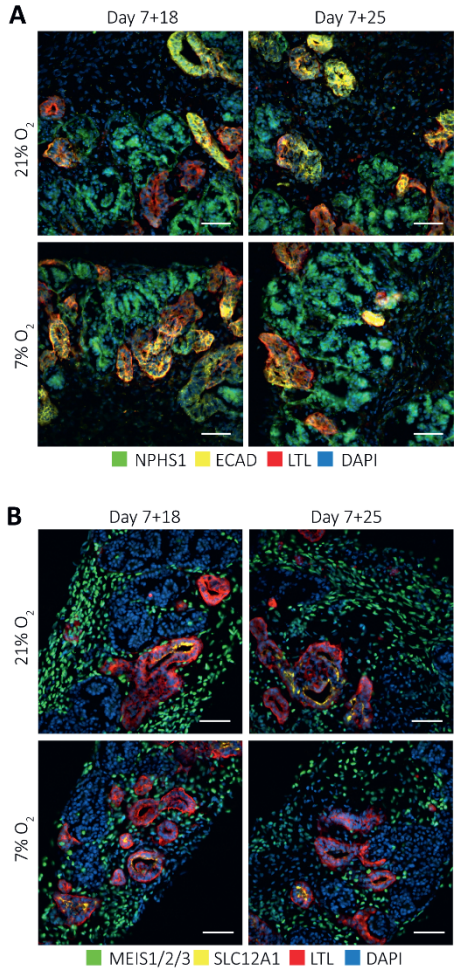

Figure 2: Kidney organoids cultured at 7% and 21% O_2 develop the same cell types. Immunofluorescence staining for A. podocytes (NPHS1; green), proximal tubules (LTL; red) and distal tubules (ECAD; yellow) and nuclei (DAPI; blue), and B. interstitial cells (MEIS1/2/3; green), loop of Henle (SLC12A1; yellow) and proximal tubules (LTL; red), showed these different cell types in all conditions. (n=3, N=3). Scale bars: 50 μm.

Nephrons express varied levels of nuclear HIF1α and a constant nuclear expression of HIF2α

Nuclear HIF translocation during kidney development is crucial for nephrogenesis and angiogenesis. We investigated which cells showed responsiveness to hypoxia in terms of nuclear translocation of HIF1α and HIF2α. For this, we performed immunofluorescence staining of HIF1α and HIF2α on vertically cut cryosections throughout the whole kidney organoids at days 7+18 and 7+25. Qualitative analysis showed that HIF1α was differentially expressed in hypoxia and normoxia (Figure 3A). At day 7+25, particularly the podocytes had more nuclear translocation in both normoxia and hypoxia compared to other cell types. Furthermore, in normoxia, podocytes at the bottom of the organoid, towards the medium interface, expressed nuclear HIF1α, while in hypoxia this was seen in podocytes throughout the whole organoid. In all conditions and time points, interstitial cells and most tubules did not express nuclear HIF1α. HIF2α was expressed in the nuclei of all cells of the kidney organoids at days 7+18 and 7+25 (Figure 3B). Particularly the interstitial cells had heterogeneous expression. We did not detect differences between organoids cultured in normoxia or hypoxia in terms of HIF2α nuclear translocation.

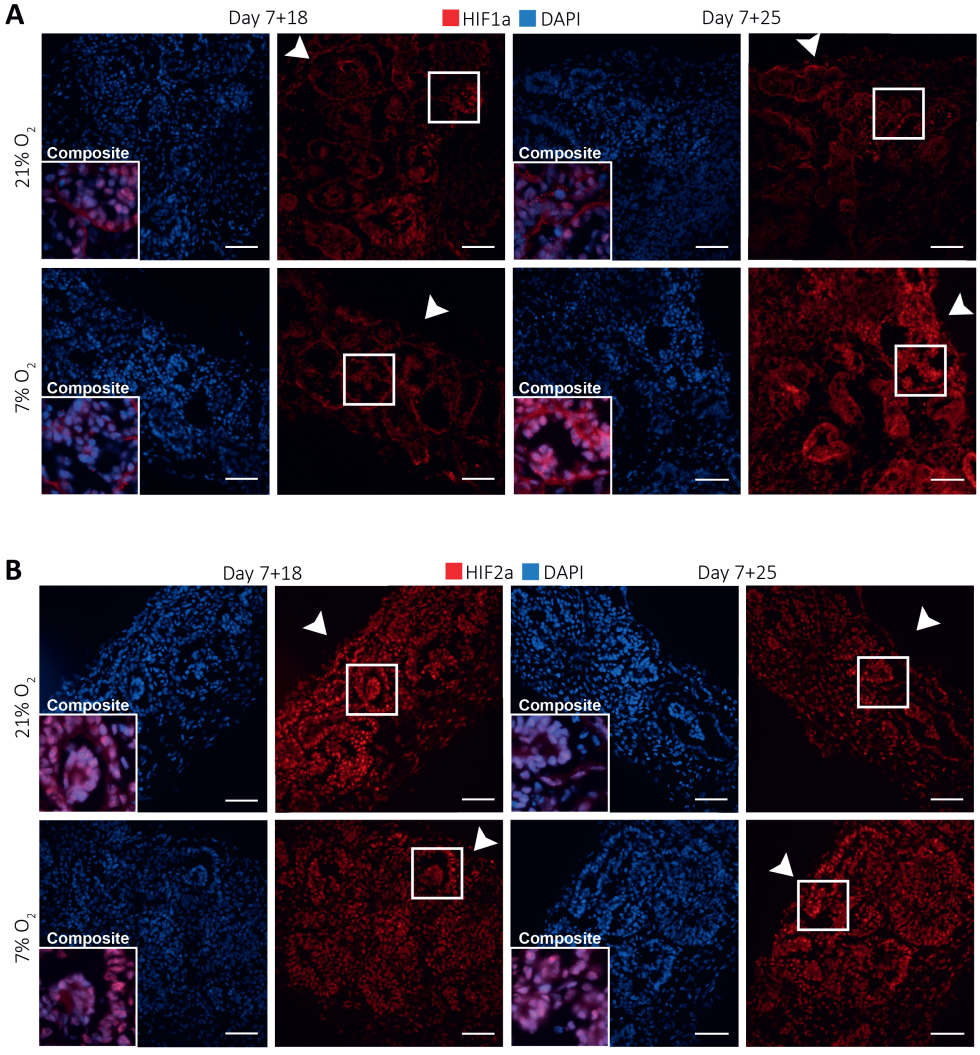

Figure 3: Kidney organoids cultured in both 7% and 21% O_2 show differential nuclear translocation of HIF1a and HIF2a. A. Immunofluorescence staining for HIF1a (red) and DAPI (blue) shows increased nuclear translocation in podocytes (composite), particularly in 7% O_2 at day 7+25. Scale bar: 50 μm. B. HIF2a (red) and DAPI (blue) immunofluorescence staining shows nuclear translocation in most cells within the organoid irrespective of the oxygen concentration or time point. (n=3, N=3). Scale bar: 50 μm. Arrowheads indicate the (air-exposed) surface of the organoids.

VEGF-A protein expression in proximal tubules

VEGF-A is a major angiogenic factor primarily produced in distal tubules, collecting duct and podocytes.[41] It is regulated by hypoxia by the binding of nuclear, dimerized HIFs to the HRE promotor. We performed immunofluorescence on vertically cut cryosections throughout whole organoids to determine if there was a difference in expression between normoxia- and hypoxia-cultured organoids (Figure 4A), and which cell types expressed VEGF-A (Figure 4B). We found expression on the apical side of some tubular structures, mainly in normoxia and to a lesser extent in hypoxia (Figure 4A, B). VEGF-A was significantly less expressed in hypoxia compared to normoxia at both time points ($p = 0.02$ at d7+18, $p = 0.013$ at d7+25), but there was no difference between the two time points ($p = 0.362$ in normoxia, $p = 0.461$ in hypoxia) (Figure 4D). The VEGF-A+ tubules in both normoxia and hypoxia co-expressed both SLC12A1 marking the loop of Henle (thick ascending limb) and LTL marking proximal tubules (Figure 4B). We validated this co-expression of SLC12A1, LTL and VEGF-A on adult kidney sections and in scRNA sequencing datasets of organoids (Supplementary Figure S3). Glomerular expression of VEGF-A in the normoxia and hypoxia organoids rarely found. We hypothesized that the lower VEGF-A expression in the proximal tubules in hypoxia could be due to a switch to a more soluble VEGF-A isoform or that the time point of secretion would be different. Therefore, soluble VEGF-A was measured using a Luminex assay validated for the VEGF-A165 isoform in the culture medium on days 7+7, 7+12, 7+17, 7+21, 7+24 (Figure 4C). There was an increase over time from day 7+7 until 7+17 for organoids in both hypoxia and normoxia. After day 7+17, the soluble VEGF-A decreased until day 7+21. There was no significant difference between organoids in normoxia or hypoxia ($p = 0.544$). The protein expression of the antiangiogenic isoform VEGF-A165b normalized to GAPDH expression was determined by Western blot (Figure 4E, Supplementary Figure S4). VEGF-A165b was significantly upregulated in normoxia from day 7+18 to day 7+25 ($p = 0.003$), while there was a significant reduction in hypoxia compared to normoxia at day 7+25 ($p = 0.001$).

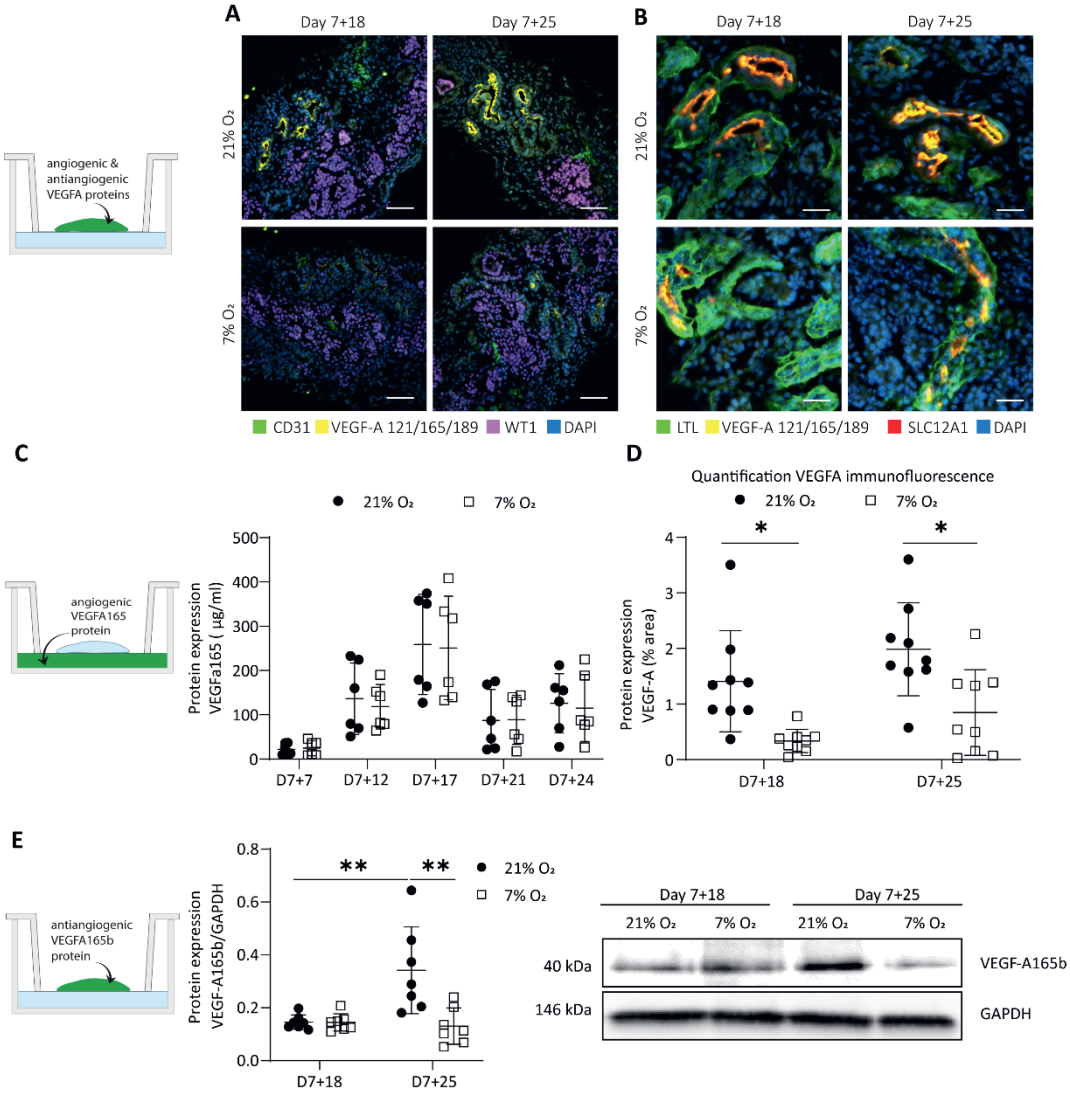

Figure 4: Expression of hypoxia-responsive VEGF-A in organoids cultured in 21% and 7% O_2. A. Immunofluorescence for VEGF-A (121, 165, 189 isoforms; yellow), endothelial cells (CD31; green), podocytes (WT1; magenta) and nuclei (DAPI; blue) displays a reduction of VEGF-A in 7% O_2 compared to 21% O_2 at both day 7+18 and day 7+25. (n=3, N=3). Scale bar: 50 µm. B. Immunofluorescence shows localization of VEGF-A to the apical side of proximal tubules co-positive for loop of Henle marker (SLC12A1; red). (n=3, N=3). Scale bar: 25 µm. C. VEGF-A165 protein expression measured in the culture

medium was differentially expressed over time, but not significantly different in hypoxia compared to normoxia. (n=3, N=2). D. Quantification of immunofluorescence images confirm that VEGF-A was significantly lower expressed in hypoxia compared to normoxia. (n=3, N=3) E. The anti-angiogenic VEGF-A165b isoform was significantly upregulated over time in normoxia and significantly downregulated in hypoxia compared to normoxia at day 7+25. (n=2, N=3). *= $p \leq 0.02$, ** = $p < 0.003$.

Differential expression of angiogenesis-regulating genes in hypoxic culture

VEGF-A is known to exist in various splice variants with distinct biological functions. *VEGF-A165* is the most prominent variant, followed by *189* and *121* in the adult human kidney.[42] We investigated *VEGF-A* variant expression in the organoids by quantitative polymerase chain reaction (qPCR). VEGF-A189 was significantly higher in hypoxia cultures than in normoxia, with a 1.8 fold-change (FC) at day 7+18 ($p = 0.001$) and 1.9 fold-change at day 7+25 ($p = 0.032$) relative to the control samples expression (day 7+18 normoxia) (Figure 5A). VEGF-A165 was significantly upregulated at day 7+18 relative to the control samples (FC = 2.06; $p = 0.0014$), but there was no significant difference between organoids in normoxia or hypoxia at day 7+25 (Figure 5B). VEGF-A121 was significantly upregulated in hypoxia compared to normoxia at both day 7+18 (FC: 1.49; $p = 0.0004$) and day 7+25 (FC: 1.617; $p = 0.002$)(Figure 5C). The ANOVA main effect analysis showed that time did have a limited effect on the observed differences in VEGF-A variant expression (VEGFA189: $p = 0.243$; VEGF-A121: $p = 0.085$; VEGF-A165: $p = 0.047$) and could largely be attributed to the hypoxic culture (VEGF-A189: $p < 0.0001$; VEGF-A121: $p < 0.0001$; VEGFA165: $p = 0.0001$). We also determined mRNA expression of *ANG*, the gene encoding angiogenin, another hypoxia-regulated angiogenic factor, in our kidney organoid culture. Similar to *VEGF-A165, ANG* mRNA was significantly upregulated over time ($p < 0.0001$) but with no differences between hypoxia and normoxia cultures (Figure 5D).

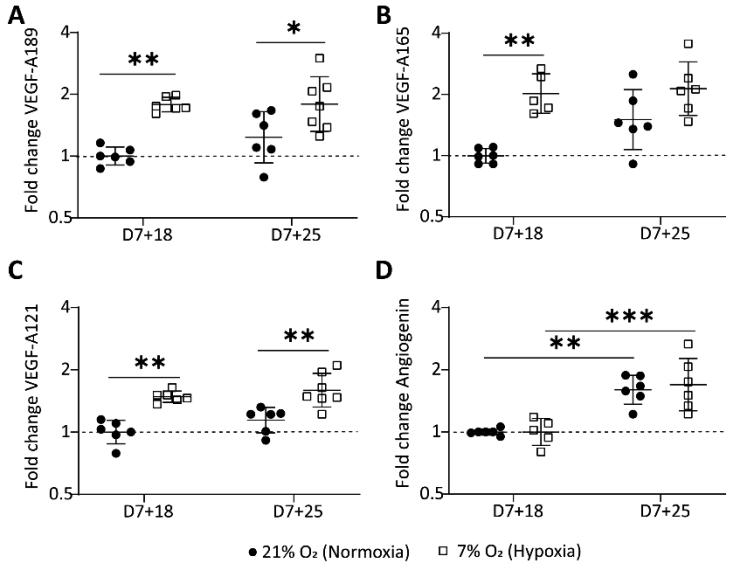

Figure 5: Hypoxic organoid culture differentially upregulates VEGF-A variants. (A). VEGF-189 is significantly upregulated at both time points in the hypoxic culture. (B). VEGF-A165 is significantly upregulated at day 7+18 in the hypoxic culture and (C). VEGF-121 is significantly upregulated at both time points in the hypoxic culture. D. Angiogenin mRNA is significantly upregulated over time in both the normoxic and hypoxic culture. The data is plotted relative to day 7+18 normoxia (n=3, N=3 with excluded technical failures). *= $p \leq 0.03$, ** = $p \leq 0.002$, *** = $p \leq 0.0004$.

Hypoxia-induced angiogenesis: homogenous micro-vessel formation and sprouting

Hypoxia is well known to enhance angiogenesis in both development and pathologies.[43] In both, endothelial cells undergo sprouting to form new blood vessels. In the normoxia culture, endothelial cells largely reside on the surface of the organoids and are therefore directly exposed to the non-physiological oxygen concentrations (Supplementary Figure S5). We investigated the effect of hypoxia on the endothelial patterning by whole mount immunostaining with the endothelial marker CD31. Whole mount imaging and quantification in 3D revealed enhanced micro-vessel formation with more homogenous morphology, enhanced branching and sprouting in organoids cultured in hypoxia compared to normoxia (Figures 6A, C). We observed a reduced intensity of CD31 (not quantified) in hypoxia and normoxia at day 7+25 (Figure 6B). However, the endothelial phenotype was maintained, as confirmed by co-expression of CD31 and VE-cadherin in both normoxia- and hypoxia-cultured organoids at day 7+25 (Supplementary Figure S6). We set up an automatic 3D segmentation and quantification pipeline and found that hypoxia induced a significant increase in the fraction of endothelial cells of the total organoid volume (40.3 ± 12.50%) compared to normoxia (14.3 ± 2.60%) (p = 0.019; Figure 6E) at day 7+18 that was not observed at day 7+25 (p = 0.318). Interestingly, the average vessel length was significantly higher in hypoxia compared to normoxia at day 7+25 (hypoxia: 170 ± 26 μm; normoxia: 97 ± 11 μm; p = 0.014) (Figure 6D). There was no significant difference at D7+18 (p = 0.068). Three-dimensional segmentation additionally revealed that the endothelial network in organoids cultured in normoxia largely resided in a two-dimensional plane (parallel to the transwell), while in hypoxia culture, the network was mainly interconnected in three dimensions (Supplementary video 1 and 2).

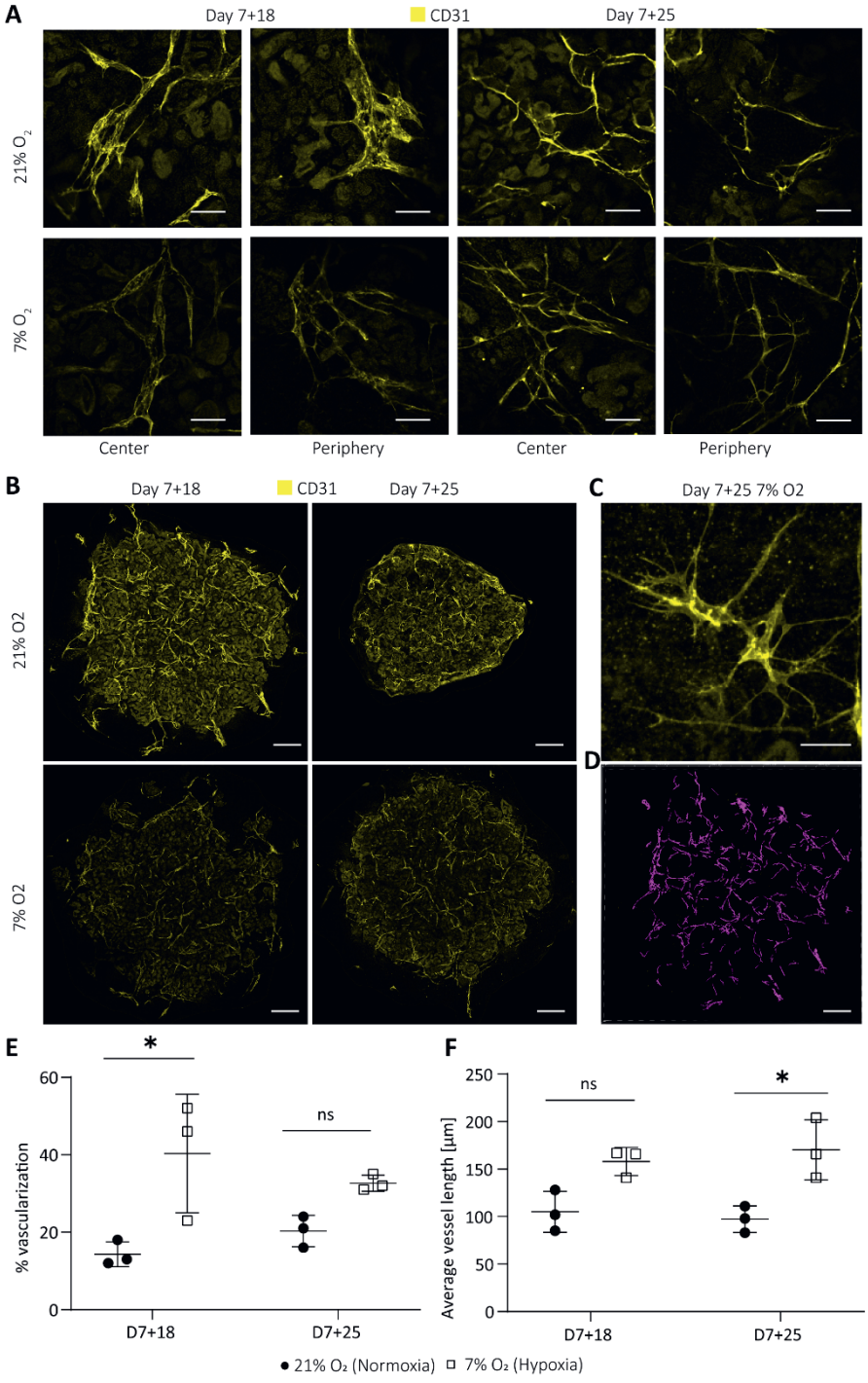
A
Day 7+18
CD31
Day 7+25
21% O2
7% O2
Center
Periphery
Center
Periphery
B
Day 7+18
CD31
Day 7+25
21% O2
7% O2
C
Day 7+25 7% O2
D
E
% vascularization
60
40
20
0
*
ns
D7+18
D7+25
F
Average vessel length [µm]
250
200
150
100
50
0
ns
*
D7+18
D7+25
21% O2 (Normoxia)
7% O2 (Hypoxia)

Figure 6: Hypoxic organoid culture promotes interconnected microvasculature formation and sprouting. A. The endothelial network (CD31; yellow) has a more homogeneous morphology and enhanced interconnectivity and branching in organoids cultured in 7% O_2. B. Z-intensity projected images of whole mount imaged organoids show less intense CD31 staining, likely due to smaller vessel size. C. Hypoxia-induced sprouting of endothelial vessels at day 7+25. D. Example of 3D segmentation of endothelial network of a day 7+18 normoxia organoid. Scale bars: 50 μm (A, C); 600 μm (B, D). Quantification in 3D reveals E. an increase in the volume fraction of endothelial cells at day 7+18 in hypoxia and F. an increased average vessel length in hypoxia compared to normoxia at D7+25. (n=1, N=3). * = $p \leq 0.019$.

Discussion

Our aim was to investigate if a lower oxygen concentration applied to the kidney organoid culture that mimics the *in vivo* hypoxic environment during nephrogenesis could improve angiogenesis and organoid vascularization. The mRNA expression of endothelial markers (*CD31*, *KDR*) in the normoxic culture was downregulated over time (Supplementary Figure S7), indicating the need for stimuli to activate angiogenesis. We opted for a long-term hypoxic culture (20 days), because long-term hypoxia (hours to days, depending on the model) enhances the expression of angiogenic cytokines and growth factors such as PDGF and VEGF in comparison to acute hypoxia that is known to activate the release of inflammatory factors.[44,45] VEGF-A in particular is known to be crucial for endothelial cell differentiation, proliferation and migration[46], as well as glomerular capillary formation, podocyte survival and slit diaphragm integrity in autocrine podocyte signaling.[47] We therefore included VEGF-A mRNA and protein expression in our investigations.

Kidney organoids developed similarly in normoxic and hypoxic conditions. The hypoxic culture did not impair nephron specification and organization, nor organoid size (Figure 1B–C, Figure 2A–B), indicating that hypoxia did not interfere with normal organoid development. Our measurements of oxygen concentration on the bottom of the organoid culture plate (1.0 ± 0.21% in hypoxia on day 7+25) were lower compared to the poorly vascularized medullas in adults (1.9% O_2 at atmospheric pressure derived from the measured 15 mmHg).[31] We therefore expected our hypoxic culture to more closely resemble avascular, hypoxic kidneys during early development, although *in vivo* data are still lacking.[48] This similarity

indicates that growing organoids at 7% O_2 could mimic the *in vivo* hypoxic environment and help study organoid maturation in a more physiological model.

In addition to oxygen levels, we found a similar transcriptional program activated in the kidney organoids as in the developing human kidney. Specifically, severe hypoxia and consequently HIF stabilization was found to be essential in nephrogenesis[41], with HIF-1α expressed in cortical and medullary collecting duct, nephrogenic zone and glomerular cells.[33] While the collecting duct lineage does not exist in the organoids, podocytes deeper within the organoid, showed nuclear HIF-1α expression at day 7+18 in normoxia (Figure 3A). According to our measurements, these podocytes would reside in regions close to 7.53 ± 1.47% O_2. Likely, only podocytes experiencing less than 5% O_2 showed nuclear translocation of HIF-1α.[29] Indeed, even peripheral podocytes of the hypoxia-cultured organoids, where the oxygen concentration was 1.0 ± 0.21% at the bottom of the organoids, showed nuclear HIF-1α translocation (Figure 3A). While certainly not all podocytes responded by nuclear HIF-1α translocation, the hypoxic culture clearly induces nuclear HIF-1α in podocytes throughout the organoids.

Comparable to HIF-1α, nuclear HIF-2α is important to *in vivo* kidney development, where it is known to be expressed only in interstitial cells and podocytes[13], as shown in week 14 fetal kidneys[33], as well as in developing tubules in newborns[41]. In our kidney organoids, HIF-2α expression was not limited to interstitial cells and podocytes, but was expressed in all cell types examined in both hypoxia and normoxia (Figure 3B). There were clear differences in intensity of nuclear HIF-2α in interstitial cells within the organoids in normoxia and hypoxia, while the nephrons equally expressed nuclear HIF-2α. The reason for this observed difference is unclear. Clarification is also needed for why all interstitial cells, even in the most oxygenated condition (day 7+18 normoxia), do express nuclear HIF-2α. There is a need for further investigation, since recent findings in mice suggest that chronic HIF-2α expression in stromal progenitors impairs kidney development, in particular nephron formation, tubular maturation, and the differentiation of FOXD1+ stromal cells into smooth muscle, renin, and mesangial cells.[49] This was found to be regulated by the inhibition of PhD2 and PhD3.[50] The fact that the organoids do not mature further and mesangial cells and renin cells are thought to be absent in this kidney

organoid model[51], could indicate impaired *in vitro* differentiation of FOXD1+ progenitor cells. Therefore, future research could investigate the role of HIF-2α nuclear translocation in this context.

In vivo, pericytes derived from FOXD1+ progenitors are known to show HIF-2α nuclear translocation that induces EPO production. However, in our organoids, HIF-2α nuclear translocation did not induce EPO mRNA transcription in either normoxia or hypoxia (Supplementary Figure S8). The fact that EPO was not transcribed in the organoids in normoxia and hypoxia could potentially be due to a fibrotic stromal population found in the organoids[36] and subsequent hyper-methylation of the EPO 5′ and HRE, inhibiting HIF2/HIFβ dimer binding, as found in adult fibrotic kidneys[52]. Future research could clarify mechanistically, if nuclear HIF-2α is actually leading to target gene transcriptions or if this is inhibited, consequently being one reason for limited organoid maturation.[49]

As with HIF-2α expression, we found differences in the expression of VEGF-A in our kidney organoids compared to fetal human developing kidneys. Comparing the normoxic and hypoxic organoid culture, a decrease in VEGF-A protein expression could be seen. VEGF-A, being one of the most important angiogenic factors, is known for its function in nephrogenesis to induce blood vessel formation in glomeruli through branching angiogenesis and consequently to induce maturation of glomerular cells.[53] In fetal human developing kidneys, VEGF-A is expressed in the epithelial cells in the s-shaped body and collecting duct.[32] Later in nephrogenesis, VEGF-A uptake by convoluted tubules has been observed.[54] In the organoids, VEGF-A was localized on the apical side of LTL+ proximal tubules, co-expressing the LoH marker SLC12A1. We rarely detected expression in podocytes, which is needed to initiate the formation of glomerular capillaries.[55] Consequently, glomeruli containing endothelial cells is a rare event in the organoids. The amount of VEGF-A expression differed between differentiations. However, VEGF-A was reliably less expressed in hypoxia. The location of VEGF-A at the apical side of SCL12A1+ tubules remained the same in hypoxia (Figure 4 A–B, D). We hypothesized that there could be differences in the VEGF-A isoform and transcript variant expression, which could remain hidden by targeting three isoforms with the same antibody as performed in Figures 4A, B. *In vivo*, podocytes are the main source of VEGF-A and synthesize

three VEGF-A isoforms (VEGF-A-121, VEGF-A-165, VEGF-A-189) by alternative mRNA splicing.[47]

VEGF-A variants were differentially expressed in the organoids in hypoxia (Figures 5A–C), consistent with previous studies.[56] *VEGF-A189* was significantly upregulated in organoids cultured in hypoxia, which is associated with microvessel formation[42] and enhanced migration of endothelial cells[57]. Being positively charged in some domains, encoded for by exons 6a, 6b and 7, VEGF-A189 binds negatively charged extracellular matrix and heparan sulphate proteoglycans on cell surfaces, remaining spatially localized and becomes biologically active upon mobilization by heparinase.[58,59] This allows the attraction of vessels into hypoxic tissue. Enhanced cell migration is also confirmed in a variety of cell lines cultured at 0.5% O_2 and modified to overexpress VEGF-A189.[60] In contrast to VEGF-189, VEGF-A121 lacks both exon 6 and 7 and is therefore a readily diffusible, active isoform. Hypoxia-induced pro-angiogenic VEGF-A gene alternative splicing is also known for the VEGF-A121 and VEGF-A165 variants.[56] Their upregulation in the hypoxic culture could indicate an overall higher availability of the three isoforms throughout the organoid. While we could not prove the localization of these isoforms in the organoids due to unavailability of isoform-specific antibodies, we did find an improved patterning of the endothelial network in hypoxia compared to normoxia. Microvessels were homogenously sprouting (Figures 6A–C) with larger vessel length (Figure 6F) and larger connectivity in 3D (Supplementary video 1 and 2) in hypoxia. In normoxia, there was comparatively less connectivity, hetereogenous vessel morphologies and planar growth.

The VEGF-A165b isoform was downregulated in hypoxia compared to normoxia (Figure 4E). VEGF-A165b is a low efficacy agonist, binding VEGFR2 with a stronger affinity and thereby reducing binding of VEGF-A165, resulting in strongly decreased signal transduction via the VEGFR2 receptor.[61,62] VEGF-A165b is upregulated in quiescent vessels and in adult kidneys[61], inhibiting endothelial cell migration[54], and is downregulated in nephrogenesis during capillary loop formation[54,63]. Downregulation of the VEGF-A165b isoform in hypoxia at day 7+25 could indicate increased binding of VEGF-A165 to the VEGFR2 receptor, enhanced signal transduction and consequently the initiation of angiogenesis. Earlier research

confirms the phosphorylation of SRSF1 splice factor by hypoxia targeting the exon 8a proximal splice site, leading to the expression of angiogenic VEGF-A isoforms.[56] While the increased vessel sprouting observed in the hypoxia-cultured organoids is an indication of angiogenesis[64] (Figure 6A–C), more research is needed to prove causality with the downregulated VEGF-A165b isoform. Furthermore, to our knowledge, alternative splicing of VEGF-A in non-pathological developmental angiogenesis is insufficiently studied and would be highly valuable in the context of organoid vascularization and maturation. Finally, *in vivo* glomerular maturation is VEGF-A dose dependent, however, it is only hypothesized that the antiangiogenic isoforms have a dose dependent effect in glomerulogenesis as well.[54]

The results of our study show that modulation of the oxygen concentrations in kidney organoid culture can improve the patterning of endothelial cells and therefore is potentially a relevant factor to integrate in regular organoid culture. Sprouting and interconnected vessels in hypoxia indicated the activation of angiogenesis, which is important for further nephron maturation. Future research is, however, needed to confirm the mechanism by which this enhanced patterning of the endothelial network takes place and to elucidate the roles of the different VEGF-A isoforms. This understanding will help to further enhance the endothelial network in kidney organoids and can potentially be applied to other systems as well. An important challenge in this context will be to understand the batch variations in VEGFA expression and number of endothelial cells in the organoids. Furthermore, we hypothesize that a culture in a hypoxic chamber could be a more controlled environment to study the effects of a hypoxic culture on organoid development. This setup would allow medium changes at the desired hypoxia instead of at ambient oxygen concentrations and would consequently avoid repeated reoxygenation of the organoids. Future research could investigate the effects of hypoxia on nephrons beyond structural development and cell type specific marker expression, such as mitochondrial functionality and cell type specific changes in metabolism. Ideal would be a comparison of the transcriptome of fetal human kidneys with organoids in different oxygen concentrations. Finally, it remains to be determined how VEGF-A expression by podocytes can be increased to allow vascularization and maturation of glomeruli.

Conclusion

In conclusion, kidney organoid culture in physiological hypoxia induced the formation of a homogenous and interconnected endothelial network, while maintaining renal cell types and their spatial organization. We found that *VEGF-A189*, *VEGF-A165* and *VEGF-A121* mRNA is upregulated in hypoxia. At day 7+25 VEGF-A165 is no longer upregulated. Protein expression analysis of the antiangiogenic VEGF-A165b isoform confirmed significant downregulation in hypoxia at day 7+25, being a potential reason for the enhanced endothelial sprouting. While further vessel maturation, i.e. tube formation and glomerular vascularization, are still unresolved, we believe that culture in physiological hypoxia is an important driving force for organoid vascularization and is translatable to other organoid models in a model-specific manner.

Acknowledgements

The authors wish to thank the Physiology department at the Maastricht University for the opportunity to use their hypoxia incubator and Hang Nguyen for reviewing this manuscript. Furthermore, the authors would like to thank Carlos Julio Peniche Silva and Daniel Carvalho from the MERLN Institute for initial support with the oxygen measurements, Sven Hildebrand from Cognitive Neuroscience at Maastricht University for vivid discussions on tissue clearing and Jasmin Dehnen for the support with designing variant-specific primer pairs.

References

1 Takasato, M., Er, P. X., Chiu, H. S. & Little, M. H. Generation of kidney organoids from human pluripotent stem cells. *Nat Protoc* **11**, 1681-1692, doi:10.1038/nprot.2016.098 (2016).

2 Schumacher, A. *et al.* Defining the variety of cell types in developing and adult human kidneys by single-cell rna sequencing. *NPJ Regen Med* **6**, 45, doi:10.1038/s41536-021-00156-w (2021).

3 Gupta, N., Dilmen, E. & Morizane, R. 3d kidney organoids for bench-to-bedside translation. *J Mol Med (Berl)* **99**, 477-487, doi:10.1007/s00109-020-01983-y (2021).

4 Nishinakamura, R. Human kidney organoids: Progress and remaining challenges. *Nat Rev Nephrol* **15**, 613-624, doi:10.1038/s41581-019-0176-x (2019).

5 Takasato, M. & Wymeersch, F. J. Challenges to future regenerative applications using kidney organoids. *Curr. Opin. Biomed. Eng.* **13**, 144-151, doi:10.1016/j.cobme.2020.03.003 (2020).

6 Rossi, G., Manfrin, A. & Lutolf, M. P. Progress and potential in organoid research. *Nat Rev Genet* **19**, 671-687, doi:10.1038/s41576-018-0051-9 (2018).

7 Place, T. L., Domann, F. E. & Case, A. J. Limitations of oxygen delivery to cells in culture: An underappreciated problem in basic and translational research. *Free Radic Biol Med* **113**, 311-322, doi:10.1016/j.freeradbiomed.2017.10.003 (2017).

8 Ma, T., Grayson, W. L., Frohlich, M. & Vunjak-Novakovic, G. Hypoxia and stem cell-based engineering of mesenchymal tissues. *Biotechnol Prog* **25**, 32-42, doi:10.1002/btpr.128 (2009).

9 Worsdorfer, P. & Ergun, S. The impact of oxygen availability and multilineage communication on organoid maturation. *Antioxid Redox Signal* **35**, 217-233, doi:10.1089/ars.2020.8195 (2021).

10 Okkelman, I. A., Foley, T., Papkovsky, D. B. & Dmitriev, R. I. Live cell imaging of mouse intestinal organoids reveals heterogeneity in their oxygenation. *Biomaterials* **146**, 86-96, doi:https://doi.org/10.1016/j.biomaterials.2017.08.043 (2017).

11 Ding, B. *et al.* Three-dimensional renal organoids from whole kidney cells: Generation, optimization, and potential application in nephrotoxicology in vitro. *Cell Transplant* **29**, 963689719897066, doi:10.1177/0963689719897066 (2020).

12 Grobstein, C. Trans-filter induction of tubules in mouse metanephrogenic mesenchyme. *Exp Cell Res* **10**, 424-440, doi:10.1016/0014-4827(56)90016-7 (1956).

13 Buchholz, B., Schley, G. & Eckardt, K. U. The impact of hypoxia on nephrogenesis. *Curr Opin Nephrol Hypertens* **25**, 180-186, doi:10.1097/MNH.0000000000000211 (2016).

14 Li, J., Gao, X., Qian, M. & Eaton, J. W. Mitochondrial metabolism underlies hyperoxic cell damage. *Free Radic Biol Med* **36**, 1460-1470, doi:10.1016/j.freeradbiomed.2004.03.005 (2004).

15 Jagannathan, L., Cuddapah, S. & Costa, M. Oxidative stress under ambient and physiological oxygen tension in tissue culture. *Curr Pharmacol Rep* **2**, 64-72, doi:10.1007/s40495-016-0050-5 (2016).

16 Brueckl, C. *et al.* Hyperoxia-induced reactive oxygen species formation in pulmonary capillary endothelial cells in situ. *Am J Respir Cell Mol Biol* **34**, 453-463, doi:10.1165/rcmb.2005-0223OC (2006).

17 Shang, T. *et al.* Hypoxia promotes differentiation of adipose-derived stem cells into endothelial cells through demethylation of ephrinb2. *Stem Cell Res Ther* **10**, 133, doi:10.1186/s13287-019-1233-x (2019).

18 Bekhite, M. M. *et al.* Hypoxia, leptin, and vascular endothelial growth factor stimulate vascular endothelial cell differentiation of human adipose tissue-derived stem cells. *Stem Cells Dev* **23**, 333-351, doi:10.1089/scd.2013.0268 (2014).

19 Podkalicka, P. *et al.* Hypoxia as a driving force of pluripotent stem cell reprogramming and differentiation to endothelial cells. *Biomolecules* **10**, doi:10.3390/biom10121614 (2020).

20 Yuan, C. *et al.* Coculture of stem cells from apical papilla and human umbilical vein endothelial cell under hypoxia increases the formation of three-dimensional vessel-like structures in vitro. *Tissue Eng Part A* **21**, 1163-1172, doi:10.1089/ten.TEA.2014.0058 (2015).

21 Salomon, C. *et al.* Exosomal signaling during hypoxia mediates microvascular endothelial cell migration and vasculogenesis. *PLoS One* **8**, e68451, doi:10.1371/journal.pone.0068451 (2013).

22 Prado-Lopez, S. *et al.* Hypoxia promotes efficient differentiation of human embryonic stem cells to functional endothelium. *Stem Cells* **28**, 407-418, doi:10.1002/stem.295 (2010).

23 Han, Y., Kuang, S. Z., Gomer, A. & Ramirez-Bergeron, D. L. Hypoxia influences the vascular expansion and differentiation of embryonic stem cell cultures through the temporal expression of vascular endothelial growth factor receptors in an arnt-dependent manner. *Stem Cells* **28**, 799-809, doi:10.1002/stem.316 (2010).

24 Loughna, S., Yuan, H. T. & Woolf, A. S. Effects of oxygen on vascular patterning in tie1/lacz metanephric kidneys in vitro. *Biochem Biophys Res Commun* **247**, 361-366, doi:10.1006/bbrc.1998.8768 (1998).

25 Tufro-McReddie, A. *et al.* Oxygen regulates vascular endothelial growth factor-mediated vasculogenesis and tubulogenesis. *Dev Biol* **183**, 139-149, doi:10.1006/dbio.1997.8513 (1997).

26 Fischer, B. & Bavister, B. D. Oxygen tension in the oviduct and uterus of rhesus monkeys, hamsters and rabbits. *Journal of reproduction and fertility* **99**, 673-679, doi:10.1530/jrf.0.0990673 (1993).

27 Lee, Y. M. *et al.* Determination of hypoxic region by hypoxia marker in developing mouse embryos in vivo: A possible signal for vessel development. *Developmental dynamics : an official publication of the American Association of Anatomists* **220**, 175-186, doi:10.1002/1097-0177(20010201)220:2<175::Aid-dvdy1101>3.0.Co;2-f (2001).

28 Fajersztajn, L. & Veras, M. M. Hypoxia: From placental development to fetal programming. *Birth Defects Res* **109**, 1377-1385, doi:10.1002/bdr2.1142 (2017).

29 Hemker, S. L., Sims-Lucas, S. & Ho, J. Role of hypoxia during nephrogenesis. *Pediatric nephrology (Berlin, Germany)* **31**, 1571-1577, doi:10.1007/s00467-016-3333-5 (2016).

30 Gerosa, C. *et al.* Low vascularization of the nephrogenic zone of the fetal kidney suggests a major role for hypoxia in human nephrogenesis. *Int Urol Nephrol* **49**, 1621-1625, doi:10.1007/s11255-017-1630-y (2017).

31 Keeley, T. P. & Mann, G. E. Defining physiological normoxia for improved translation of cell physiology to animal models and humans. *Physiol Rev* **99**, 161-234, doi:10.1152/physrev.00041.2017 (2019).

32 Tufro, A. Vegf spatially directs angiogenesis during metanephric development in vitro. *Dev Biol* **227**, 558-566, doi:10.1006/dbio.2000.9845 (2000).

33 Bernhardt, W. M. *et al.* Expression of hypoxia-inducible transcription factors in developing human and rat kidneys. *Kidney Int* **69**, 114-122, doi:10.1038/sj.ki.5000062 (2006).

34 Takasato, M. *et al.* Kidney organoids from human ips cells contain multiple lineages and model human nephrogenesis. *Nature* **526**, 564-568, doi:10.1038/nature15695 (2015).

35 van den Berg, C. W. *et al.* Renal subcapsular transplantation of psc-derived kidney organoids induces neo-vasculogenesis and significant glomerular and tubular maturation in vivo. *Stem Cell Rep.* **10**, 751-765, doi:10.1016/j.stemcr.2018.01.041 (2018).

36 Geuens, T. *et al.* Thiol-ene cross-linked alginate hydrogel encapsulation modulates the extracellular matrix of kidney organoids by reducing abnormal type 1a1 collagen deposition. *Biomaterials* **275**, 120976, doi:10.1016/j.biomaterials.2021.120976 (2021).

37 Schindelin, J. *et al.* Fiji: An open-source platform for biological-image analysis. *Nat Methods* **9**, 676-682, doi:10.1038/nmeth.2019 (2012).

38 Schneider, C. A., Rasband, W. S. & Eliceiri, K. W. Nih image to imagej: 25 years of image analysis. *Nat Methods* **9**, 671-675, doi:10.1038/nmeth.2089 (2012).

39 Xie, F., Xiao, P., Chen, D., Xu, L. & Zhang, B. Mirdeepfinder: A mirna analysis tool for deep sequencing of plant small rnas. *Plant Mol Biol*, doi:10.1007/s11103-012-9885-2 (2012).

40 Klingberg, A. *et al.* Fully automated evaluation of total glomerular number and capillary tuft size in nephritic kidneys using lightsheet microscopy. *J Am Soc Nephrol* **28**, 452-459, doi:10.1681/ASN.2016020232 (2017).

41 Freeburg, P. B., Robert, B., St John, P. L. & Abrahamson, D. R. Podocyte expression of hypoxia-inducible factor (hif)-1 and hif-2 during glomerular development. *J Am Soc Nephrol* **14**, 927-938, doi:10.1097/01.asn.0000059308.82322.4f (2003).

42 Vempati, P., Popel, A. S. & Mac Gabhann, F. Extracellular regulation of vegf: Isoforms, proteolysis, and vascular patterning. *Cytokine & growth factor reviews* **25**, 1-19, doi:10.1016/j.cytogfr.2013.11.002 (2014).

43 Otrock, Z. K., Mahfouz, R. A., Makarem, J. A. & Shamseddine, A. I. Understanding the biology of angiogenesis: Review of the most important molecular mechanisms. *Blood Cells Mol Dis* **39**, 212-220, doi:10.1016/j.bcmd.2007.04.001 (2007).

44 Michiels, C., Arnould, T. & Remacle, J. Endothelial cell responses to hypoxia: Initiation of a cascade of cellular interactions. *Biochim Biophys Acta* **1497**, 1-10, doi:10.1016/s0167-4889(00)00041-0 (2000).

45 Haddad, J. J. & Harb, H. L. Cytokines and the regulation of hypoxia-inducible factor (hif)-1alpha. *Int Immunopharmacol* **5**, 461-483, doi:10.1016/j.intimp.2004.11.009 (2005).

46 Abhinand, C. S., Raju, R., Soumya, S. J., Arya, P. S. & Sudhakaran, P. R. Vegf-a/vegfr2 signaling network in endothelial cells relevant to angiogenesis. *J Cell Commun Signal* **10**, 347-354, doi:10.1007/s12079-016-0352-8 (2016).

47 Guan, F., Villegas, G., Teichman, J., Mundel, P. & Tufro, A. Autocrine vegf-a system in podocytes regulates podocin and its interaction with cd2ap. *Am J Physiol Renal Physiol* **291**, F422-428, doi:10.1152/ajprenal.00448.2005 (2006).

48 Freeburg, P. B. & Abrahamson, D. R. Hypoxia-inducible factors and kidney vascular development. *J Am Soc Nephrol* **14**, 2723-2730, doi:10.1097/01.asn.0000092794.37534.01 (2003).

49 Gerl, K. *et al.* Activation of hypoxia signaling in stromal progenitors impairs kidney development. *Am J Pathol* **187**, 1496-1511, doi:10.1016/j.ajpath.2017.03.014 (2017).

50 Kobayashi, H. *et al.* Hypoxia-inducible factor prolyl-4-hydroxylation in foxd1 lineage cells is essential for normal kidney development. *Kidney Int* **92**, 1370-1383, doi:10.1016/j.kint.2017.06.015 (2017).

51 Yousef Yengej, F. A., Jansen, J., Rookmaaker, M. B., Verhaar, M. C. & Clevers, H. Kidney organoids and tubuloids. *Cells* **9**, 1326, doi:10.3390/cells9061326 (2020).

52 Shih, H. M., Wu, C. J. & Lin, S. L. Physiology and pathophysiology of renal erythropoietin-producing cells. *J Formos Med Assoc* **117**, 955-963, doi:10.1016/j.jfma.2018.03.017 (2018).

53 Kim, B. S., Chen, J., Weinstein, T., Noiri, E. & Goligorsky, M. S. Vegf expression in hypoxia and hyperglycemia: Reciprocal effect on branching angiogenesis in epithelial-endothelial co-cultures. *J Am Soc Nephrol* **13**, 2027-2036, doi:10.1097/01.asn.0000024436.00520.d8 (2002).

54 Bevan, H. S. *et al.* The alternatively spliced anti-angiogenic family of vegf isoforms vegfxxxb in human kidney development. *Nephron Physiol* **110**, p57-67, doi:10.1159/000177614 (2008).

55 Eremina, V. & Quaggin, S. E. The role of vegf-a in glomerular development and function. *Curr Opin Nephrol Hypertens* **13**, 9-15, doi:10.1097/00041552-200401000-00002 (2004).

56 Farina, A. R. *et al.* Hypoxia-induced alternative splicing: The 11th hallmark of cancer. *J Exp Clin Cancer Res* **39**, 110, doi:10.1186/s13046-020-01616-9 (2020).

57 Dahan, S. *et al.* Vegfa's distal enhancer regulates its alternative splicing in cml. *NAR Cancer* **3**, zcab029, doi:10.1093/narcan/zcab029 (2021).

58 Roodink, I. *et al.* Development of the tumor vascular bed in response to hypoxia-induced vegf-a differs from that in tumors with constitutive vegf-a expression. *Int J Cancer* **119**, 2054-2062, doi:10.1002/ijc.22072 (2006).

59 Cebe Suarez, S. *et al.* A vegf-a splice variant defective for heparan sulfate and neuropilin-1 binding shows attenuated signaling through vegfr-2. *Cell Mol Life Sci* **63**, 2067-2077, doi:10.1007/s00018-006-6254-9 (2006).

60 Salton, M., Voss, T. C. & Misteli, T. Identification by high-throughput imaging of the histone methyltransferase ehmt2 as an epigenetic regulator of vegfa alternative splicing. *Nucleic Acids Res* **42**, 13662-13673, doi:10.1093/nar/gku1226 (2014).

61 Peach, C. J. *et al.* Molecular pharmacology of vegf-a isoforms: Binding and signalling at vegfr2. *International Journal of Molecular Sciences* **19**, 1264 (2018).

62 Mamer, S. B., Wittenkeller, A. & Imoukhuede, P. I. Vegf-a splice variants bind vegfrs with differential affinities. *Scientific Reports* **10**, 14413, doi:10.1038/s41598-020-71484-y (2020).

63 Stolz, D. B. & Sims-Lucas, S. Unwrapping the origins and roles of the renal endothelium. *Pediatric nephrology (Berlin, Germany)* **30**, 865-872, doi:10.1007/s00467-014-2798-3 (2015).

64 Tahergorabi, Z. & Khazaei, M. A review on angiogenesis and its assays. *Iran J Basic Med Sci* **15**, 1110-1126 (2012).

Supplementary Figures and Tables

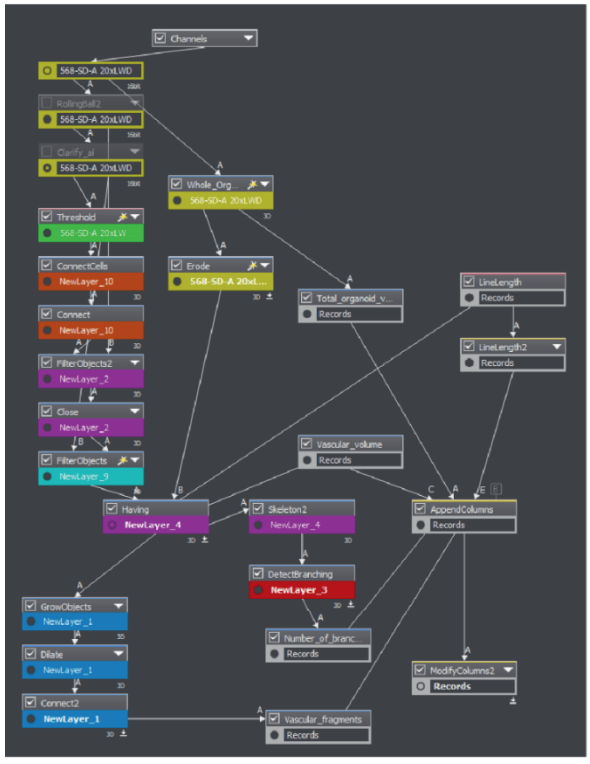

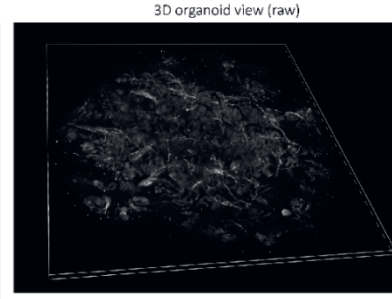

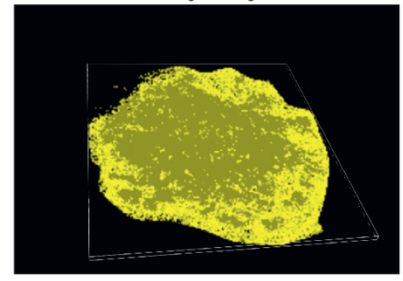

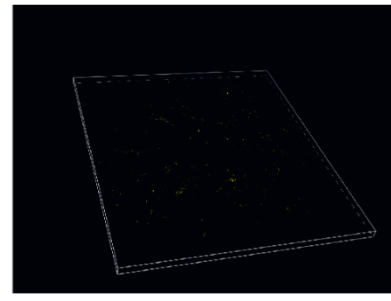

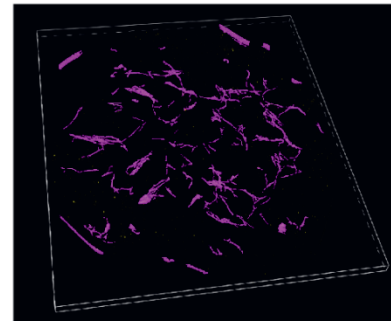

Supplementary figure S1: Segmentation and quantification pipeline of the endothelial network in 3D. Detailed description can be found in the methods section. Briefly, after clarifying the image, the CD31 signal was thresholded, and after conservative filtering, the vessels were skeletonized and segmented.

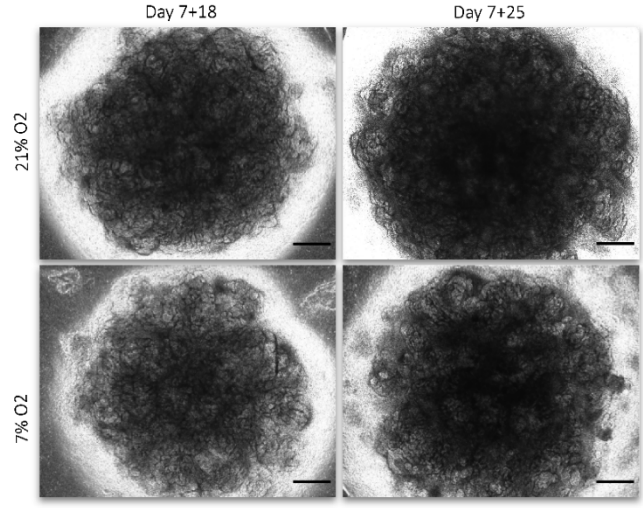

Supplementary figure S2: Brightfield images of organoids in normoxia and hypoxia. Kidney organoids in 21% O_2 and 7% O_2 develop similar morphologies. Scale bars: 1 mm

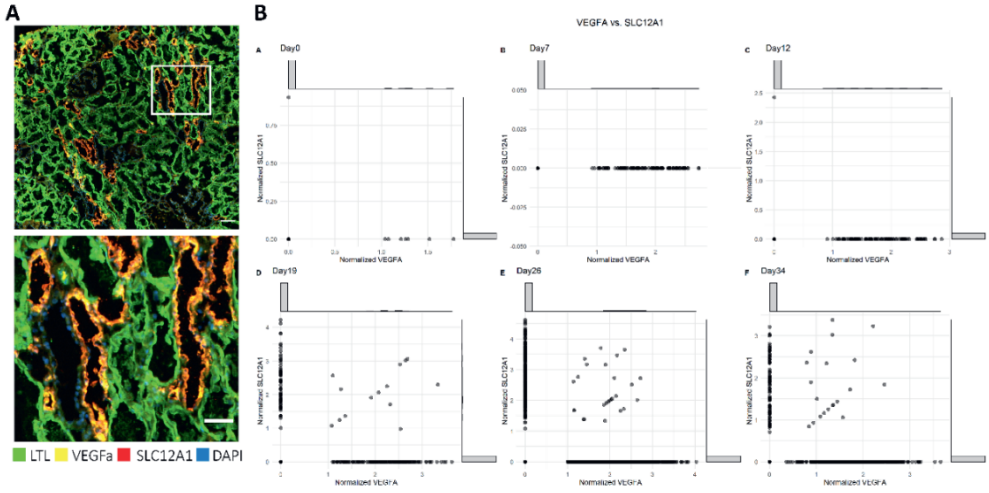

Supplementary figure S3: Vascular endothelial growth factor alpha (VEGF-A) marker validation on adult human kidney and in single cell RNA sequencing datasets of kidney organoids. VEGF-A is co-expressed with Solute carrier family 12 member 1 (SLC12A1) in both adult human kidney sections (A) and single cell RNA sequencing data (B) of Wu et al (2018). Scale bars: 50 μm

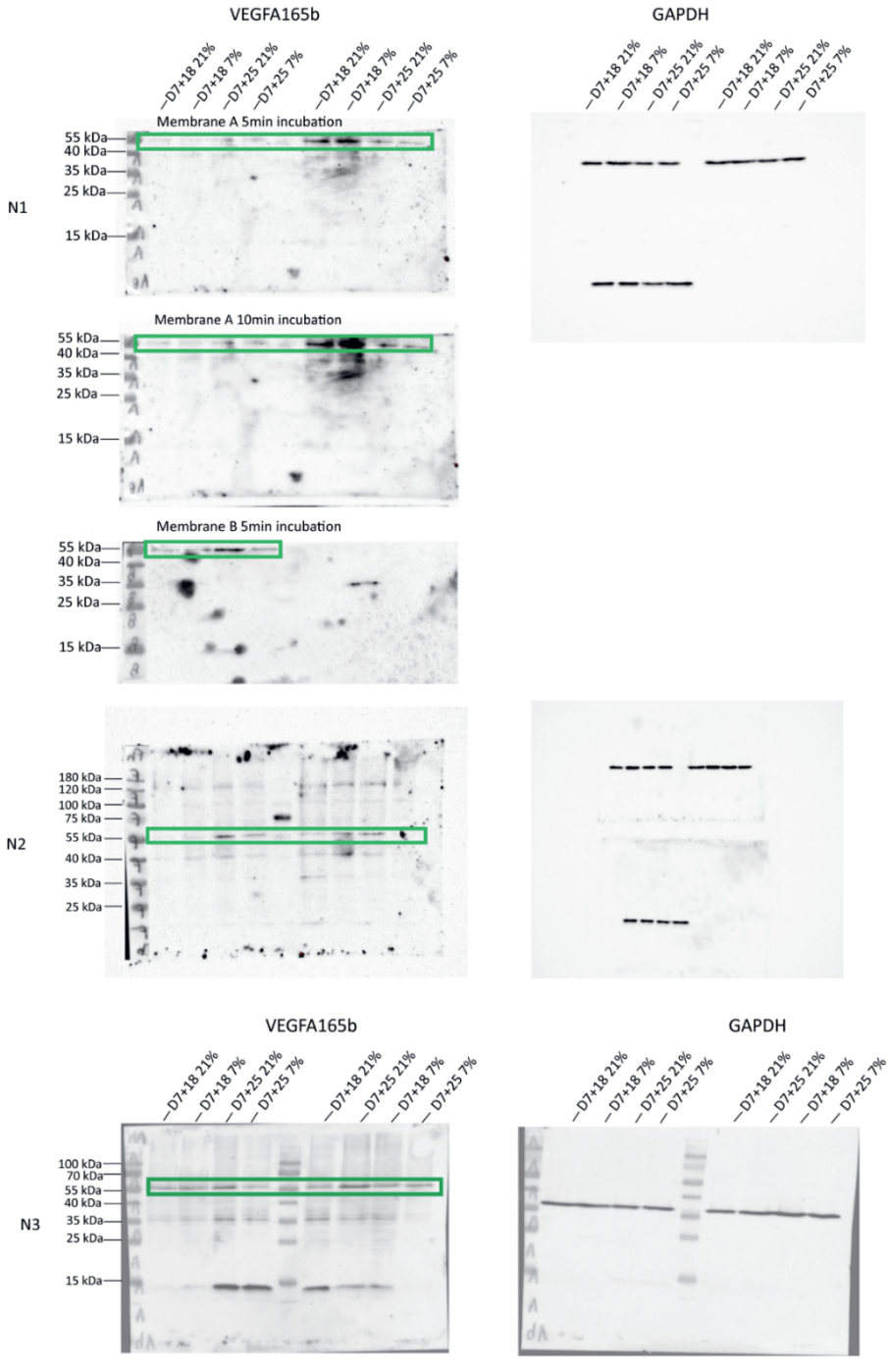
VEGFA165b
GAPDH
D7+18 21%
D7+18 7%
D7+25 21%
D7+25 7%
N1
Membrane A 5min incubation
55 kDa
40 kDa
35 kDa
25 kDa
15 kDa
Membrane A 10min incubation
Membrane B 5min incubation
N2
180 kDa
120 kDa
100 kDa
75 kDa
N3
70 kDa

Supplementary figure S4: Raw blots of VEGF-A165b and GAPDH, indicating the downregulation of VEGF-A165b in hypoxia compared to normoxia at D7+25.

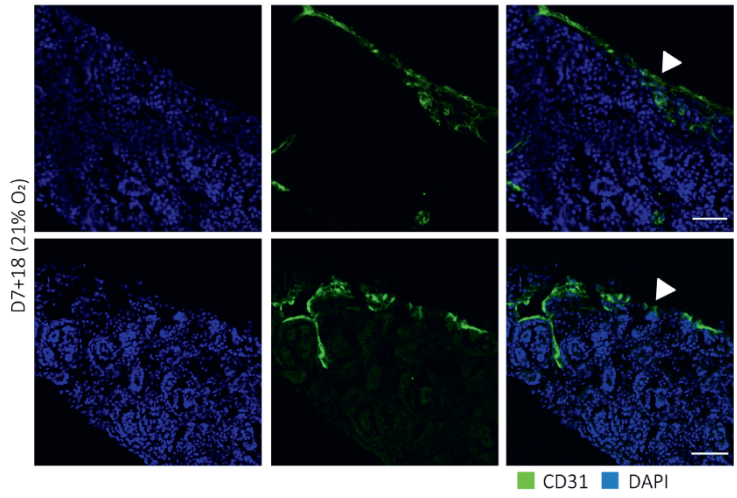

Supplementary figure S5: Localization of endothelial cells in kidney organoids. Immunofluorescence staining of D7+18 (21% O2) shows that endothelial cells are largely located on the surface of the organoids (arrow indicating the air-exposed surface) and only rarely infiltrate into the organoids or reside on the bottom and leaving them directly exposed to the hyperoxic incubator air. Scale bars: 50 µm (top row), 70 µm (bottom row).

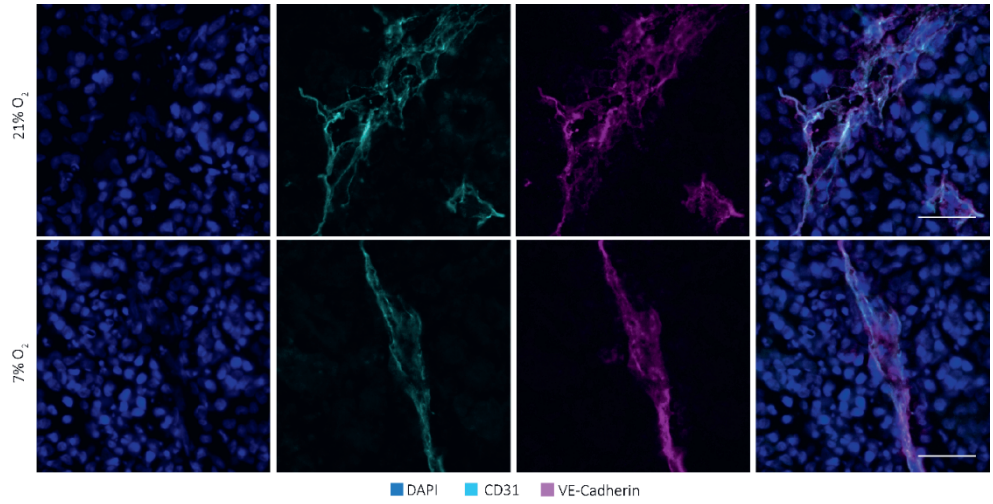

Supplementary figure S6: CD31 and VE-cadherin expression at day 7+25 at 21% and 7% O_2. Co-expression of CD31 and VE-cadherin indicates maintenance of the endothelial phenotype at day 7+25 in culture in both 21% and 7% O_2. Scale bar: 30 μm

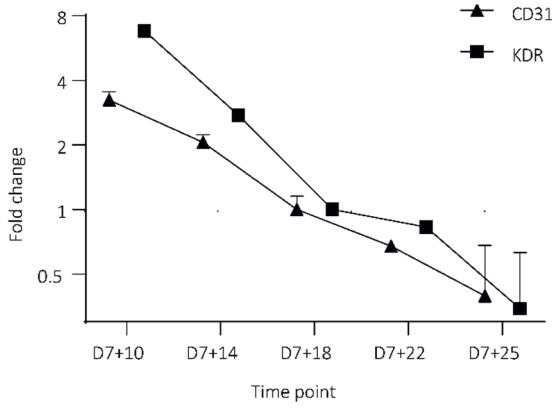

Supplementary figure S7: Gene expression of CD31 and KDR is downregulated over time in 21% O_2 indicating a diminishing endothelial network.

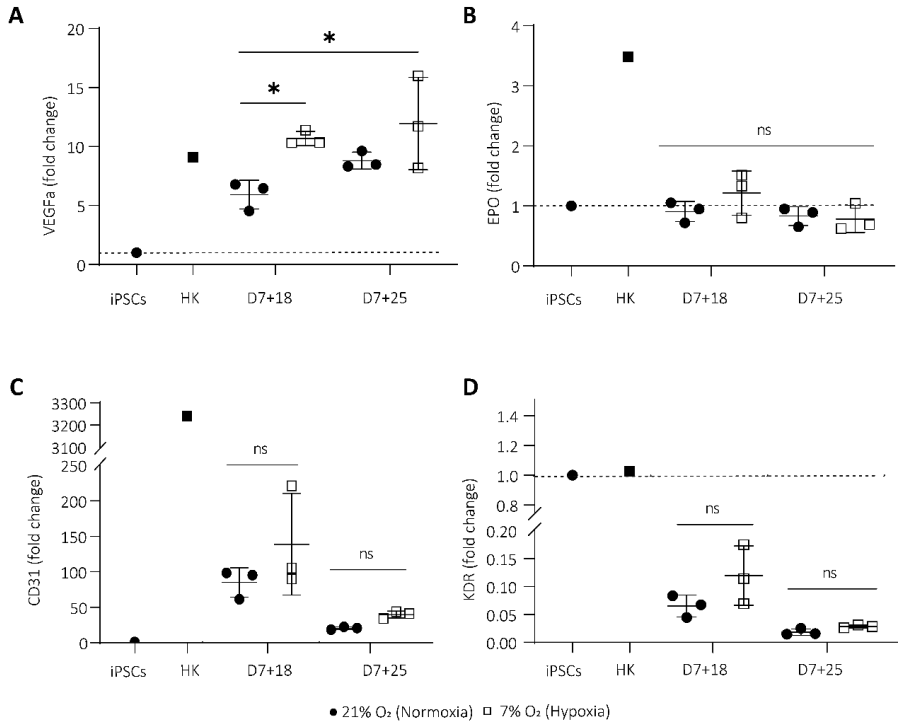

Supplementary figure 8: Gene expression of VEGF-A (all variants), EPO, CD31 and KDR in 21% O_2 and 7% O_2 of a single experiment. VEGF-A mRNA is significantly upregulated at 7% O_2 (A). There is no significant difference between 21% O_2 and 7% O_2 in EPO (B), CD31 (C) and KDR (D) gene expression. Human kidney and iPSCs were plotted as reference. (n=3, N=1)

Supplementary Table 1: List of antibodies and stains used for immunofluorescence of cryosections and whole organoids.

Target	Host	Dilution	Supplier	Cat. no.
Primary antibodies and stains				
CD31	Sheep	1:300	R&D Systems	AF809
E-cadherin (ECAD)	Mouse	1:300	BD Bioscience	610182
HIF1α	Mouse	1:300	Abcam	ab16066
HIF2α	Mouse	1:250	Santa Cruz Biotechnology	sc-46691
Lotus tetragonolobus lectin (LTL), Biotinylated	N/A	1:300	Vector Laboratories	B-1325-2
MEIS 1/2/3	Mouse	1:300	Santa Cruz Biotechnology	SC-101850
Nephrin (NPHS1)	Sheep	1:300	R&D Systems	AF4269
SLC21A1	Rabbit	1:200	Sigma-Aldrich	HPAG14967
VEGF-A	Mouse	1:250	Santa Cruz Biotechnology	SC-7269
VEGF-A165b	Mouse	1:500	R&D Systems	MAB3045
WT1	Rabbit	1:500	Abcam	ab89901
Secondary antibodies and stains				
Anti-Mouse 488	Goat	1:400	Thermo Fisher Scientific	10696113
Anti-Mouse 568	Goat	1:400	Thermo Fisher Scientific	A-11031
Anti-Mouse 647	Goat	1:400	Thermo Fisher Scientific	A-21236
Anti-Rabbit 568	Donkey	1:400	Thermo Fisher Scientific	10617183
Anti-Sheep 488	Donkey	1:400	Thermo Fisher Scientific	10473982
Anti-Sheep 568	Donkey	1:400	Thermo Fisher Scientific	A-21099
Goat Anti-Mouse IgG (H + L)-HRP Conjugate	Mouse	1:3000	Bio-Rad	1706516
Streptavidin 647	N/A	1:400	Thermo Fisher Scientific	S21374

Supplementary Table 2: List of qPCR primers.

NCBI gene ID	Gene symbol	Forward primer (5′ to 3′)	Reverse primer (5′ to 3′)
283	ANG	CAAGGCCATCTGTGAAAACAAG	CAGGGGGAACCTCCATGTAG
2056	EPO	GACATAGTGGCCATGGATGAAG	CGAGGCCAAAGCAGATGAG
2597	GADPH[a]	CTGGGCTACACTGAGCACC	AAGTGGTCGTTGAGGGCAATG
3791	KDR	GGCCCAATAATCAGAGTGGCA	CCAGTGTCATTTCCGATCACTTT
5175	PECAM1	AACAGTGTTGACATGAAGAGCC	TGTAAAACAGCACGTCATCCTT
5692	PSMB4[b]	TGGCTCGTTTCCGCAACAT	GAAATCAGCGTAGTCGCCAG
7422	VEGF-A	AGGGCAGAATCATCACGAAGT	AGGGTCTCGATTGGATGGCA
7422	VEGF-A 121	AGGCCAGCACATAGGAGAGA	GCCTCGGCTTGTCACATTTTT
7422	VEGF-A 165	GAGCAAGACAAGAAAATCCC	CCTCGGCTTGTCACATCTG
7422	VEGF-A 189	TAAGTCCTGGAGCGTTCCCT	ACGCGAGTCTGTGTTTTTGC

[a] second housekeeping gene used to validate the results

[b] housekeeping gene used for analysis

Supplementary videos can be viewed online: https://doi.org/10.3389/fbioe.2022.860138.

Chapter 7

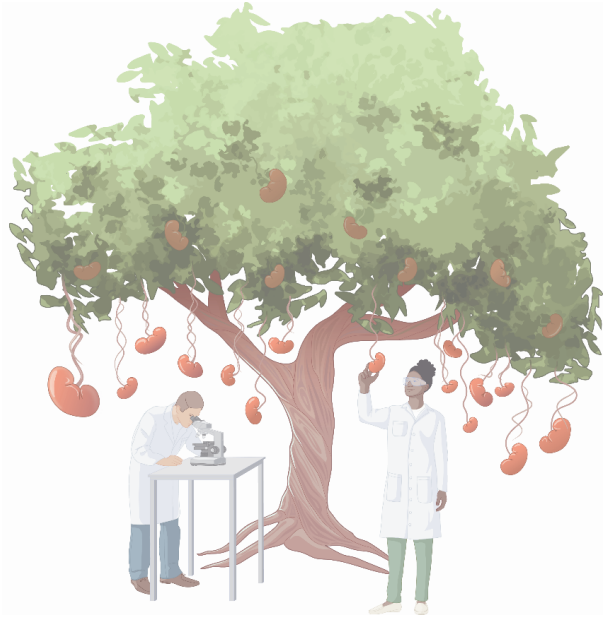

General discussion

In the last decade, organoids have evolved as a versatile tool for disease modeling and drug testing, but also as a potential cell source for regenerative medicine therapies. One example is stem cell–derived kidney organoids, in which nephron progenitor cells, differentiated from pluripotent stem cells, self-organize and further differentiate into a variety of renal cells that are needed for functionality *in vivo* and to make more realistic models *in vitro*. While the emergence of organoids has advanced the fields of tissue engineering and regenerative medicine towards more physiologically relevant results *in vitro*, many challenges still persist. Particularly, the stem cell–derived kidney organoids that can qualify for transplantation to regenerate kidney function are limited by their immaturity, which has been attributed to their stem cell origin and the *in vitro* induction of their differentiation and maturation. While it remains to be determined which extent of maturity is needed for functional success upon transplantation, it is nonetheless clear that the stem cell–derived kidney organoids currently fall short.

In this thesis, we suggest that research to generate functional stem cell–derived kidney organoids should be guided by knowledge of the development of human fetal kidneys *in vivo*. Generally, this approach is applied in the field to determine growth factors and small molecules to induce lineage-specific stem cell differentiation. However, the same approach has largely been lacking in other parameters of the culture environment, such as oxygen supply, extracellular matrix (ECM), cellular heterogeneity, and medium composition. In line with this, the assessment of kidney organoids should ideally include a comparison to human fetal tissue as a control or literature from human fetal tissue as a reference, and not only the rodent tissue or human adult kidneys that are commonly used instead. Furthermore, based on the known importance of the precise microanatomic build up of the kidney for its function, we argue that morphological assessment by electron microscopy should be a mandatory method to assess kidney organoid cultures.

This chapter contains a general discussion to put the findings from this thesis into perspective for future research. Additionally, important future directions are discussed, particularly those needed to advance kidney organoids for transplantation.

Creating correct kidney organoid morphology: current knowledge and future implications

Kidney organoid morphology: immature and incorrect

With the overall aim to replicate nephrogenesis as it occurs *in vivo*, **Chapter 3** and **Chapter 4** assess the morphological development of human fetal kidneys and human kidney organoids. The findings show that kidney organoid development is morphologically both immature and incorrect. **Chapter 4** shows that tubular development is largely immature given the absence of, for instance, the lumen, intracellular vesicles, and complete cellular polarization. Therefore, different organoid tubule types could not be morphologically distinguished. Similarly, podocytes lack secondary foot processes, possess microvilli, and are connected by tight junctions. As shown in **Chapter 3**, all these features can be detected frequently around weeks 8–10 and exclusively close to the nephrogenic zone later in development, which confirms their immaturity.

In addition to immaturity, numerous features in the kidney organoids are incorrect compared to human fetal kidneys. One major difference is the absence of a vascular network in the organoids. Facilitated by a whole mount imaging protocol described in **Chapter 5**, **Chapter 6** shows that endothelial cells grow in a planar fashion largely on the organoids' surfaces. Culture in physiological hypoxia resulted in a more connected, three-dimensional endothelial network. However, perfusable tubes were still absent and endothelial cells were lacking within glomeruli. Accordingly, the glomerular basement membrane (GBM) was deposited in large irregular areas around podocytes (**Chapter 4**) instead of a thin trilaminar layer in between podocytes and endothelial cells (**Chapter 3**). Further examples of striking differences between kidney organoids and human fetal kidneys are the excessive glycogen and ECM deposits, and the disorganized patterning of nephrons. These features are discussed in further detail below in the context of current literature and future research.

Culture environment to determine cellular metabolism

Comparing kidney organoids with human fetal kidneys led us to notice they possessed several abnormal features. Particularly, the amount of intracellular glycogen was striking, and we therefore questioned whether the culture environment was ideal. In **Chapter 4**, we found the coexistence of intracellular glycogen deposits with lipid droplet accumulation, excessive ECM deposition, nuclear YAP expression, EGFR upregulation and mitochondrial damage in the kidney organoids, the combination of which is known for diabetic nephropathy. Consequently, we confirmed that the culture medium was hyperglycemic. Similarly, in **Chapter 6**, we hypothesized that the culture environment was not ideal in terms of oxygen concentration and found that culture in physiological hypoxia improved endothelial patterning. Modulation of cellular metabolism is an interesting link between the two chapters and we propose that future research should focus on this to determine cell-specific needs in glucose and oxygen metabolism.

One factor in the kidney organoid culture affecting cellular metabolism, is the glucose content in the culture medium. The preferred metabolism and glucose requirements differ between stem cells and differentiated cells.[1] Cellular metabolism influences cell fate in terms of stemness and differentiation,[2] and recent research showed that metabolic signals can even predict cell fate prior to commitment.[3] Furthermore, it is generally known that metabolic enzymes play an important role in regulating the epigenome in a loci-specific manner, and metabolites act as co-factors for chromatin-modifying enzymes,[4] thereby influencing cellular phenotypes. Thus, cellular metabolism is an essential determinant of cellular phenotype. For example, pluripotent stem cell culture in glycolysis-supporting medium decreases spontaneous differentiation and maintains pluripotency[5], while inhibition of glycolysis supports differentiation.[6] The same holds true in developing kidneys: inhibiting glycolysis enhances nephrogenesis and induces a mesenchymal-to-epithelial transition in cultured isolated metanephric mesenchyme from embryonic kidneys.[7] Similarly, the culture of kidney organoids in either endothelial growth medium (promoting glycolysis) or renal epithelial growth medium (promoting oxidative phosphorylation) showed that the latter increased overall mitochondrial respiration (oxygen consumption rate).[8] However, individual cell types could not be

distinguished in this study, which could be essential given the known cellular differences in metabolism in the adult kidney.[9,10] From a morphological point of view, a significant increase in tubular branching was present in kidney organoids cultured in renal epithelial growth medium. The direct influence of different glucose concentrations on induced pluripotent stem cell–derived renal cells or organoids has not been investigated. Yet, based on the above and the fact that hyperglycemic culture can lead to abnormal cellular changes as shown morphologically in **Chapter 4**, it is likely that oxidative phosphorylation–supporting medium with lower glucose would be beneficial compared to the currently used culture medium.

Like the medium composition, oxygen availability determines cellular metabolism. Hypoxia is known to increase the reprogramming efficacy of somatic cells to pluripotent stem cells by supporting the glycolytic metabolism of stem cells.[11,12] Similarly, in the fetal kidney, nephron progenitors remain in a hypoxic, non-vascularized niche, and an increase in oxygen through vascularization supports their differentiation into nephrons; yet physiological hypoxic levels are needed for cellular function.[13,14] This need is confirmed by the expression of hypoxia-inducible factors, which ensure oxygen homeostasis throughout nephrogenesis.[15] Yet, the oxygen concentrations throughout the cortex and medulla during nephrogenesis remain to be determined. As known in adults, it can be expected that differences exist between the cortex and medulla; however, additional gradients throughout the fetal cortex likely exist due to the differences in nephron maturity based on anatomical location (**Chapter 3**). Better insights into the oxygenation of developing kidneys could help to further improve kidney organoid culture methods.

Like in adult kidneys, it is likely that local differences and gradients of oxygen exist within the kidney organoids given their size and the different oxygen consumption rates of different cell types. These differences and gradients could then co-influence cellular differentiation. Endothelial cells may be an example of this effect since different renal endothelial phenotypes are thought to be induced by different metabolic profiles.[9] It remains to be determined if kidney organoids contain different subtypes of endothelial cells and what their corresponding metabolic profiles are. Potentially, the tubular lipid accumulations and the impaired fatty acid oxidation in kidney organoids described in **Chapter 4** and in the literature[16] also apply to the

endothelial cells. Endothelial cells do not persist in the organoid culture and are known to need high levels of fatty acid oxidation to protect themselves against ROS and eventual dysfunction.[17] Impaired fatty acid oxidation in endothelial cells also leads to a disrupted vessel network and eventually to an increase of the endothelial-to-mesenchymal transition.[18,19] However, a reduction in oxygen, described in **Chapter 6**, showed an improved endothelial network and therefore raises the question about which metabolic pathway changed. Similar to previous studies, determining the presence of CPT1A, a rate-controlling enzyme in fatty acid oxidation, in endothelial cells could be informative for this question. Understanding specific cellular needs in oxygen availability throughout nephrogenesis will likely lead to more physiological culture protocols and potentially solve some of the current issues of the organoid culture.

Importantly, glucose and oxygen cannot be regarded as separate factors in cell culture since they are intertwined in metabolic pathways. Glucose metabolism is needed to allow oxidative phosphorylation to occur to generate large amounts of ATP. Similarly, glucose content and oxygen concentration in the organoid culture are likely to interfere with each other. For instance, sustained hyperglycemia leads to an increase in oxygen consumption and therefore decreased intrarenal oxygen tension *in vivo,* which is a mechanism known in diabetic nephropathy.[20] Another example are normal and diabetic fibroblasts cultured in hyperglycemia, which were both unable to upregulate vascular endothelial growth factor alpha (VEGF-A) in response to hypoxia due to a decrease in hypoxia-inducible factor (HIF) 1 alpha functionality.[21] A similar mechanism could explain our findings in **Chapter 6**, where hypoxia-cultured organoid cells did not upregulate their VEGF-A protein expression as in normal nephrogenesis *in vivo*, and only downregulated an antiangiogenic variant. Another interplay of glucose and oxygen is suggested by the fact that pharmacological activation of HIFs *in vivo* prevents diabetes-induced changes in oxygen metabolism and could therefore prevent diabetic nephropathy.[22] Impaired HIF functionality leads to tissue hypoxia in diabetic kidneys *in vivo*, consequently further damaging the tissue. However, assuring by means of pharmacological activation that HIF translocates into the nucleus, as in homeostasis, prevented mitochondrial leak respiration, oxygen metabolism, tubulointerstitial damage and loss of kidney function *in vivo*.[22] It might be possible that the culture in

physiological oxygen in **Chapter 6** reduces the effects associated with a hyperglycemic culture in **Chapter 4**. Regardless, HIF functionality needs to be guaranteed in all cell types.

Recently, the first studies investigated the metabolism of fetal kidneys and kidney organoids. The preferred metabolic pathways in week 9 and week 18 human fetal kidneys were determined in a recent study using spatial transcriptomics.[23] Their findings focused on early differentiation within the nephrogenic zone, showing that pre-tubular aggregate cells relied both on glycolysis and oxidative phosphorylation at week 9, but were metabolically inactive at week 18. Interestingly, this inactivity occurs much earlier than the cessation of nephrogenesis around week 35.[24] Only recently, research mapped the metabolic trajectory of nephron progenitor cells to differentiated nephron cells in week 13, 16 and 18 human fetal kidneys, showing a switch from glycolysis to fatty acid beta oxidation in proximal tubular cells.[16] In comparison, kidney organoids remained metabolically immature and failed to use mitochondrial fatty acid beta oxidation. This absence is in line with our findings of accumulating lipid droplets in organoid tubules (**Chapter 4**). In a suspension kidney organoid study using a different differentiation and culture protocol, kidney organoids preferred mitochondrial oxidative phosphorylation.[25] Clearly, there are differences between kidney organoid culture models, and the latest findings including those of **Chapter 4** show the importance of modifying the culture to achieve a metabolism comparable to human fetal kidneys of similar age.

In sum, medium composition and oxygen availability determine cellular metabolism, which directly affects the cellular phenotype. Therefore, both medium composition and oxygen concentrations should be carefully determined to produce complete and functional kidney organoids. Because the findings of this thesis are largely morphological, conclusions on the functional implications are challenging. To strengthen the evidence of this thesis, future research could further investigate the metabolic states of the individual kidney organoid cell types. Knowing the preferred metabolic pathway of the organoid cell types compared to human fetal kidneys could inform cellular needs in terms of nutrients and oxygen supply to be implemented to improve the organoid culture. Future studies could potentially study cell-specific metabolism by redox imaging methods that determine the

NADH/FAD ratio by their autofluorescence[26] or the NAD(P)H ratio by their fluorescence decay rate in 3D.[27,28] Additionally, cell lines expressing a biosensor such as CytochromeC-GFP can allow real-time determination of mitochondrial health.[29] The determination of the cellular metabolism in organoids is one of the most recent developments in the field, therefore much remains to be learned.

Source and impact of aberrant ECM depositions

Another aberrant feature of the kidney organoids is the presence of large ECM depositions. **Chapter 4** showed that, over time, the GBM accumulates in a disorganized fashion. Given the absence of endothelial cells within glomeruli, as shown in **Chapter 4** and **Chapter 6**, their contribution to the formation of the GBM is unlikely and therefore dissimilar to what occurs *in vivo*.[30] Interestingly, differences appear to exist between culture protocols and iPSC lines, since a comparable culture protocol confirmed the expression of collagen type IV subtypes, typical of GBM, by endothelial cells, and also their existence within glomeruli.[31] Neither the frequency of this event nor any basement membrane thickening or bulky deposition has been described. In **Chapter 4**, we hypothesize that the aberrant matrix deposition results from a hyperglycemic culture, since both an increase in matrix deposition and changes of MMP expression were associated with diabetic nephropathy and experimental *in vivo* and *in vitro* models.[32-35] This hypothesis is supported by increased collagen type IV deposition in human blood vessel organoids in hyperglycemic culture, and was even more pronounced for diabetic patient–derived organoids.[36] Another potential source of the aberrant matrix is the off-target chondrocytes present in the kidney organoids, which may have transdifferentiated from mesangial or endothelial cells in a high glucose environment.[37,38]

The composition of the bulky ECM described in **Chapter 4** remains to be determined. Given the different location (glomeruli instead of stroma) and time point of emergence (after D7+18 instead of before) of the ECM in the organoids, it is not expected to be the type 1 collagen we previously described.[39] The observations that podocytes polarize when attached to the matrix and that endothelial cells are absent within glomeruli suggest either a high matrix stiffness or a matrix composition not

supporting endothelial growth. Interestingly, podocytes are known to express more mature markers when cultured on stiff substrates (up to 12 kPa).[40] In contrast, endothelial cells need softer substrates *in vitro* to internalize VEGF-A and form tubes (maximum 4 kPa) and *in vivo* show increased permeability when vessel matrix stiffens (above 2.5 kPa).[41-43] In **Chapter 6**, we show that endothelial cells largely reside on the organoid's surface, potentially due to a lower stiffness compared to the ECM accumulations within the organoid around podocytes or the transwell filter to which they adhered. Culture in physiological hypoxia led to an increase of endothelial vessel length and a three-dimensional network, however, hollow tubes failed to form and vessels did not infiltrate glomeruli. Further investigations are needed to unravel the role of the ECM in this context. Additionally, as discussed in **Chapter 6**, hyperoxia can increase mitochondrial ROS[44] to serve as a signaling molecule, and pathologically upregulated levels of ROS can lead to excessive matrix deposition.[45] Future research should find the source of the aberrant ECM by determining the ECM composition and gene expression of major ECM proteins in the surrounding cell types, for instance by *in situ* hybridization. Spatial proteomics could be used to compare the matrisome of organoids cultured in different oxygen concentrations and glucose concentrations to evaluate if these adaptations lead to a reduction of aberrant ECM.

Improving nephron patterning by increasing the progenitor pool complexity?

One more major distinction between the kidney organoids and human fetal kidneys is the patterning of nephrons. In **Chapter 4**, we show that nephrons in kidney organoids lack orientation, organization of segments, and correct epithelial polarization, making it challenging to distinguish different cell types. Yet, correct patterning is essential for proper function. Kidneys are built up hierarchically, thus both nephrons and vasculature have a tree-like shape. During nephrogenesis, multiple generations of nephrons are formed with increasing maturity towards the medulla. In the kidney organoid model, the nephron progenitors differentiate into a single generation of nephrons simultaneously and with limited maturity.[46] This observation raises the question if mature nephrons can be generated from a single generation or if there is crosstalk between the different stages of maturity

throughout a kidney. *In vitro* culture of one or more isolated generations could provide an answer to this.

Comparing our kidney organoid culture to the latest developments in kidney organoid research, we also argue that the initial differentiation into a larger variety of progenitor cells is an essential step to achieve the correct morphology. While the field aims to generate a tissue from a single cell type (iPSCs) thereby allowing more efficient and controllable cultures as well as the intercommunication of progenitor cells like *in vivo*, future research might deviate from this path. Recent research indicates that differentiating diverse progenitor populations (ureteric bud, nephron and stromal progenitors) separately from mouse pluripotent stem cells, and reuniting them at a later stage, creates more kidney-like patterning (Figure 1). While the patterning does not occur when, for instance, stromal progenitors are not separately induced and added to the culture.[47] Given this fact and the known limited number of cell types in the kidney organoids, one might conclude that to date we are not able to simultaneously induce the necessary variety of progenitors and that separate induction could be more successful.

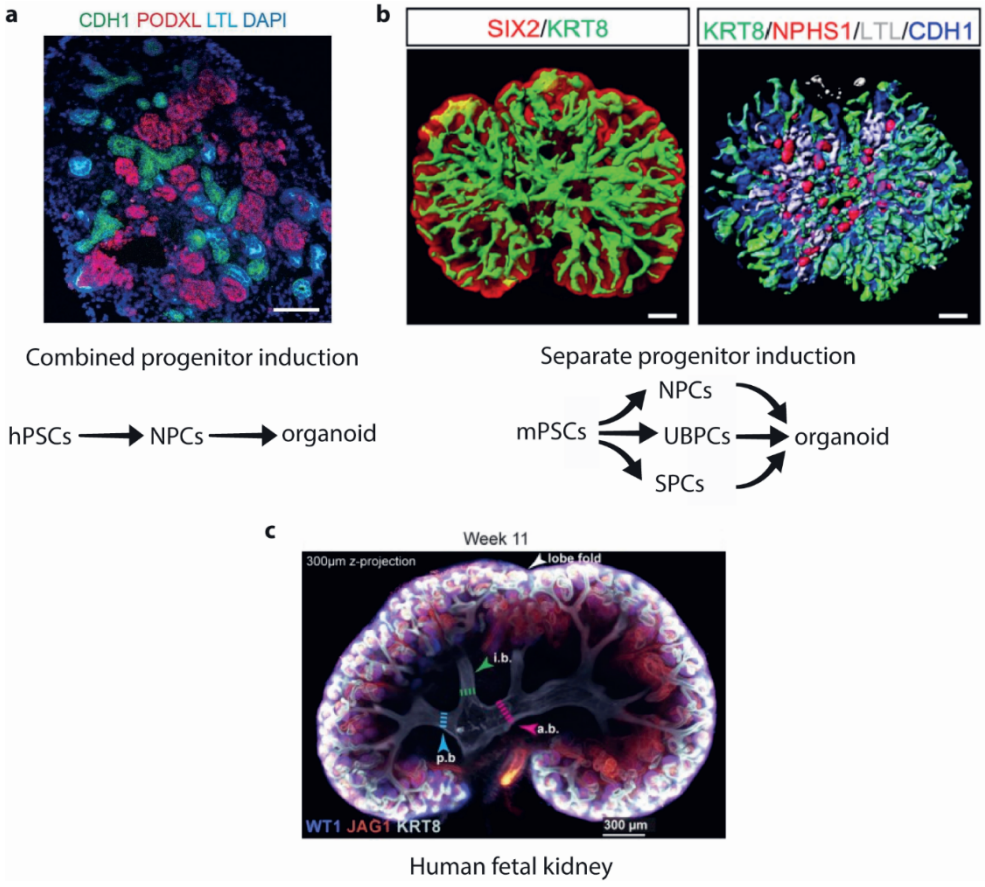

Figure 1: Improved hierarchical morphology and connectivity in kidney organoid culture potentially due to separate induction of progenitor populations. a. Image of a kidney organoid derived from human pluripotent stem cells (hPSCs), which were differentiated to nephron progenitor cells (NPCs) and further matured within organoids into different cell types. Adapted with permission from Morizane, et al. [48] b. Image of a kidney organoid derived from mouse pluripotent stem cells (mPSCs) that were separately induced to NPCs, stromal progenitor cells (SPCs) and ureteric bud progenitor cells (UBPCs), and recombined for maturation. Adapted with permission from Tanigawa, et al. [47] c. Morphology of a human fetal kidney at a similar age as the kidney organoids. Adapted with permission from Lindstrom, et al. [49]

Indeed, mimicking the diversity of cell types of fetal kidneys in our kidney organoids could be critical for a more realistic *in vitro* model. We found approximately 32 cell types in fetal kidneys in contrast to the 5–6 cell types in the

kidney organoid model of this thesis (**Chapter 2**).[50,51] Clearly, many major cell types are lacking in our kidney organoid model, but their importance in nephrogenesis remains to be determined. For instance, different tubular segments such as S1–S3 proximal tubules, loop of Henle, and the connecting tubule have not been generated in organoids. Furthermore, various stromal cells are considered absent, and the existence of intra- and extra-glomerular mesangial cells is not confirmed. Last but not least, non-renal cell types such as vascular cells and immune cells are confirmed to exist in early-stage fetal kidneys, but are absent in the kidney organoids. For most cell types, it remains to be determined whether the inclusion of these cells in our kidney organoid model will stimulate improved nephron patterning.

Increasing culture control and robustness

Besides choosing a culture medium supporting the right metabolic pathways, we believe it is necessary to highlight that control over the medium composition should be guaranteed. In the past years, the morphology of the kidney organoids of this thesis has changed and the degree of off-target populations has increased, despite the fact that both the protocol and cell line were kept the same. Similar observations were made by researchers around the globe (personal communication at conferences), and theories have been posited that the medium composition had changed. As researchers using medium with unknown compositions, we are not notified about changes in formulations by vendors, who are not obligated to disclose this information. We urge vendors to be more transparent about their medium composition to facilitate controlled research, since unknown modifications can have serious effects for research. Furthermore, researchers need the freedom to modify culture media according to their findings. As such, it would have been ideal to modify the APEL2 medium in **Chapter 4** by reducing the amount of glucose to substantiate the findings. However, given the unconfirmed medium composition, this reduction is not a straightforward task. Undoubtedly, high automation and quality control need to be preserved to minimize batch-to-batch variations. In the meantime, scientists, particularly stem cell researchers, remain dependent on commercial media.

Controlling research conditions also includes culture robustness, defined by the use of a variety of cell lines. In this thesis, the work is based on a single iPSC line. While our results are in line with previously published research of the same organoid model with different iPSC lines, they would be more powerful if reproduced with different iPSC lines for the following reasons. Genetic mutations are known to persist during reprogramming and differentiation and can therefore affect the outcomes of organoid studies. Large studies confirmed indeed that the genetic background of the donor drives the variability of iPSCs from the epigenome to cell differentiation capacity, and cellular morphology.[52-54] Another important driver of the variability of iPSCS, and consequently the organoid culture, is the genomic instability of iPSCs. During reprogramming and at any point in culture, genetic variations can occur, however point mutations are thought to occur more frequently during reprogramming than during prolonged culture.[55] Yet, the deletion of tumor-suppressor genes early in culture and increasing duplication of oncogenes throughout the culture remains a matter of concern.[56]

An additional factor highly influencing the reproducibility of this kidney organoid culture is cell–cell contact, which determines both differentiation and stemness. IPSC colonies are characterized by spontaneously differentiating cells at the rim of colonies, where cell–cell contact is lost.[5] While differentiation into cardiomyocytes, for example, requires the loss of cell–cell contact,[57] epithelial differentiation, as needed for nephrogenesis, requires cell–cell contact. Previously, the largest variation was determined between batches and not between individual organoids of the same batch, indicating that manual aggregation and placement on transwell filters is a small issue.[58] In contrast, it is more likely that iPSC seeding density and treatment during 2D differentiation are most prone to induce the variation between batches.

Potential translation to other organoid models

While **Chapter 3** and **Chapter 4** showed that kidney organoids are both morphologically immature and incorrect compared to human fetal kidneys, several findings are similar to features of diabetic kidneys and hyperglycemic cultures. We argue that this is a wider issue since (from personal communication and the

literature[31]) other stem cell–based (kidney) organoid models also possess aberrant glycogen deposits and can be cultured only for a limited time. Furthermore, in our study in **Chapter 6**, we argue that the kidney organoid culture is hyperoxic. Transwell cultures of organoids are common to models of organs that are supposed to be exposed to air (such as ocular[59], skin[60] and lung[61] organoids), therefore 21% oxygen might be correct for these cultures. However, for other organs and therefore organoid models, this air–liquid interface is unusual and hyperoxic. Our findings argue this case for kidney organoids and we therefore urge the modification of protocols.

Conclusion

To conclude, we recommend future research focus on adapting the medium composition, specifically reducing the glucose concentration, and modulating the oxygen concentration. This change will likely allow the generation of more physiological kidney organoids with improved cellular phenotypes and morphology. We emphasize that the kidney organoid model of this thesis has been cultured for more than eight years around the world, and yet the hyperglycemic features have never been described. We believe this highlights the need for more extensive microscopic assessment of organoid cultures and that cellular morphology together with state-of-the-art technology (such as metabolomics and spatial transcriptomics) can dictate future research. Finally, returning to the main message of this thesis, we are convinced that human fetal tissues should guide research of stem cell–derived organoids as long as immaturity is a challenge.

References

1 Carey, B. W., Finley, L. W., Cross, J. R., Allis, C. D. & Thompson, C. B. Intracellular alpha-ketoglutarate maintains the pluripotency of embryonic stem cells. *Nature* **518**, 413-416, doi:10.1038/nature13981 (2015).

2 Dohla, J. *et al.* Metabolic determination of cell fate through selective inheritance of mitochondria. *Nat Cell Biol* **24**, 148-154, doi:10.1038/s41556-021-00837-0 (2022).

3 Arguello-Miranda, O., Liu, Y., Wood, N. E., Kositangool, P. & Doncic, A. Integration of multiple metabolic signals determines cell fate prior to commitment. *Mol Cell* **71**, 733-744 e711, doi:10.1016/j.molcel.2018.07.041 (2018).

4 Haws, S. A., Leech, C. M. & Denu, J. M. Metabolism and the epigenome: A dynamic relationship. *Trends Biochem Sci* **45**, 731-747, doi:10.1016/j.tibs.2020.04.002 (2020).

5 Yamamoto, T., Arita, M., Kuroda, H., Suzuki, T. & Kawamata, S. Improving the differentiation potential of pluripotent stem cells by optimizing culture conditions. *Sci Rep* **12**, 14147, doi:10.1038/s41598-022-18400-8 (2022).

6 Tsogtbaatar, E., Landin, C., Minter-Dykhouse, K. & Folmes, C. D. L. Energy metabolism regulates stem cell pluripotency. *Front Cell Dev Biol* **8**, 87, doi:10.3389/fcell.2020.00087 (2020).

7 Liu, J. *et al.* Regulation of nephron progenitor cell self-renewal by intermediary metabolism. *J Am Soc Nephrol* **28**, 3323-3335, doi:10.1681/ASN.2016111246 (2017).

8 Garreta, E. *et al.* Fine tuning the extracellular environment accelerates the derivation of kidney organoids from human pluripotent stem cells. *Nat Mater* **18**, 397-405, doi:10.1038/s41563-019-0287-6 (2019).

9 Dumas, S. J. *et al.* Phenotypic diversity and metabolic specialization of renal endothelial cells. *Nat Rev Nephrol* **17**, 441-464, doi:10.1038/s41581-021-00411-9 (2021).

10 Bhargava, P. & Schnellmann, R. G. Mitochondrial energetics in the kidney. *Nat Rev Nephrol* **13**, 629-646, doi:10.1038/nrneph.2017.107 (2017).

11 Yoshida, Y., Takahashi, K., Okita, K., Ichisaka, T. & Yamanaka, S. Hypoxia enhances the generation of induced pluripotent stem cells. *Cell Stem Cell* **5**, 237-241, doi:10.1016/j.stem.2009.08.001 (2009).

12 Mathieu, J. *et al.* Hypoxia-inducible factors have distinct and stage-specific roles during reprogramming of human cells to pluripotency. *Cell Stem Cell* **14**, 592-605, doi:10.1016/j.stem.2014.02.012 (2014).

13 Hemker, S. L., Sims-Lucas, S. & Ho, J. Role of hypoxia during nephrogenesis. *Pediatr Nephrol* **31**, 1571-1577, doi:10.1007/s00467-016-3333-5 (2016).

14 Gerosa, C. *et al.* Low vascularization of the nephrogenic zone of the fetal kidney suggests a major role for hypoxia in human nephrogenesis. *Int Urol Nephrol* **49**, 1621-1625, doi:10.1007/s11255-017-1630-y (2017).

15 Bernhardt, W. M. *et al.* Expression of hypoxia-inducible transcription factors in developing human and rat kidneys. *Kidney Int* **69**, 114-122, doi:10.1038/sj.ki.5000062 (2006).

16 Wang, G. *et al.* Spatial dynamic metabolomics identifies metabolic cell fate trajectories in human kidney differentiation. *Cell Stem Cell* **29**, 1580-1593 e1587, doi:10.1016/j.stem.2022.10.008 (2022).

17 Kalucka, J. *et al.* Quiescent endothelial cells upregulate fatty acid beta-oxidation for vasculoprotection via redox homeostasis. *Cell Metab* **28**, 881-894 e813, doi:10.1016/j.cmet.2018.07.016 (2018).

18 Patella, F. *et al.* Proteomics-based metabolic modeling reveals that fatty acid oxidation (fao) controls endothelial cell (ec) permeability. *Mol Cell Proteomics* **14**, 621-634, doi:10.1074/mcp.M114.045575 (2015).

19 Xiong, J. *et al.* A metabolic basis for endothelial-to-mesenchymal transition. *Mol Cell* **69**, 689-698 e687, doi:10.1016/j.molcel.2018.01.010 (2018).

20 Palm, F., Cederberg, J., Hansell, P., Liss, P. & Carlsson, P. O. Reactive oxygen species cause diabetes-induced decrease in renal oxygen tension. *Diabetologia* **46**, 1153-1160, doi:10.1007/s00125-003-1155-z (2003).

21 Thangarajah, H. *et al.* The molecular basis for impaired hypoxia-induced vegf expression in diabetic tissues. *Proc Natl Acad Sci U S A* **106**, 13505-13510, doi:10.1073/pnas.0906670106 (2009).

22 Nordquist, L. *et al.* Activation of hypoxia-inducible factors prevents diabetic nephropathy. *J Am Soc Nephrol* **26**, 328-338, doi:10.1681/ASN.2013090990 (2015).

23 Wu, H. *et al.* Integrating spatial transcriptomics with single-cell transcriptomics reveals a spatiotemporal gene landscape of the human developing kidney. *Cell Biosci* **12**, 80, doi:10.1186/s13578-022-00801-x (2022).

24 Rumballe, B. A. *et al.* Nephron formation adopts a novel spatial topology at cessation of nephrogenesis. *Dev Biol* **360**, 110-122, doi:10.1016/j.ydbio.2011.09.011 (2011).

25 Wang, Q. *et al.* The dynamics of metabolic characterization in ipsc-derived kidney organoid differentiation via a comparative omics approach. *Front Genet* **12**, 632810, doi:10.3389/fgene.2021.632810 (2021).

26 Foomani, F. H. *et al.* Optical metabolic imaging of mitochondrial dysfunction on hadh mutant newborn rat hearts. *IEEE J Transl Eng Health Med* **9**, 1800407, doi:10.1109/JTEHM.2021.3104966 (2021).

27 Blacker, T. S. *et al.* Separating nadh and nadph fluorescence in live cells and tissues using flim. *Nat Commun* **5**, 3936, doi:10.1038/ncomms4936 (2014).

28 Kolenc, O. I. & Quinn, K. P. Evaluating cell metabolism through autofluorescence imaging of nad(p)h and fad. *Antioxid Redox Signal* **30**, 875-889, doi:10.1089/ars.2017.7451 (2019).

29 Przepiorski, A. *et al.* Modeling oxidative injury response in human kidney organoids. *Stem Cell Res Ther* **13**, 76, doi:10.1186/s13287-022-02752-z (2022).

30 Byron, A. *et al.* Glomerular cell cross-talk influences composition and assembly of extracellular matrix. *J Am Soc Nephrol* **25**, 953-966, doi:10.1681/ASN.2013070795 (2014).

31 Morais, M. *et al.* Kidney organoids recapitulate human basement membrane assembly in health and disease. *Elife* **11**, doi:10.7554/eLife.73486 (2022).

32 Garcia-Fernandez, N. *et al.* Matrix metalloproteinases in diabetic kidney disease. *J Clin Med* **9**, doi:10.3390/jcm9020472 (2020).

33 Marshall, C. B. Rethinking glomerular basement membrane thickening in diabetic nephropathy: Adaptive or pathogenic? *Am J Physiol Renal Physiol* **311**, F831-F843, doi:10.1152/ajprenal.00313.2016 (2016).

34 Thrailkill, K. M., Clay Bunn, R. & Fowlkes, J. L. Matrix metalloproteinases: Their potential role in the pathogenesis of diabetic nephropathy. *Endocrine* **35**, 1-10, doi:10.1007/s12020-008-9114-6 (2009).

35 Xu, X. *et al.* A glimpse of matrix metalloproteinases in diabetic nephropathy. *Curr Med Chem* **21**, 3244-3260, doi:10.2174/09298673216661407160920 52 (2014).

36 Wimmer, R. A. *et al.* Human blood vessel organoids as a model of diabetic vasculopathy. *Nature* **565**, 505-510, doi:10.1038/s41586-018-0858-8 (2019).

37 Tang, R. *et al.* High glucose mediates endothelial-to-chondrocyte transition in human aortic endothelial cells. *Cardiovasc Diabetol* **11**, 113, doi:10.1186/1475-2840-11-113 (2012).

38 Guidotti, S. *et al.* Glycogen synthase kinase-3beta inhibition links mitochondrial dysfunction, extracellular matrix remodelling and terminal differentiation in chondrocytes. *Sci Rep* **7**, 12059, doi:10.1038/s41598-017-12129-5 (2017).

39 Geuens, T. *et al.* Thiol-ene cross-linked alginate hydrogel encapsulation modulates the extracellular matrix of kidney organoids by reducing abnormal type 1a1 collagen deposition. *Biomaterials* **275**, 120976, doi:10.1016/j.biomaterials.2021.120976 (2021).

40 Melica, M. E. *et al.* Substrate stiffness modulates renal progenitor cell properties via a rock-mediated mechanotransduction mechanism. *Cells* **8**, doi:10.3390/cells8121561 (2019).

41 Kohn, J. C. *et al.* Cooperative effects of matrix stiffness and fluid shear stress on endothelial cell behavior. *Biophys J* **108**, 471-478, doi:10.1016/j.bpj.2014.12.023 (2015).

42 Sack, K. D., Teran, M. & Nugent, M. A. Extracellular matrix stiffness controls vegf signaling and processing in endothelial cells. *J Cell Physiol* **231**, 2026-2039, doi:10.1002/jcp.25312 (2016).

43 Vernon, R. B., Angello, J. C., Iruela-Arispe, M. L., Lane, T. F. & Sage, E. H. Reorganization of basement membrane matrices by cellular traction promotes the formation of cellular networks in vitro. *Lab Invest* **66**, 536-547 (1992).

44 Resseguie, E. A., Staversky, R. J., Brookes, P. S. & O'Reilly, M. A. Hyperoxia activates atm independent from mitochondrial ros and dysfunction. *Redox Biol* **5**, 176-185, doi:10.1016/j.redox.2015.04.012 (2015).

45 Eble, J. A. & de Rezende, F. F. Redox-relevant aspects of the extracellular matrix and its cellular contacts via integrins. *Antioxid Redox Signal* **20**, 1977-1993, doi:10.1089/ars.2013.5294 (2014).

46 Howden, S. E., Vanslambrouck, J. M., Wilson, S. B., Tan, K. S. & Little, M. H. Reporter-based fate mapping in human kidney organoids confirms nephron lineage relationships and reveals synchronous nephron formation. *EMBO Rep* **20**, e47483, doi:10.15252/embr.201847483 (2019).

47 Tanigawa, S. *et al.* Generation of the organotypic kidney structure by integrating pluripotent stem cell-derived renal stroma. *Nat Commun* **13**, 611, doi:10.1038/s41467-022-28226-7 (2022).

48 Morizane, R. *et al.* Nephron organoids derived from human pluripotent stem cells model kidney development and injury. *Nat Biotechnol* **33**, 1193-1200, doi:10.1038/nbt.3392 (2015).

49 Lindstrom, N. O. *et al.* Conserved and divergent features of human and mouse kidney organogenesis. *J Am Soc Nephrol* **29**, 785-805, doi:10.1681/ASN.2017080887 (2018).

50 Wu, H. *et al.* Comparative analysis and refinement of human psc-derived kidney organoid differentiation with single-cell transcriptomics. *Cell Stem Cell* **23**, 869-881 e868, doi:10.1016/j.stem.2018.10.010 (2018).

51 Combes, A. N., Zappia, L., Er, P. X., Oshlack, A. & Little, M. H. Single-cell analysis reveals congruence between kidney organoids and human fetal kidney. *Genome Med* **11**, 3, doi:10.1186/s13073-019-0615-0 (2019).

52 Rouhani, F. *et al.* Genetic background drives transcriptional variation in human induced pluripotent stem cells. *PLoS Genet* **10**, e1004432, doi:10.1371/journal.pgen.1004432 (2014).

53 Kilpinen, H. *et al.* Common genetic variation drives molecular heterogeneity in human ipscs. *Nature* **546**, 370-375, doi:10.1038/nature22403 (2017).

54 Carcamo-Orive, I. *et al.* Analysis of transcriptional variability in a large human ipsc library reveals genetic and non-genetic determinants of heterogeneity. *Cell Stem Cell* **20**, 518-532 e519, doi:10.1016/j.stem.2016.11.005 (2017).

55 Yoshihara, M., Hayashizaki, Y. & Murakawa, Y. Genomic instability of ipscs: Challenges towards their clinical applications. *Stem Cell Rev Rep* **13**, 7-16, doi:10.1007/s12015-016-9680-6 (2017).

56 Laurent, L. C. *et al.* Dynamic changes in the copy number of pluripotency and cell proliferation genes in human escs and ipscs during reprogramming and time in culture. *Cell Stem Cell* **8**, 106-118, doi:10.1016/j.stem.2010.12.003 (2011).

57 Buikema, J. W. *et al.* Wnt activation and reduced cell-cell contact synergistically induce massive expansion of functional human ipsc-derived cardiomyocytes. *Cell Stem Cell* **27**, 50-63 e55, doi:10.1016/j.stem.2020.06.001 (2020).

58 Phipson, B. *et al.* Evaluation of variability in human kidney organoids. *Nature methods* **16**, 79-87, doi:10.1038/s41592-018-0253-2 (2019).

59 Chacon, M. *et al.* Qobur - a new in vitro human corneal epithelial model for preclinical drug screening. *Eur J Pharm Biopharm* **136**, 164-173, doi:10.1016/j.ejpb.2019.01.023 (2019).

60 Kim, Y. *et al.* Establishment of a complex skin structure via layered co-culture of keratinocytes and fibroblasts derived from induced pluripotent stem cells. *Stem Cell Res Ther* **9**, 217, doi:10.1186/s13287-018-0958-2 (2018).

61 Leibel, S. L., McVicar, R. N., Winquist, A. M., Niles, W. D. & Snyder, E. Y. Generation of complete multi-cell type lung organoids from human embryonic and patient-specific induced pluripotent stem cells for infectious disease modeling and therapeutics validation. *Curr Protoc Stem Cell Biol* **54**, e118, doi:10.1002/cpsc.118 (2020).

Chapter 8

Impact

Social and economic relevance and target groups

The aim of this thesis was to create further understanding of human fetal kidney development and to use this knowledge to better understand and improve kidney organoids. Developments in kidney organoid culture are relevant to researchers and clinicians aiming to model diseases, test drugs and develop renal replacement therapies.[1] Yet, to be functional replicates of adult human tissue, kidney organoids still have to mature further in terms of their cellular and structural complexity and functionality. The knowledge generated in this thesis supports these aims by highlighting important differences between kidney organoid and fetal kidney development and providing suggestions for culture improvement.

In the long term, kidney organoids might be an alternative treatment for patients with kidney failure and could therefore mitigate the donor tissue shortage and the need for dialysis. Both dialysis and donor kidney transplantation are not long-term solutions for patients since they do not prevent the progression of chronic kidney disease. Accordingly, a high risk of death remains. The 10-year graft failure from deceased donors is 49.7% and for grafts from living donors, it is 34.1%.[2] At the same time, the donor shortage remains an unresolved issue and the high prevalence of patients with chronic kidney disease (>10% worldwide[3]) drives research for an alternative treatment. Self-organizing kidney organoids produce nephrons of micro-anatomic detail similar to human nephrons and therefore show unprecedented potential for transplantation to restore kidney function. The work of this thesis has brought more insight into the functional ultrastructure, cellular organization and importance of the culture environment in kidney organoids, thereby helping to progress the field further towards a functional graft.

Importantly, the target groups eligible for receiving organoids as a tissue graft still need to be better defined. Chronic kidney disease is a multifactorial disease in which high age, cardiovascular disease, uremia, diabetes and chronic inflammation can co-exist and this might affect the functionality and lifetime of transplanted grafts.[4] Accordingly, animal studies will be needed that validate organoid survival and functionality in hosts with comparable co-factors.

Products

Adapting the kidney organoid culture protocol according to suggestions made in this thesis will likely lead to organoids with more physiological morphology and may thereby increase nephron functionality. For instance, the reduction of glucose in the culture medium (**Chapter 4**) may prevent the emergence of features of diabetic nephropathy and result in cell types with physiological metabolism. In contrast, due to the identification of features of diabetic nephropathy in this thesis, the current hyperglycemic culture could be implemented as a model of early diabetic nephropathy to increase our understanding of the development of renal pathologies and allow *in vitro* testing of reno-protective treatments in diabetic patients.

Innovation

The research of this thesis focused mainly on the development of human fetal kidneys and human kidney organoids and is innovative in a variety of approaches. To date, kidney morphology has been mainly studied in rodents or adult human tissues. However, given the fact that stem cell–derived organoids are immature and the field focused on gene expression analyses, we provided deeper insights into the ultrastructural development of human fetal kidneys in **Chapter 3**. This knowledge is applied in **Chapter 4**, showing that the comparison to fetal tissue is essential to validate whether organoids develop correctly. As such, we could find that kidney organoids possess features of hyperglycemic cultures and early diabetic nephropathy, which the field has not found with different approaches over the course of the past decade. **Chapter 5** explains the technical details of tissue clearing on kidney organoids, a state-of-the-art method for large organoid models that enables cell type identification and assessment in 3D. Following up on this, **Chapter 6** uses this technology to quantify the irregular endothelial network in 3D, which to date succeeded in such detail only in actual vascular networks. Furthermore, the research of **Chapter 6** was innovative in that the impact of a lower oxygen concentration in kidney organoids had not been suggested or studied. In contrast, many organoid cultures struggle with a pathological hypoxic and necrotic core and we show that culture of kidney organoids in physiological hypoxia improves the vascular network.

Overall, these findings show that detailed microscopic assessment of organoids should be a mandatory part of organoid assessment and that age-matched controls (such as human fetal kidneys) can support the creation of better organoid models.

Implementation

There is an urgent need for alternative treatments for patients with chronic kidney disease since it affects more than 10% of the global population and is the leading cause of mortality worldwide.[3] Clearly, current treatments are not a long-term solution. This gap creates great opportunities for tissue-engineered products. The implementation of kidney organoids as a renal replacement therapy is therefore promising. However, extensive research is still required to translate into the clinic.

One challenge for clinical translation is related to the dimension of kidney organoids compared to human kidneys. An adult human kidney contains from 200,000 to 2.5 million nephrons[5] and, together with a second kidney, filter an average of 200 liters of blood every day. A kidney organoid is estimated to contain approximately 100 nephrons.[6] Consequently, 2,000–25,000 organoids with nephrons of equal functionality are required to fully replace one kidney, though some patients may benefit still from the equivalent of a partial kidney. To date, the engineering of human adult-sized kidneys *in vitro,* to achieve equal functionality, has not succeeded. Generally speaking, culturing tissues of centimeter-scale dimensions is hindered by the lack of nutrient and oxygen delivery through blood vessels. On top of that, the kidney is one of the most complex organs owing to its hierarchical anatomy, complex ultrastructure, and large number of distinct cell types. It is imaginable that researchers will need to develop ways to recreate kidney grafts of larger dimensions, such as bioengineering a framework into which kidney organoids can be integrated as functional units, thereby overcoming the struggle of culturing tissue with large dimensions. Indeed, recent research shows promise in the upscaling of organoids for clinical translation and automization of the culture. These are essential steps to reduce costs and increase culture robustness.

Another factor that is both an opportunity and a challenge is the cell source of kidney organoids. IPSC–derived kidney organoids generate the best replication of kidney

tissue today in terms of cellular and structural complexity. IPSCs also hold the promise to be applied as an autologous therapy, since they can be fabricated from patient's healthy somatic cells. The first clinical trial involving iPSCs was in 2014 and since then numerous trials are ongoing, showing the potential of this cell source.[7] However, chronic kidney diseases often affect the elderly. It therefore can be expected that the creation of reliable and safe iPSCs from these patients is not as straightforward as an age-dependent linear increase in mutations is known to occur throughout the culture.[8] Additionally, organoids successfully replicate genetic mutations limiting their applications for patients with hereditary kidney diseases. Furthermore, two of the Yamanaka-factors (*c-Myc* and *Klf-4*) used for iPSC generation are potent oncogenes[9] and cancer-associated mutations, such as in the *TP53* gene, have been shown to accumulate during iPSC culture[10,11]. IPSCs are also being investigated for their potential to serve as an allogeneic, off-the-shelf cell source for tissue-engineered grafts.[12] This will allow a quicker, more standardized and therefore more cost-effective treatment. Personalized cell therapies are extremely expensive, in the range of hundreds of thousands of dollars.[12] Therefore, off-the-shelf therapy is highly desired. Yet, additional modifications could be needed to avoid rejection of autologous grafts. It may require donor patient matching and the detection of major histocompatibility complex (MHC)-specific neoepitopes that are currently known to occur due to mutations of mitochondrial DNA during iPSC culture and differentiation[13], and might be an additional risk for rejection. Yet, results are conflicting regard the long-term protection from rejection when MHC-specific matching of iPSC–derived cells was performed in non-human primates.[14,15] Additional CRISPR-mediated gene editing could be desired to create hypoimmune iPSCs, for instance by inactivating MHC class I and class II genes whilst over-expressing CD47[16], to evade allogeneic immune responses. Clearly, iPSC–derived grafts in general are close to be used as a therapy, however iPSC–derived kidney organoid cultures still require improvements.

Regarding the two main culture modifications suggested in this thesis, their implementation is expected to be feasible in clinical and research laboratories. The suggested reduction in glucose from **Chapter 4** will require additional research to confirm the ideal concentration, after which the current medium can be exchanged.

The same is the case for the oxygen concentration as suggested in **Chapter 6.** Consequently, laboratories will need oxygen-adjustable cell culture incubators.

Overall, this thesis provides deeper insights into human nephrogenesis and, in comparison with kidney organoids, revealed challenges of the culture. While these challenges need to be addressed to generate functional grafts, considering the progress made since the invention of kidney organoids, and the body of knowledge building this field, the future developments hold great promise.

References

1 Khoshdel-Rad, N., Ahmadi, A. & Moghadasali, R. Kidney organoids: Current knowledge and future directions. *Cell Tissue Res.* **387**, 207-224, doi:10.1007/s00441-021-03565-x (2022).

2 Hart, A. *et al.* Optn/srtr 2017 annual data report: Kidney. *Am. J. Transplant.* **19**, 19-123, doi:https://doi.org/10.1111/ajt.15274 (2019).

3 Kovesdy, C. P. Epidemiology of chronic kidney disease: An update 2022. *Kidney Int Suppl (2011)* **12**, 7-11, doi:10.1016/j.kisu.2021.11.003 (2022).

4 Hickson, L. J., Eirin, A. & Lerman, L. O. Challenges and opportunities for stem cell therapy in patients with chronic kidney disease. *Kidney Int* **89**, 767-778, doi:10.1016/j.kint.2015.11.023 (2016).

5 Bertram, J. F., Douglas-Denton, R. N., Diouf, B., Hughson, M. D. & Hoy, W. E. Human nephron number: Implications for health and disease. *Pediatr Nephrol* **26**, 1529-1533, doi:10.1007/s00467-011-1843-8 (2011).

6 Humphreys, B. D. & Knepper, M. A. Prioritizing functional goals as we rebuild the kidney. *JASN* **30** (2019).

7 Kim, J. Y., Nam, Y., Rim, Y. A. & Ju, J. H. Review of the current trends in clinical trials involving induced pluripotent stem cells. *Stem Cell Rev Rep* **18**, 142-154, doi:10.1007/s12015-021-10262-3 (2022).

8 Lo Sardo, V. *et al.* Influence of donor age on induced pluripotent stem cells. *Nat Biotechnol* **35**, 69-74, doi:10.1038/nbt.3749 (2017).

9 Attwood, S. W. & Edel, M. J. Ips-cell technology and the problem of genetic instability—can it ever be safe for clinical use? *J. Clin. Med.* **8**, 288 (2019).

10 Merkle, F. T. *et al.* Human pluripotent stem cells recurrently acquire and expand dominant negative p53 mutations. *Nature* **545**, 229-233, doi:10.1038/nature22312 (2017).

11 Kuijk, E. *et al.* The mutational impact of culturing human pluripotent and adult stem cells. *Nat. Commun.* **11**, 2493, doi:10.1038/s41467-020-16323-4 (2020).

12 Ando, M. & Nakauchi, H. 'Off-the-shelf' immunotherapy with ipsc-derived rejuvenated cytotoxic t lymphocytes. *Exp Hematol* **47**, 2-12, doi:https://doi.org/10.1016/j.exphem.2016.10.009 (2017).

13 Deuse, T. *et al.* De novo mutations in mitochondrial DNA of ipscs produce immunogenic neoepitopes in mice and humans. *Nat Biotechnol* **37**, 1137-1144, doi:10.1038/s41587-019-0227-7 (2019).

14 Aron Badin, R. *et al.* Mhc matching fails to prevent long-term rejection of ipsc-derived neurons in non-human primates. *Nat. Commun.* **10**, 4357, doi:10.1038/s41467-019-12324-0 (2019).

15 Morizane, A. *et al.* Mhc matching improves engraftment of ipsc-derived neurons in non-human primates. *Nat. Commun.* **8**, 385, doi:10.1038/s41467-017-00926-5 (2017).

16 Deuse, T. *et al.* Hypoimmunogenic derivatives of induced pluripotent stem cells evade immune rejection in fully immunocompetent allogeneic recipients. *Nat Biotechnol* **37**, 252-258, doi:10.1038/s41587-019-0016-3 (2019).

Epilogue

Summary

Human kidneys are remarkably complex organs in which many different cell types cooperate to filter blood, regulate water, sodium and mineral levels, and secrete various hormones and humoral factors. The cellular complexity is a mirror of the kidney's anatomical design, which therefore is no less complex. In case of acute injury or chronic disease, kidneys generally do not regenerate, eventually leading to kidney failure. Current treatment options are inadequate long-term solutions and the morbidity for patients remains high. Stem cell–derived kidney organoids, which self-organize into kidney-like tissues, are promising alternatives. Yet, since they develop from stem cells, they have many limitations that have not yet been resolved. For instance, the kidney organoids do not mature further than kidneys between the first and second trimester, and they develop off-target cells, lack functional vasculature, and deteriorate after 25 days in culture. On top of that, their functionality and micro-anatomy are largely unstudied. Therefore, this thesis aimed to create more insight into kidney organoid development with guidance from human fetal nephrogenesis. To this end, in **Chapter 2**, we identified the variety of cell types in fetal versus adult human kidneys based on gene expression. This provided us insight into the cellular complexity present early in development, as well as the difficulty to distinguish cell populations in fetal kidneys, indicating high cellular plasticity.

We continued to study human fetal development in **Chapter 3**, by investigating human fetal kidney ultrastructure of comparable age to the kidney organoids. This allowed us to define additional glomerular developmental stages, as well as features of early tubule differentiation. The latter indicated that a specific order of tubule type-specific maturation might exist and that nuclear shape and chromatin organization might be an additional informative factor of cellular maturity in tubules.

Following the ultrastructural study of human fetal kidney organoids, we continued with assessing kidney organoid development according to our recent insights into the ultrastructure during human nephrogenesis. Accordingly, in **Chapter 4**, we

detected ultrastructural features in kidney organoids that were distinct from fetal kidneys. Most striking were large glycogen and lipid deposits that increased over time in various organoid cells. Along with tubular YAP expression, excessive matrix depositions, mitochondrial abnormalities, and EGFR upregulation, the glycogen and lipid depositions hinted towards a hyperglycemic culture, since these features combined are known for renal cells cultured in hyperglycemia and diabetic kidneys. We confirmed that the glucose concentration in the standard organoid culture medium was indeed hyperglycemic and recommended future work to culture organoids in lower concentrations.

In **Chapter 5**, we tackled the issue that the kidney organoids had dimensions in the millimeter range, leading to challenges in whole-mount imaging using light microscopy. The application of tissue clearing allowed us to fully image kidney organoids stained with conjugated antibodies. In the chapter, we discuss various methods and present technical details of the most successful method for researchers to easily replicate.

Finally, we used the method developed in **Chapter 5** to quantify the endothelial network in kidney organoids in **Chapter 6**. In this chapter, we were again inspired by the way kidneys develop in an embryo. We hypothesized that the air–liquid interface culture at 21% oxygen was hyperoxic. Since human kidneys initially develop in hypoxia and are later not exposed to oxygen concentrations above 9% oxygen, we estimated that 7% oxygen might be a more physiological choice. The endothelial cells in the kidney organoid culture are largely residing on the organoid surface, directly exposed to the hyperoxic air. Furthermore, it is well-known that the angiogenesis-stimulating factor vascular endothelial growth factor (VEGF) is hypoxia-regulated. We were therefore incentivized to investigate the effect of physiological hypoxia on the endothelial population. We found that the anti-angiogenic variant VEGF-A165b was downregulated in our culture in physiological hypoxia. At the same time, the length and connectivity of the endothelial network increased, indicating that a culture at 7% oxygen might be beneficial for endothelial survival.

Overall, the work of this thesis generated deeper insights into both human fetal kidney and human kidney organoid development and offers suggestions for further

improvements. This thesis also highlights the strength and necessity of microscopy as well as age-matched human tissue to understand and improve tissue-engineered constructs such as organoids.

Samenvatting

Menselijke nieren zijn opmerkelijk complexe organen waarin veel verschillende celtypen samenwerken om bloed te filtreren, het water-, natrium- en mineraalgehalte te reguleren en om verschillende hormonen en humorale factoren uit te scheiden. De cellulaire complexiteit is een weerspiegeling van het anatomische ontwerp van de nier, en is daarom niet minder complex. In het geval van acuut letsel of chronische ziekte regenereren de nieren over het algemeen niet, wat uiteindelijk leidt tot nierfalen. De huidige behandelingsopties zijn ontoereikende lange termijn-oplossingen en de morbiditeit voor patiënten blijft hoog. Van stamcellen afgeleide nierorganoïden, die zichzelf organiseren tot nierachtige weefsels, zijn veelbelovende alternatieven. Echter, omdat ze zich ontwikkelen uit stamcellen, hebben ze veel beperkingen die nog niet zijn opgelost. De organoïden van de nieren rijpen bijvoorbeeld niet verder dan de nieren tussen het eerste en tweede trimester, en ze ontwikkelen cellen die niet in de nier thuishoren, missen een functioneel vaatstelsel en verslechteren na 25 dagen in cultuur. Bovendien zijn hun functionaliteit en micro-anatomie grotendeels onbestudeerd. Het doel van dit proefschrift was daarom om meer inzicht te genereren in de ontwikkeling van nierorganoïden door middel van kennis uit de menselijke foetale nefrogenese. Hiertoe hebben we in **Hoofdstuk 2** de diversiteit aan celtypen in foetale versus volwassen menselijke nieren geïdentificeerd op basis van genexpressie. Dit gaf ons inzicht in de cellulaire complexiteit die vroeg in de ontwikkeling aanwezig is, evenals de moeilijkheid om cel populaties in foetale nieren te onderscheiden, wat wijst op een hoge cellulaire plasticiteit.

We gingen door met het bestuderen van de ontwikkeling van de menselijke foetus in **Hoofdstuk 3**, door onderzoek te doen naar de ultrastructuur van menselijke foetale nieren van vergelijkbare leeftijd als de nierorganoïden. Hierdoor konden we extra glomerulaire ontwikkelingsstadia definiëren, evenals kenmerken van vroege tubulusdifferentiatie. Dit laatste gaf aan dat er een specifieke volgorde van type-specifieke rijping van tubuli zou kunnen bestaan en dat nucleaire vorm en chromatine-organisatie een aanvullende informatieve factor zou kunnen zijn voor cellulaire volwassenheid in tubuli.

Na de ultrastructurele studie van organoïden van menselijke foetale nieren, gingen we verder met het beoordelen van de ontwikkeling van nierorganoïden volgens onze recente inzichten in de ultrastructuur tijdens nefrogenese bij de mens. Dienovereenkomstig ontdekten we in **Hoofdstuk 4** ultrastructurele kenmerken in nierorganoïden die anders waren dan foetale nieren. Het meest opvallend waren de grote glycogeen- en vetafzettingen die in de loop van de tijd toenamen in verschillende organoïde cellen. Samen met tubulaire YAP-expressie, overmatige matrixafzettingen, mitochondriale afwijkingen en EGFR-hoogregulatie, wezen de glycogeen- en lipide-afzettingen op een hyperglycemische cultuur, aangezien deze gecombineerde kenmerken bekend zijn voor niercellen gekweekt in hyperglycemie en diabetische nieren. We bevestigden dat de glucoseconcentratie in het standaard organoïde kweekmedium inderdaad hyperglycemisch was en adviseren toekomstig werk om organoïden in lagere concentraties te kweken.

In **Hoofdstuk 5** pakten we het probleem aan dat de organoïden van de nieren afmetingen hadden in het millimeterbereik, wat leidde tot uitdagingen bij de beeldvorming van een gehele organoïde met behulp van lichtmicroscopie. De toepassing van weefsel-clearing stelde ons in staat om nier-organoïden gekleurd met geconjugeerde antilichamen volledig in beeld te brengen. In het hoofdstuk bespreken we verschillende methoden en presenteren we technische details van de meest succesvolle methode die onderzoekers gemakkelijk kunnen repliceren.

Ten slotte hebben we de in **Hoofdstuk 5** ontwikkelde methode gebruikt om het endotheliale netwerk in nierorganoïden in **Hoofdstuk 6** te kwantificeren. In dit hoofdstuk werden we opnieuw geïnspireerd door de manier waarop nieren zich in een embryo ontwikkelen. Onze hypothese was dat de lucht-vloeistof-interfacecultuur bij 21% zuurstof hyperoxisch was. Aangezien menselijke nieren zich aanvankelijk in hypoxie ontwikkelen en later niet worden blootgesteld aan zuurstofconcentraties van meer dan 9% zuurstof, schatten we dat 7% zuurstof een meer fysiologische keuze zou kunnen zijn. De endotheelcellen in de nier-organoïdecultuur bevinden zich grotendeels op het organoïde-oppervlak, direct blootgesteld aan de hyperoxische lucht. Bovendien is het algemeen bekend dat de angiogenese-stimulerende vasculaire endotheliale groeifactor (VEGF) door hypoxie wordt gereguleerd. We werden daarom geïnspireerd om het effect van fysiologische

hypoxie op de endotheel populatie te onderzoeken. We ontdekten dat de anti-angiogene variant *VEGF-A165b* in onze cultuur omlaag was gereguleerd in fysiologische hypoxie. Tegelijkertijd namen de lengte en connectiviteit van het endotheel-netwerk toe, wat aangeeft dat een kweek met 7% zuurstof gunstig kan zijn voor de overleving van het endotheel.

Over het algemeen heeft het werk van dit proefschrift geleid tot diepere inzichten in de ontwikkeling van zowel menselijke foetale nieren als de ontwikkeling van menselijke nierorganoïden en biedt het suggesties voor verdere verbeteringen. Dit proefschrift belicht ook de kracht en noodzaak van microscopie, en van op leeftijd afgestemd menselijk weefsel om lab-gemaakte weefsels zoals organoïden te begrijpen en te verbeteren.

Zusammenfassung

Menschliche Nieren sind bemerkenswert komplexe Organe, in denen viele verschiedene Zelltypen zusammenarbeiten, um Blut zu filtern, Wasser-, Natrium- und Mineralstoffspiegel zu regulieren und verschiedene Hormone und humorale Faktoren abzusondern. Die zelluläre Komplexität ist ein Spiegel des anatomischen Aufbaus der Niere, die daher nicht weniger komplex ist. Im Falle einer akuten Verletzung oder einer chronischen Erkrankung regenerieren sich die Nieren im Allgemeinen nicht, was letztendlich zu einem Nierenversagen führt. Die derzeitigen Behandlungsoptionen sind keine langfristigen Lösungen, und die Morbidität für Patienten bleibt hoch. Aus Stammzellen gewonnene Nierenorganoide organisieren sich selbst zu nierenähnlichen Geweben und sind eine vielversprechende Alternative. Da sie sich jedoch aus Stammzellen entwickeln, haben sie viele Einschränkungen, die noch nicht behoben wurden. Zum Beispiel reifen die Nierenorganoide nicht weiter als fötale Nieren zwischen dem ersten und zweiten Trimester, sie entwickeln Off-Target-Zellen, es fehlt ihnen an funktionellen Gefäßen und sie zerfallen nach 25 Tagen in Kultur. Darüber hinaus sind ihre Funktionsweise und Mikroanatomie weitgehend unerforscht. Daher zielte diese Dissertation darauf ab, mehr Einblick in die Entwicklung von Nierenorganoiden zu gewinnen, indem sie sich an der menschlichen fötalen Nephrogenese orientiert. Zu diesem Zweck haben wir in **Kapitel 2** anhand der Genexpression die Vielfalt der Zelltypen in fötalen und erwachsenen menschlichen Nieren identifiziert. Dies verschaffte uns einen besseren Einblick in die zelluläre Komplexität, die früh in der Entwicklung anwesend ist, sowie in die Schwierigkeit Zellpopulationen in fötalen Nieren zu unterscheiden, was auf eine hohe zelluläre Plastizität hinweist.

Wir haben die Entwicklung des menschlichen Fötus in **Kapitel 3** weiter untersucht, indem wir die Ultrastruktur der menschlichen fötalen Niere untersuchten, deren Entwicklungsstadien mit den Organoiden der Niere vergleichbar ist. Dies ermöglichte es uns, zusätzliche glomeruläre Entwicklungsstadien sowie Merkmale der frühen Tubulusdifferenzierung zu definieren. Letzteres weist darauf hin, dass eine spezifische Reihenfolge der Tubulustyp-spezifischen Reifung existieren könnte

und, dass Kernform und Chromatinorganisation ein zusätzlicher informativer Faktor für die Zellreife in Tubuli sein könnten.

Nach der ultrastrukturellen Untersuchung menschlicher fötaler Nierenorganoide setzten wir die Bewertung der Entwicklung von Nierenorganoiden gemäß unseren jüngsten Erkenntnissen über die Ultrastruktur während der menschlichen Nephrogenese fort. Dementsprechend entdeckten wir in **Kapitel 4** ultrastrukturelle Merkmale in Nierenorganoiden, die sich von fötalen Nieren unterschieden. Am auffälligsten waren große Glykogen- und Lipidablagerungen, die sich im Laufe der Zeit in verschiedenen organoiden Zellen vermehrten. Zusammen mit der tubulären YAP-Expression, übermäßigen Matrixablagerungen, mitochondrialen Anomalien und EGFR-Hochregulierung deuteten die Glykogen- und Lipidablagerungen auf eine hyperglykämische Kultur hin, da die Kombination dieser Merkmale bekannt sind für hyperglykämische Kulturen von Nierenzellen und diabetischen Nieren. Wir bestätigten, dass die Glukosekonzentration des Organoid-Kulturmediums tatsächlich hyperglykämisch war, und empfahlen zukünftigen Forschungen Organoide in niedrigeren Glukosekonzentrationen zu kultivieren.

In **Kapitel 5** haben wir uns mit dem Problem befasst, dass die Nierenorganoide Abmessungen im Millimeterbereich hatten, was zu Herausforderungen bei der Ganz-organoid-Bildgebung mit Lichtmikroskopie führte. Die Anwendung des „Gewebe-Clearings" ermöglichte es uns, mit konjugierten Antikörpern gefärbte Nierenorganoide vollständig abzubilden. In diesem Kapitel diskutieren wir verschiedene Methoden und präsentieren technische Details der erfolgreichsten Methode, die Forscher leicht replizieren können.

Schließlich haben wir in **Kapitel 6** die in **Kapitel 5** entwickelte Methode verwendet, um das endotheliale Netzwerk in Nierenorganoiden zu quantifizieren. In diesem Kapitel wurden wir erneut von der Art und Weise inspiriert, wie sich Nieren in einem Embryo entwickeln. Wir stellten die Hypothese auf, dass die Luft-Flüssigkeits-Grenzflächenkultur bei 21% Sauerstoff hyperoxisch war. Da sich menschliche Nieren zunächst in Hypoxie entwickeln und später keinen Sauerstoffkonzentrationen über 9% ausgesetzt sind, schätzten wir, dass 7% Sauerstoff eine physiologischere Wahl sein könnten. Die Endothelzellen in der Nierenorganoidkultur befinden sich größtenteils auf der Organoid-oberfläche und

sind direkt der hyperoxischen Luft ausgesetzt. Darüber hinaus ist bekannt, dass der Angiogenese-stimulierende vaskuläre endotheliale Wachstumsfaktor (VEGF) Hypoxie-reguliert ist. Dies hat uns inspiriert, die Wirkung von physiologischer Hypoxie auf die Endothelpopulation zu untersuchen. Wir fanden heraus, dass die anti-angiogene Variante *VEGF-165b* in unserer Kultur bei physiologischer Hypoxie herunterreguliert war. Gleichzeitig nahm die Länge und Konnektivität des endothelialen Netzwerks zu, was darauf hinweist, dass eine Kultur mit 7% Sauerstoff für das Überleben des Endothels von Vorteil sein könnte.

Insgesamt lieferte die Arbeit dieser Dissertation tiefere Einblicke in die Entwicklung sowohl der menschlichen fötalen Niere als auch der menschlichen Nierenorganoide und bietet Vorschläge für weitere Verbesserungen. Diese Dissertation hebt auch die Stärke und Notwendigkeit der Mikroskopie sowie altersangepassten menschlichen Gewebes hervor, um durch Gewebezüchtung hergestellte Konstrukte wie Organoide zu verstehen und zu verbessern.

About the author

Anika Schumacher was born on 9th of March 1989 in Ulm-Söflingen (Germany). Still in school, she dreamt of studying in big lecture halls and learning in the library from thick scientific books. Later, in her search for a suitable study, she was drawn to studies that would enable her to help patients in need. Biomedical Engineering, which had enough complexity and potential to help others, was the final choice without a single day of regret. She studied both the Bachelor and Master Biomedical Engineering at the University of Twente in Enschede (the Netherlands), the latter specialized in Bionanotechnology and Advanced Biomanufacturing. During her Bachelor internship, she gained her first practical experience in the group of Prof. Dr Leon Terstappen at the University of Twente on the isolation of circulating tumor cells. The next practical experience was in the group of Prof. Dr Pamela Habibovic at the Maastricht University on the effects of calcium phosphates with inorganic coatings to prevent Staphylococcus aureus induced osteomyelitis. In the group of Prof. Dr Molly Stevens at the Karolinska Institutet in Stockholm (Sweden), she worked on 3D printing of scaffolds to culture neurons obtained by direct conversion from fibroblasts. Finally, she started her PhD in September 2017 in the group of Dr Vanessa LaPointe at the Maastricht University (the Netherlands), later to be co-supervised by Prof. Dr Martijn van Griensven. With the freedom to choose a PhD topic, she decided to join the RegmedXB consortium to focus her research on kidney organoids and to validate their accuracy in replicating human kidneys. Since September 2022, she works as a staff member at the Transplantation Immunology department of the Maastricht University Medical Center, where she happily can do work that more directly affects patients by performing molecular diagnostics together with a great team headed by Dr Lotte Wieten in the field of transplantation. At the same time, she is setting up a research line that brings together the fields of Regenerative Medicine and Transplantation Immunology to support the translation of regenerative technologies into the clinic.

List of publications

Schumacher, A., Joris, V., van Griensven, M. et al. *Ultrastructural comparison of human kidney organoids and human fetal kidneys reveals features of hyperglycemic culture*. bioRxiv, 2023.03. 27.534124 (2023). https://doi.org/10.1101/2023.03.27.534124

Schumacher, A., Nguyen, T.Q., Broekhuizen, R. et al. *Structural development of the human fetal kidney: new stages and cellular dynamics in nephrogenesis.* bioRxiv, 2023.03. 24.534074 (2023). https://doi.org/10.1101/2023.03.24.534074

Wieland, F., **Schumacher, A.**, Roumans, N. et al. *Methodological approaches in aggregate formation and microscopic analysis to assess pseudoislet morphology and cellular interactions*. Open Res Europe, 2:87. (2022). https://doi.org/10.12688/openreseurope.14894.2

Ruiter, F.A.A., Morgan, F.L.C., Roumans, N., **Schumacher, A** et al. *Soft, Dynamic Hydrogel Confinement Improves Kidney Organoid Lumen Morphology and Reduces Epithelial–Mesenchymal Transition in Culture. Advanced Science.* 9(20):2200543. (2022). https://doi.org/10.1002/advs.202200543

Schumacher, A, Roumans, N, Rademakers, et al. *Enhanced Microvasculature Formation and Patterning in iPSC–Derived Kidney Organoids Cultured in Physiological Hypoxia*. Front. Bioeng. Biotechnol. 10:860138. (2022) https://doi.org/10.3389/fbioe.2022.860138

Schumacher, A., Rookmaaker, M.B., Joles, J.A. et al. *Defining the variety of cell types in developing and adult human kidneys by single-cell RNA sequencing*. npj Regen Med 6, 45 (2021). https://doi.org/10.1038/s41536-021-00156-w

Geuens, T., Ruiter, F.A.A., **Schumacher, A.**, et al. *Thiol-ene cross-linked alginate hydrogel encapsulation modulates the extracellular matrix of kidney organoids by reducing abnormal type 1a1 collagen deposition.* Biomaterials. 275, 120976, (2021). https://doi.org/10.1016/j.biomaterials.2021.120976

Schumacher, A., Vranken, T., Malhotra, A. et al. *In vitro antimicrobial susceptibility testing methods: agar dilution to 3D tissue-engineered models*. Eur J Clin Microbiol Infect Dis 37, 187–208 (2018). https://doi.org/10.1007/s10096-017-3089-2

Acknowledgements

Vanessa LaPointe, I would like to express my gratitude for your support throughout my PhD in your group. Your reliability in financing this work has been invaluable. It allowed me to not only design my projects as needed without a heavy burden of strong financial boundaries, but also to attend international conferences that have broadened my horizons and enabled me to make important connections with other researchers in our field. Furthermore, I have truly appreciated your timely feedback on our written pieces and presentations. Your keen eye for detail and excellent understanding of tone and messaging has helped to refine our manuscripts and craft more compelling stories that resonate with our audiences. Finally, your talent for finding a better wording has been an inspiration. Your suggestions have often allowed us to communicate complex ideas more clearly and effectively, and I appreciate the extra effort you put into making sure every piece of writing is as polished and professional as possible.

Martijn van Griensven. Your big heart, positivity, and unwavering belief in me have been an inspiration throughout my PhD journey. Since the moment, I asked you if you would like to be my second supervisor, you have given me your unrestricted support, both professionally and personally. Even when things got tough, your belief in me has lifted me up and given me the courage to push forward. I cannot thank you enough for being such a great support, especially during the challenging times of the lockdown. Your dedication and guidance have been instrumental in helping me to complete my PhD, and I feel truly privileged to have had you by my side throughout this process. You were a kind and generous mentor, with unwavering commitment to my success, which keeps inspiring me for my own leadership role. I am grateful to have had such a supportive mentor like you throughout my PhD.

My gratitude extents to all **(ex-) members of the LaPointe group** (**Arianne van Velthoven, Demi Vogels, Eduardo Soares, Elisa Landi, Fiona Passanha, Fredrik Tengström, Jasmin Dehnen, Marco Schaafsma, Maria-José Eischen-Loges, Mireille Sthijns, Nadia Roumans, Paula Marks, Pere Catala, Virginie Joris)**, I am grateful to have had such a talented and motivated group of individuals working

alongside me, and although our research topics were far apart, each of you tried their best to contribute with valuable feedback during our group meetings. Thank you for that. I would like to particularly thank a few (ex-) members of the LaPointe group for their individual contribution to my PhD:

Thank you, **Timo Rademakers**, for all the invaluable assistance you provided around the lab and particularly with the microscopes and image processing. You are undoubtedly an encyclopedia for microscopy. Whenever I faced any imaging issues or technical problems, you always came up with a solution that worked like a charm. Beyond that, as a lab manager, you are very attentive to the cleanliness and organization of the laboratory, which makes our work environment comfortable and productive. Your contribution is truly indispensable, and I feel lucky to have had your support.

Virginie Joris, I would like to thank you for all the amazing work you have done in the past years, particularly when it comes to Western blotting. You are truly a genius in this area and your skills have been invaluable to my research. Moreover, your enthusiasm for laboratory work is infectious and I am sure it has inspired the whole group to work even harder, but also to prevent any unsuccessful experiments from demotivating us. Watching you take on difficult experiments with such dedication has been truly inspiring. I look forward to continuing our collaboration in the future and cannot wait to see which great things we will achieve together.

I would like to express my heartfelt gratitude to **Nadia Roumans**, for the incredible work you have done in the lab. Your consistency and reliability in working with the organoid culture have been instrumental in saving my PhD project the moment the Covid-19 lockdown started and remained helpful until the end of my PhD. Your meticulous workstyle has helped to produce many organoids and valuable qPCR results, which have been essential for this thesis. Your dedication and commitment to maintaining tidiness around the lab are a blessing and have created a safer and more efficient work environment for everyone. I also much appreciated talking about our mutual passion (gardening) outside the lab or during long organoid-spotting sessions.

Maria-José Eischen-Loges and **Gözde Sahin**, I will always remember the recharging time I spent with you during the busy PhD years. From the beautiful hikes to the delicious dinners and fun parties, each moment spent with you two has helped to

relax and recharge, and felt like a holiday. Your company is always such a joy, and I truly cherish the times we spend together. I could not imagine better paranyphms and am truly grateful to have your support throughout the last phase of my PhD. Thank you for being such great friends, down-to-earth, always understanding and supportive, even when life gets busy. Gözde, thank you also for being a constant source of inspiration with your busy free time schedule. You truly make my life feel boring in comparison! And finally, thank you both for having such great boyfriends, Ruud and Aron. I cannot wait for our next couple times.

I would like to thank the **MERLN Institute** in general for being an inspiring place to work. The MERLN Institute has been a wonderful experience, and I have cherished not only to work there, but also to learn and grow. Being part of such an exceptional and innovative research organization has certainly nurtured my professional development. One of the things that sets the MERLN Institute apart from the rest is its extraordinary openness to all different cultures. This cultural diversity is a lesson for life that shapes our way of teamwork in a positive way. A thank you to **all MERLN members** who helped me throughout these years. **Pamela Habibović** and **Lorenzo Moroni**, a particular thank you for doing the groundwork for such a great research institute, which allows the co-existence of ambition and respect. A personal thank you to **Pamela Habibović**, for your mentoring in times of need. Thank you to all other **MERLN PIs (Aart van Apeldoorn, Aurélie Carlier, Jurica Bauer, Matt Baker, Carlos Mota, Paul Wieringa, Roman Truckenmüller, Sabine van Rijt, Stefan Gieselbrecht)** for ensuring MERLN to be a great working environment. Thank you to the RegmedXB moonshot team (**Aurélie Carlier, Stefan Gieselbrecht, Roman Truckenmueller, Jasia King**) for the interesting consortium meetings during my first year.

To my co-authors **Jaap Joles, Maarten Rookmaker, Rafael Kramann, Tri Nguyen, Timo Rademakers, Nadia Roumans**, and **Virginie Joris**. I would like to thank you for valuable and timely feedback. A particular thank you to **Tri Nguyen** for enthusiastically joining my projects and sharing your knowledge, which set a great base for the studies.

Cathelijne van den Berg and **Loes Wiersma**, thank you for your initial advice on setting up the kidney organoid culture in our laboratory. **Sven Hildebrandt**, thank you for sharing your expertise on brain tissue clearing.

Dear **colleagues from the Transplant Immunology (TIM) laboratory**. I cannot thank you enough for being so welcoming. I truly think that you are a wonderful team and that over the years the most kind and helpful people have joined the lab; it feels like an honor and blessing to be part of this team. Dear **Lotte Wieten**, thank you for having faith in me, for putting potential over experience and giving me the chance to settle in the fields of immunology and organ transplantation. You are a wonderful team leader and I am entirely grateful for the possibilities you offer and will keep taking them with ambition and pleasure. Dear **Christien Voorter**, thank you for being so welcoming, putting all trust in me. I really like our regular meetings, in which I always end up being impressed by the knowledge you possess.

Dear work-roomies (**Coline Groesen, Denise Habets, Sandra Piederiet** and **Steven Koetzier**), thank you for being such great colleagues. Sharing the office with you is truly refreshing and I'm always looking forward to go to work. **Denise Habets**, your positive energy is infectious. I believe I have never met someone who can so enthousiastically and motivatingly say: "Dit wordt huilen met de pet op.", when times are busy and stressful. I wish you all the luck and success for your career. Dear **Steven Koetzier**, thank you for being a great colleague and sharing stories of your life with us during our lunch breaks. I'm looking forward to our future work together. Dear **Amber Lombardi**, I am grateful that you joined my research project. In such a short time you have already been a great help and it has been really fun working with you in the lab. You truly are a great lab-partner! I know already that I will be so proud of what we will achieve together. Dear **Burcu Duygu** and **Timo Olieslagers**, I am always looking forward to having lunch together with both of you. Often it is not possible, but definitely always a joy! I am looking forward to working together with both of you more closely in the near future. Dear **TIM (head-) technicians** and **secretaries**, thank you for receiving me with open arms and being such great and kind colleagues.

Dear **members of the Tumor Immunology lab (Birgit Gijsberg, Gerard Bos, Janine van Elssen, Lynn Janssen, Meric Birben, Nicky Beelen, Roel Klein Wolterink, Vera Valckx, Wilfred Germeraad)**, thank you for welcoming me with open arms and being incredibly open to help. Our weekly meetings are really valuable. I am learning a lot from you, which I appreciate very much.

Daniela Velasco, thank you for making the most professional figures for my thesis. You are incredibly insightful and talented. We needed such few meetings and you always quickly understood what I had in mind and turned it into a perfect figure.

Hang Nguyen, I much appreciated you helping out Vanessa with corrections of our articles. You have a beautfiful writing style and your keen eye helped shaping great chapters.

Dear **members of the Nanoscopy lab (Carmen López Iglesias, Hans Duimel, Helma Kuijpers, Kevin Knoops, Willine van de Wetering)**, thank you for your help with all kinds of microscopy related questions and the thorough and reliable work in preparing TEM sections and performing FIB-SEM imaging.

Dear **Boye, Daniela, Einav, Geraldine, Gintare, Greg, Mario, Mueid, Nello** and **Pieter,** thank you for being wonderful friends during several years of my PhD. I've overly enjoyed our time together and learned a lot from us being all from different cultures; not to speak of the delicious dinners we had from which I am still inspired today. It is sad that life has took us apart and scattered us across the world, but I am sure that someday we will meet all together again.

My biggest thank you goes out to my boyfriend **Bas Van Hooren**. Thank you for being the constant in my ever-changing life. Sharing the PhD journey has been a blessing in both the highs and lows. Working long hours together during busy times has been enjoyable, which feels like a rare thing to have in common. At the same time, I treasure our shared appreciation for the joys of free time, family, and adventure. In some ways, we are so similar, nearly identical and in others, we are the furthest extremes. Being with you during my PhD helped me develop personally in areas I would never have called my strong suit; but now I think I can. As I reflect on the many years we have been together, I am grateful for all the experiences we have shared. Our time together has been anything but boring - at times very challenging, yet also easy in its own way. Thank you to your parents, **Monique** and **Roland** for the pleasant family time in the past years and the many delicious dinners.

To **my parents**: living this far has definitely not made life easier during my PhD. However, learning from my international friends and colleagues, we could have been much further apart even and I can be lucky to have you in the neighboring country. I appreciate your interest in my work and understanding why a PhD is as time consuming and challenging as it is. Today, I have accomplished a significant

milestone, and I'm proud of myself for reaching this point. However, I know this journey would not have been possible without the strong foundation of parenting I have experienced because of you. You always believed in me and instilled in me the confidence to tackle any hurdles that came my way. So, from the bottom of my heart: thank you! I am incredibly grateful for the love and support you have given me through this journey.